OPTIMISATION OF BIODIESEL PRODUCTION WITH HETEROGENEOUS ACIDIC CATALYST USING RESPONSE SURFACE METHODOLOGY

CHON WEN-XIAN

A project report submitted in partial fulfilment of the requirements for the award of Bachelor of Engineering (Hons.) Chemical Engineering

Lee Kong Chian Faculty of Engineering and Science
Universiti Tunku Abdul Rahman

September 2018

DECLARATION

I hereby declare that this project report is based on my original work except for citations and quotations which have been duly acknowledged. I also declare that it has not been previously and concurrently submitted for any other degree or award at UTAR or other institutions.

Signature   : _____

Name   : _____

ID No.   : _____

Date   : _____

APPROVAL FOR SUBMISSION

I certify that this project report entitled **"OPTIMISATION OF BIODIESEL PRODUCTION WITH HETEROGENEOUS ACIDIC CATALYST USING RESPONSE SURFACE METHODOLOGY"** was prepared by **CHON WEN-XIAN** has met the required standard for submission in partial fulfilment of the requirements for the award of Bachelor of Engineering (Hons.) Chemical Engineering at Universiti Tunku Abdul Rahman.

Approved by,

Signature   :   _____

Supervisor   :   _____

Date   :   _____

Signature   :   _____

Co-Supervisor   :   _____

Date   :   _____

ACKNOWLEDGEMENTS

Throughout this research, I have been receiving helps and suggestions from various group of people and for that, I would like to thank them. The first person I would like to thank is my supervisor, Dr. Steven Lim for his patience and guidance throughout this research.

I would also like to thank my family as well as my friends and course mates for the constant moral support throughout this period. A special thanks to Ms. Tang Zo Ee, Mr. Danny Chin and Mr. Ong Ching Yeh for all the useful suggestions and necessary information in order for me to complete this research.

ABSTRACT

The aim of this research was to study the optimum conditions to produce biodiesel from palm fatty acid distillate (PFAD). In order to improve the esterification reaction acidic carbon catalyst from corncob waste was synthesised. The catalyst synthesised was analysed using various analytical methods, which include Fourier Transform-infrared Spectroscopy (FTIR), Temperature Programmed Reduction (TPR), Scanning Electron Microscopy-Energy Dispersive X-ray (SEM-EDX), and X-ray Dispersion (XRD). Characterisation of the carbon catalyst by FTIR analysis was done based on the presence of characteristics peaks of important functional group, such as $-SO_3H$ and $S = O$. On the other hand, it was determined in TPR analysis that 661 °C was the most ideal reduction temperature with 1300 µmol/g of hydrogen gas was consumed. Based on the results of SEM, it was observed that the morphology of corncob waste was distorted during chemical activation and calcination step. However, no difference in morphology was observed between activated carbon and carbon catalyst. The increment in sulphur content in carbon catalyst through EDX analysis proved that, the active phase, sulphonic group ($-SO_3H$) was successfully attached onto the activated carbon. It was also discovered that corncob waste, activated carbon and carbon catalyst were amorphous in nature after conducting XRD analysis. To determine the optimum conditions for esterification, Design-Expert® software coupled with Response Surface Methodology (RSM) was adopted. Central Composite Design (CCD) was the strategy selected to optimise the biodiesel yield. Parameters including reaction temperature (60 °C, 70 °C, 80 °C, 90 °C and 100 °C), time (4 h, 5 h, 6 h, 7 h and 8 h), catalyst loading (7.5 wt%, 9.0 wt%, 10.5 wt%, 12.0 wt% and 13.5 wt%), and methanol-to-PFAD molar ratio (17.5:1, 20:1, 22.5:1, 25:1 and 27.5:1) were studied in this research. After the analysis, the optimum conditions for esterification were 87.56 °C, 7 h, 9.023 wt% and 24.19:1 with the estimated biodiesel yield of 70.11 %.

TABLE OF CONTENTS

LIST OF TABLES

LIST OF FIGURES

LIST OF SYMBOLS / ABBREVIATIONS

4-BDS	4-benzenediazoniumsulphonate
ANOVA	Analysis of Variance
BB	Box-Behnken Design
CCD	Central Composite Design
C. V.	Coefficient of Variance
FAME	Fatty Acid Methyl Ester
FFA	Free Fatty Acid
FTIR	Fourier-Transform Infrared Spectroscopy
GC	Gas Chromatography
GDP	Gross Domestic Product
OVAT	One-variable-at-a-time
PFAD	Palm Fatty Acid Distillate
RSM	Response Surface Methodology
TGA	Thermogravimetric Analysis
TPR	Temperature Programmed Reduction
SEM-EDX	Scanning Electron Microscopy-Energy Dispersive X-ray
XRD	X-ray Diffraction

LIST OF APPENDICES

CHAPTER 1

INTRODUCTION

1.1   General Introduction

According to the U.S. Energy Information Administration (2017), the energy consumed by the entire world in 2015 was around 575 quadrillion btu and this figure was expected to increase in the future as a result of increasing population, urbanisation and growth of the economy.

With the urbanisation of developing countries, a movement from the agricultural sector to industrial sector can be clearly observed (Bakirtas and Akpolat, 2018). While the movement of sector provides positive impacts to these countries in many ways, such as improving the economy of the country and providing more job opportunities, it will also increase the total energy demand and eventually more resources are consumed to satisfy the demand. As the main energy supplier in the modern world today, if the usage of fossil fuel is not being controlled, the depletion of these sources with the aftermath of global energy crisis will be inevitable.

To decelerate and preventing this occurrence, great efforts have been made to search for other potential alternatives that are not only inexhaustible but also environmental friendly. According to Hua, Oliphant and Hu (2016), an investment of USD 244 billion had been made in 2012 for research on renewable energy. Besides, renewable energy policies had also been drafted by at least 144 countries in 2013 in light of the current situation.

One of the potential renewable energies to be focused is biodiesel. Fatty acid methyl esters (FAME) or simply known as, biodiesel, is a product of animal fat or vegetable oil and methanol after undergoing transesterification process. Due to its possibility to replace fossil fuel as the main fuel, countless research have been made to develop it further.

1.2 Relationship between Economic Growth, Demand of Fossil Fuel-based Energy and the Aftermaths

As mentioned in Section 1.1, the energy demand is also directly affected by the growth of the economy. Taking Malaysia as an example, in order for Malaysia to become a fully developed country, the establishment of a competitive economy is necessary. According to the World Bank (2017), the gross domestic product (GDP) in Malaysia is expected to progress well. Since, the economy of a country is a function of total energy consumption, the energy consumed is also shown to be in an upward trend. This claim was supported by Bujang, Bern and Brumm (2016) and they opined that based on the current growth of economy, the primary energy demand in Malaysia by 2030 was estimated to rise to 146.7 Mtoe.

Apart from that, the energy required by vehicles is supplied by fossil fuel. With the increase of demand for energy from transport sector, it can be inferred that the annual usage of fossil fuel will only continue to grow unless it is replaced by suitable alternatives. A research was conducted by Muda and Tey (2012) on the depletion time of fossil fuels in Malaysia. The authors had applied mathematical models to estimate the depreciation time of fossil fuels, which is shown in Figure 1.1. Based on the results found, it was concluded that petroleum will deplete by 2026, while the natural gas reserves can still withstand for at least another 52 years. Meanwhile, the coal in Malaysia will be exhausted within 64 years. Unless actions are taken, it is anticipated that fossil fuel will deplete within this century, which could potentially cause serious consequences.
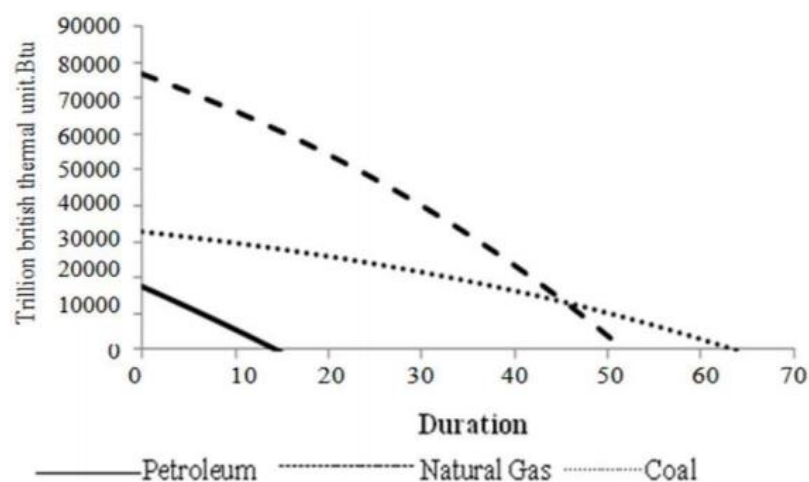
Figure 1.1: The Depreciation Time of Each Fossil Fuels based on the Modified Klass Model (Muda and Tey, 2012)

Furthermore, vehicles that use petrol and diesel often emit substances that pollute the surrounding air, which mainly consist of carbon dioxide, CO_2, and carbon monoxide, CO (Hajjari, et al., 2017). These substances are generated due to incomplete combustion in the engine of the vehicles. This will only worsen the current situation of global warming and causes climate change around the world.

A research was done by Specht, Redemann and Lorenz (2016) to further understand the effect of CO_2 concentration towards global warming. According to the findings from complex mathematical models applied, the relationship between the concentration of CO_2 and the temperature of the Earth surface was determined as shown in Figure 1.2. From the figure, it is observed that by doubling the concentration of CO_2, the increment of temperature is 0.41 °C or 0.41 K. Therefore, the effect of CO_2 emission should not be taken lightly due to its effects on the global temperature.
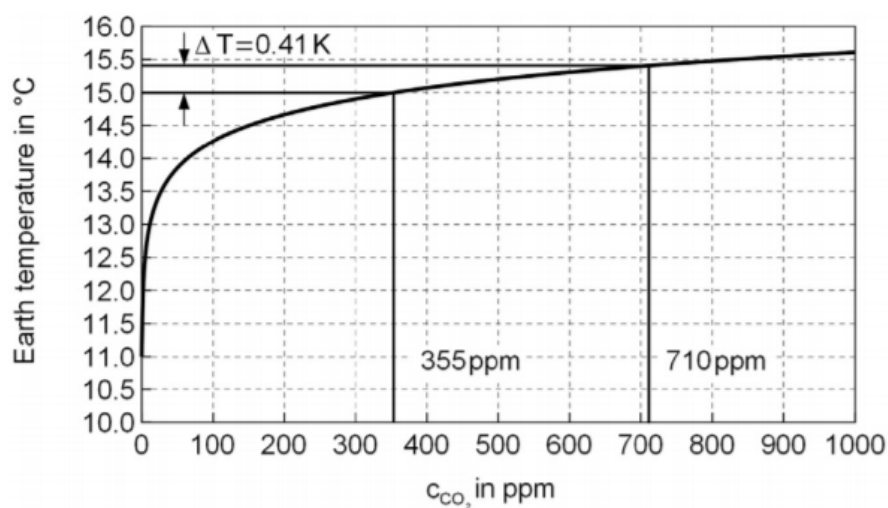
Figure 1.2: The Relationship between Concentration of Carbon Dioxide and Temperature of Earth Surface (Specht, Redemann and Lorenz, 2016)

However, according to a report by PBL Netherlands Environmental Assessment Agency in 2017, global emission of CO_2 had remained constant from 2014 to 2016 due to the decrease of emission mostly from potential superpower countries, which is shown in Table 1.1. It also stated that the emission of CO_2 by Malaysia in 2016 had a slight increment. However, no exact figures is mentioned in the report. As described by Ritter (2016), the reason for global carbon dioxide emission to remain in its position for three years in a row is mainly because of the reduction of coal usage in

the United States and China. However, it is too early to presume that the carbon dioxide emission had reached the peak and further observations are needed.

Table 1.1: Percent Decrement of CO_2 Emission in 2016 by Various Countries (PBL Netherlands Environmental Assessment Agency, 2017)

Country	Status	Percent Decrement of CO_2 Emission in 2016 (%)
United States	Superpower Country	2.0
Russian Federation	Potential Superpower Country	2.1
Brazil	Potential Superpower Country	6.1
China	Potential Superpower Country	0.3
United Kingdom	None	6.4

1.3   Biodiesel as an Alternative

However, the reduction of carbon dioxide emission mentioned in Section 1.2 is only under industrial sector. For transport sector to reduce the emission of harmful exhaust gases, particularly carbon dioxide, the most promising solution is by using biodiesel as the fuel of vehicles.

Apparently, the first vegetable oil being used as diesel is peanut oil. It was created by Rudolf Diesel. He was the inventor of diesel engine itself and the main purpose for him and the French government to do so, was to allow the African natives to be able to produce their own energy as petroleum was still unavailable in remote countries (Knothe and Razon, 2017). Today, biodiesel has been accepted globally as the substitute energy source for vehicles due to its outstanding properties.

Although there are factors that needs consideration before concluding that the performance of biodiesel is better than the current diesel or petrol, but only a few will be discussed. These factors are listed below (Hasan and Rahman, 2017).

  (i) Kinematic viscosity.

  (ii) Density.

  (iii) Cetane number.

  (iv) Calorific value.

  (v) Flashpoint.

According to the Hasan and Rahman (2017), both kinematic viscosity and density of the fuel affects the atomisation of the fuel. It is advised that fuel should have a lower kinematic viscosity. This is because, viscous fuel will reduce the effectiveness of the atomisation. It was explained by Hanna and Zoughaib (2017) that a higher kinematic viscosity reduced the degree of disintegration of the liquid fuel and, thus, reducing the effectiveness of atomisation. On the other hand, fuel with higher density will have a greater energy concentration of fuel as the high-density fuel is richer with contents than low-density fuel. However, a higher density fuel will also increase the kinematic viscosity of the fuel, hence, optimisation between these properties are required.

Cetane number is a dimensionless variable that determines the ignition properties of a fuel (Knothe and Razon, 2017). It is stated that higher cetane number will have a shorter ignition delay. The reason for shorter ignition delay is related to the origin of biodiesel. It is known that biodiesel is mainly produced from vegetable oil or animal fat, which consists of long fatty acid chains, without any the presence of branching and large aromatic group. Due to the lack of this property in diesel and petrol, therefore, diesel and petrol have a lower cetane number than biodiesel. This is also supported by Hajjari, et al. (2017) as it is claimed that biodiesel has a higher cetane number than the fuel used by vehicles today. In addition, a fuel with higher cetane number allows the engine to perform smoothly with lower noise (Mahmudul, et al., 2017).

Besides cetane number, calorific value is also another important property that determines the fuel performance. Mahmudul, et al. (2017) mentioned that the fuel itself needs to have a high calorific value to ensure a better engine performance. This is due to the fact that fuel with high calorific value increases the amount of energy released during fuel combustion. However, it was also found out that the calorific value of biodiesel of different sources is lower than diesel and petrol.

Another advantage of biodiesel is its flash point property. Ateeq (2015) explained that flash point is the lowest temperature whereby, the mixture of vaporised fuel and air is able to ignite spontaneously. This property is vital due to safety purposes, especially during transport and storage. As compared to ordinary fuels, biodiesel tends to have a higher flash point. This is also supported by Hasan and Rahman (2017). The authors also added that generally biodiesel has a flash point 50 % higher than diesel.

Apart from better fuel performance by biodiesel, biodiesel is said to be more environmental friendly than the regular fuels used today. This is due to the fact that the concentration of carbon monoxide, CO, carbon dioxide, CO_2, and other harmful gases found in the exhaust gas emitted after combustion are lower (Thangaraja, Anand and Mehta, 2016). Since, biodiesel came from animal fats or plant oils, it is biodegradable. Unlike petrol and diesel, the overall cost of biodiesel is lower because offshore mining is no longer required. Furthermore, the source of biodiesel is cheaper and easily available (Mahmudul, et al., 2017).

Nonetheless, it is reported that biodiesel emits high amount of nitrogen oxides, NO_x, which is responsible for causing acid rains (Thangaraja, Anand and Mehta, 2016). Despite that biodiesel is said to be environmental friendly, it could also cause environmental issues as well. Hasan and Rahman (2017) explained that more land will be required for plantation purpose. This could cause more deforestation, which damages the environment rather than improving the environment. Other than that, unless non-edible feedstocks are used, food shortage will happen as these feedstocks are sold at a higher price to produce biodiesel (Hajjari, et al., 2017) instead of being consumed as food.

1.4   Problem Statement

Ever since, the discovery of alternatives for fossil fuels, numerous research were made to further improve the yield of biodiesel by developing suitable catalysts or any other means. However, not many have actually attempted to optimise the yield of biodiesel using statistical tools such as Response Surface Methodology (RSM), which indirectly contributes to the increase of wastage of the raw materials as the highest possible yield of biodiesel has not been achieved from the feedstock. Hence, it is expected that through optimisation of the esterification process, the reduction of wastage is possible.

Other than reducing the amount of waste produced, Fong (2016) mentioned that the production cost of biodiesel in the market today was currently higher than diesel and petrol. In order to allow the production cost to be competitive enough, one of the solutions is to produce more biodiesel with the same amount of feedstocks used. This can achieved by optimising the biodiesel yield. By doing so, it could reduce the overall cost, especially after it is scaled up.

It is common in experiments that only a variable is manipulated while fixing the rest to determine its relationship with the responding variable. However, in this research, multiple variables are manipulated and analysed at the same time to determine the effects on the yield of biodiesel. This complicates the analysis as the effect of multiple factors could lead to different results.

The usage of transition metal as heterogeneous catalyst is common due to its ability to initiate a reaction between the reactants. Nonetheless, extensive usage of transition metals as catalyst aided in the boost of metal mining, which causes environmental damage. Moreover, unlike organic substances, transition metals are not biodegradable. This contributed to the increment of wastes produced. With the recent events to reduce the damage of human activities towards the environment, the use of environmental friendly catalyst such as the carbon-based catalyst received more attention. However, the application of carbon-based catalyst to improve a reaction is still considered to be new. Therefore, more research is needed to be done to test its capability.

1.5 Aims and Objectives

The purpose of this research is to optimise the biodiesel yield produced from palm fatty acid distillate with the following objectives that need to be achieved.

(i) To synthesise acidic catalyst from corncob waste for biodiesel production.

(ii) To characterise the synthesised catalyst for biodiesel production using FTIR, SEM-EDX, TPR and XRD.

(iii) To analyse the relationship between the reaction time, temperature, catalyst loading, and oil-to-methanol molar ratio on biodiesel production using RSM.

1.6 Scope and Limitation of the Study

This study mainly covers on the identification of the most optimised reaction conditions to undergo esterification process. Factors, which include reaction time, temperature, catalyst loading, and oil-to-methanol molar ratio will first be determined through literature review. All these factors will then be changed and the yield of biodiesel is recorded for every attempt of esterification. The results are analysed using RSM to determine the most optimised conditions for the reaction. To verify the results,

all the factors will be adjusted as according to suggested results by RSM and the entire reaction is repeated.

There are also limitations for this study as well. As a result of the manipulation of multiple variables at a time, many repetitions of experiment are required. However, due to time constraint, only a handful of results can only be obtained for analysis. Besides, due to the availability of raw materials are limited, which further restricts the number of attempts for data collection. It is also possible that the optimum point for the esterification reaction is located outside the range of conditions studied.

1.7   Contribution of the Study

Upon successful attempt to optimise the yield of biodiesel, higher yield of biodiesel is produced. Leftovers of unused oil can also be reduced because of the improvement of the yield of biodiesel. It may be insignificant in laboratory scale. However, by scaling it up to industrial level, this could not only reduce the overall wastes produced, it could also potentially reduce the cost of waste treatment and disposal. With the increase of biodiesel produced, it could also reduce the cost of biodiesel in the market, making it affordable. This could also promote the use of biodiesel as an alternative for fossil fuel and also research to further improve the yield or performance of biodiesel.

1.8   Outline of the Report

A general information on the effects of economic growth towards energy demand and consumed as well as the damage to the environment along with the introduction on biodiesel are explained in Chapter 1. In Chapter 2, different facts and results obtained from various sources that is related to this topic are reviewed. Apart from that, useful information and recommendations will be taken note in the report before conducting the research. The overall procedure of the research will be shown in Chapter 3. The results obtained based on the different data will then be analysed in Chapter 4. These results will also be compared with other sources referred. In Chapter 5, a conclusion on the research will be made. Suitable recommendations for future reference are also provided in order to improve the results obtained.

CHAPTER 2

LITERATURE REVIEW

2.1 Methods to Produce Biodiesel

Generally, there are different methods available today to produce biodiesel. This includes micro-emulsification, thermal cracking process, esterification and transesterification, which will be explained in this section (Aalam and Saravanan, 2015).

2.1.1 Micro-emulsification

Micro-emulsion was described by Arpornpong, et al. (2014) as isotropic, and thermodynamically stable mixture of liquids. It is usually produced by simply mixing water, oil, surfactant and co-surfactant. According to Rajalingam, et al. (2016), by producing biodiesel through this method, problems related to the viscosity of the biodiesel, which is mentioned in section 1.3 can be solved. Furthermore, the usage of alkyl nitrate as an additive will improve the cetane number of biodiesel. However, the authors also mentioned that biodiesels produced through micro-emulsification will have issues that lower the engine performance. Some of the issues are incomplete combustion and deposition of carbon residues in the engine.

2.1.2 Thermal Cracking

Thermal cracking or pyrolysis, is a method used to breakdown large and long hydrocarbon molecules into smaller molecules by subjecting the molecules to extreme heat and pressure (Alsobaai, 2013). This method is considered advantageous because of its ability to process feedstocks with low quality. However, it is stated by Avhad and Marchetti (2015) that the control of selectivity for desired products is one of the issues faced by this method. In general, there are two stages of thermal cracking. Parvizsedghy, Sadrameli and Towfighi Darian (2015) explained that, the first stage involves the decomposition of triglyceride molecules, which, causes the formation of acids by breaking the C–O bonds. The acids produced will then be broken down into various hydrocarbons in the second stage which share the similar fuel properties as the ordinary diesels.

2.1.3   Esterification and Transesterification

One of the widely used method for producing biodiesel is through esterification. As shown in the Figure 2.1, esters are typically formed by reacting carboxylic acid and alcohol. This reaction is usually slow and reversible (Clark, 2015).
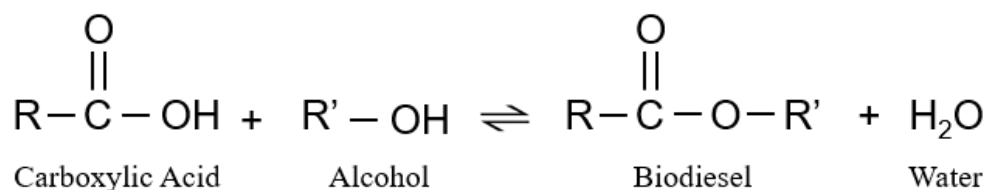
Figure 2.1: Illustration of Esterification Process

Similar to esterification process, it requires alcohol notably, methanol to produce biodiesel. But, there is a difference between esterification and transesterification process. Instead of using acids, esters are used in transesterification to react with alcohol to yield biodiesel. An illustration is shown in Figure 2.2. Again, without the use of any catalyst, this process is slow and reversible (Silva, et al., 2014).
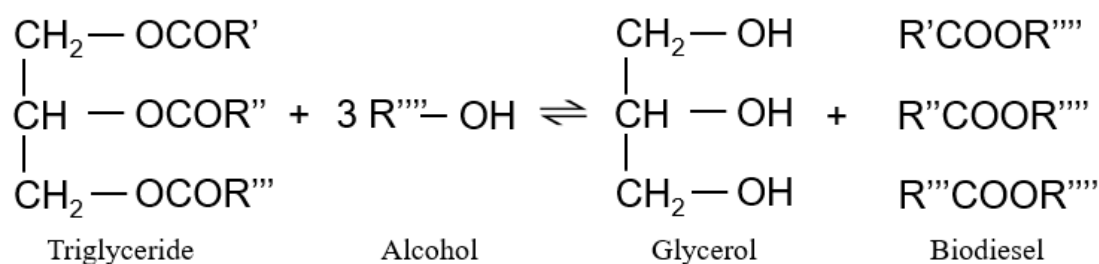
Figure 2.2: Illustration of Transesterification of Triglyceride

Thus, to improve the yield of both methods, the use of catalyst is highly suggested. Normally, the catalysts selected in industries are basic in nature. This is due to the fact that, base catalysts are not as corrosive as its acidic counterpart. Moreover, base catalyst improves the reaction rate greatly, which resulted in higher yield within a given time frame. However, saponification process may happen due to the reaction between the free fatty acids (FFA) in the feedstock and base catalyst (Ejikeme, et al., 2010).

Hence, acid catalyst is being developed to counter this problem. According to Lemoine and Thompson (2014), acid catalyst prevents the occurrence of saponification process, which could improve the yield of biodiesel. In addition, it also

reduces the overall operation cost as the treatment for separating soap from biodiesel is not required.

2.2   Review on Reaction Conditions of Esterification

As mentioned in Section 2.1.3, the process to produce biodiesel through esterification is rather slow with lower yield due to the possibility of backward reaction. Therefore, numerous research had been done in recent years to improve this process. Typically, conditions that have pronounce effect to the final result are experimented to achieve the objective. In this case, the objective is to obtain the highest yield of biodiesel with the following variables shown in Table 2.1.

Table 2.1: List of Variables and Objective

Variables	Objective
Reaction temperature	
Time	
Methanol-to-oil ratio	Biodiesel yield
Catalyst loading	

There are different approaches to analyse the effects of variables change to the objective. One of the most commonly known method is one-variable-at-a-time (OVAT). As the name implies, this method works by altering only one of the variables, while fixing the rest as constants. It is normally used to determine the effects and significance of a variable towards a certain parameter. With respect to this research, the significance of reaction temperature, time, methanol-to-oil ratio and catalyst loading are discussed.

According to Theam, et al. (2015), one of the most important variable that needs to be considered is the temperature of the reaction. Reaction activity of the molecules to perform esterification reaction depends on the temperature it is subjected to. It was also stated by Hidayat, et al. (2015) that other than the improvement of reaction rate at higher temperature, the mass transfer limitation between the reactants and catalyst was also improved, which allow higher biodiesel yield as well. Thus, it is inferred that a higher amount of product is generated from the reaction, if the reaction is performed at a higher temperature.

The theory mentioned was further supported by the results obtained from the Theam, et al. (2015). In the research, the esterification process with the use of palm fatty acid distillate (PFAD) was conducted within the range of 50 °C and 90 °C while the rest of the parameters were fixed at 90 min, catalyst loading of 2 wt% and the ratio of 10:1. As seen in Figure 2.3, the conversion of PFAD to biodiesel increases steadily as the subjected temperature increases until it reaches the peak at 70 °C. The reason for the constant conversion after 70 °C is mainly because of the evaporation of methanol from the mixture, which affects the molar ratio between methanol and PFAD. Hence, due to the contribution of molar ratio between methanol and PFAD to the biodiesel yield, it can be concluded that any decrease of methanol content will have negative impact on the biodiesel yield.
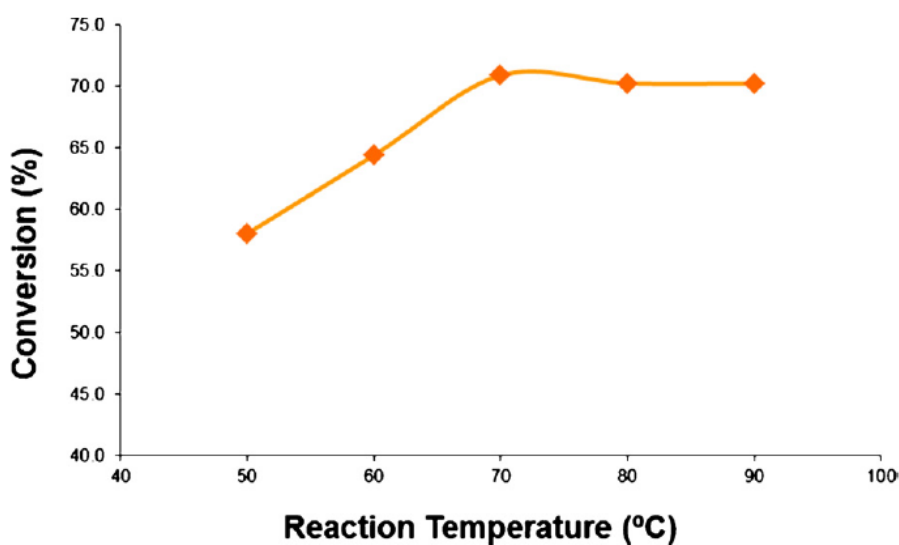
Figure 2.3: Effect of Temperature on Conversion of PFAD (Theam, et al., 2015)

The next variable that will be explained is the reaction time for esterification process. Hosseini, Janaun and Choong (2015) claimed that longer reaction time is able to improve biodiesel yield. This was because more time is provided for the reaction to proceed. In Figure 2.4, at 80 °C, catalyst loading of 2.5 wt%, and molar ratio of 15:1, the conversion of PFAD continues to increase from 60 min to 240 min. The conversion then remains constant at time after 240 min. On a side note, the acid value shown in Figure 2.4 indicates the difference in amount of PFAD at different time during the esterification process. Similar to the conversion of PFAD, the changes of PFAD remains constant at time after 240 min.
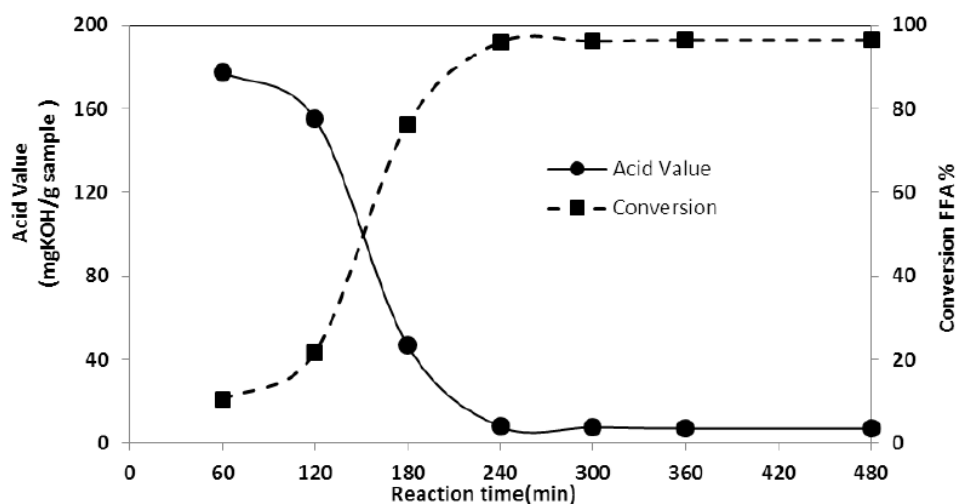
Figure 2.4: Effect of Reaction Time on PFAD Conversion and Acid Value (Hosseini, Janaun and Choong, 2015)

However, in a research by Olutoye, et al. (2014), instead of remaining constant, the biodiesel content shown in Figure 2.5, tends to decrease after a certain amount of time regardless of the use of different catalysts. This is primarily due to the Le Chatelier's principle. According to this principle, in a reversible reaction, if the amount of products strongly outweigh the amount of reactants, the position of equilibrium will shift to the left in order to reach equilibrium (Clark, 2013). In this case, the authors stated that, as time goes by, the amount of water produced along with biodiesel will also increase. This causes the occurrence of hydrolysis of biodiesel, whereby the backward reaction took place instead. This ultimately reduced the yield of biodiesel.
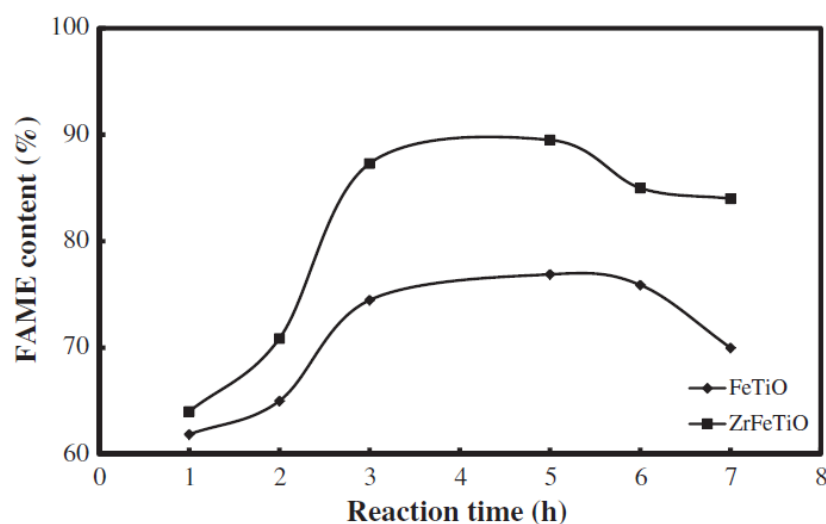
Figure 2.5: Effect of Time and Catalyst Used on FAME Production (Olutoye, et al., 2014)

As mentioned previously, the molar ratio between methanol and PFAD is another crucial factor that will affect the yield of biodiesel. Again, due to the fact that the esterification reaction is reversible, thus, higher amount of methanol is needed to minimise the occurrence of backward reaction. With the addition of excess methanol, an imbalance in the reaction will occur in order to allow a system to be in equilibrium. However, for a system to reach equilibrium, the amount of reactants should always be equal to the amount of products. Hence, in an attempt for the system to be equilibrium, more biodiesel is produced.

This theory is backed by a research of Akinfalabi, et al. (2017). The authors conducted the research by varying the molar ratio of the two substances from 3:1 to 13:1, while fixing the temperature at 60 °C, time at 2 h and catalyst loading of 2 wt%. The findings presented in Figure 2.6 showed that the conversion of PFAD initially increased until it reached the peak at molar ratio of 9:1 before decreased slightly at higher molar ratio. The cause of the decrement is also due to Le Chatelier's principle, which was explained above.
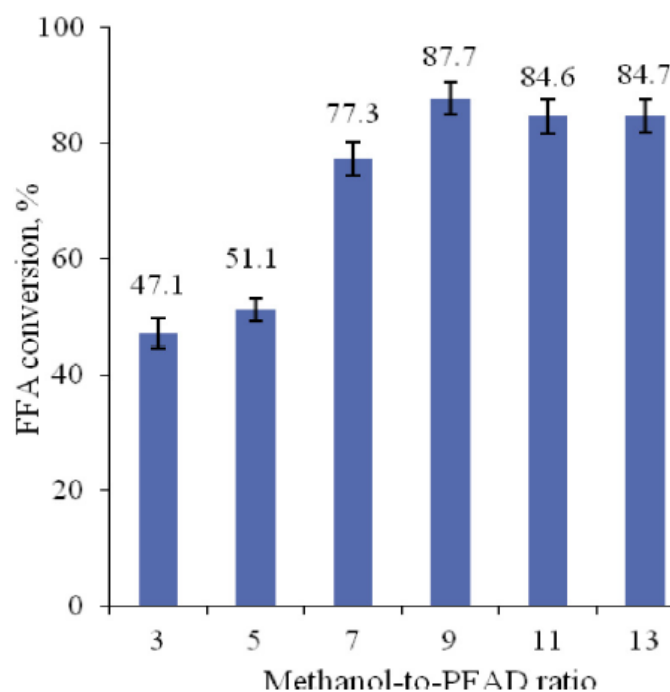
Figure 2.6: Effect of Molar Ratio on PFAD Conversion (Akinfalabi, et al., 2017)

Catalyst loading is another important factor should be considered. Farnetti, Monte and Kašpar (2009) stated that catalyst was defined as a substance used to improve the reaction rate as well as the likelihood for the reaction to happen without

being consumed. To further improve the reaction rate, Hidayat, et al. (2015) suggested to increase catalyst loading, because the increment will increase the number of active sites available in catalysts for the reaction to proceed. In a study by Lokman, et al. (2015), it was found out that the increase of catalyst loading from 0.5 wt% to 2.5 wt% at 70 °C, time at 2 h, and molar ratio of 10:1 improved the yield tremendously. However, as shown in Figure 2.7, a further increase of catalyst loading from 2.5 wt % did not show any improvement as it was said that the mass transfer rate had reached its optimum point.
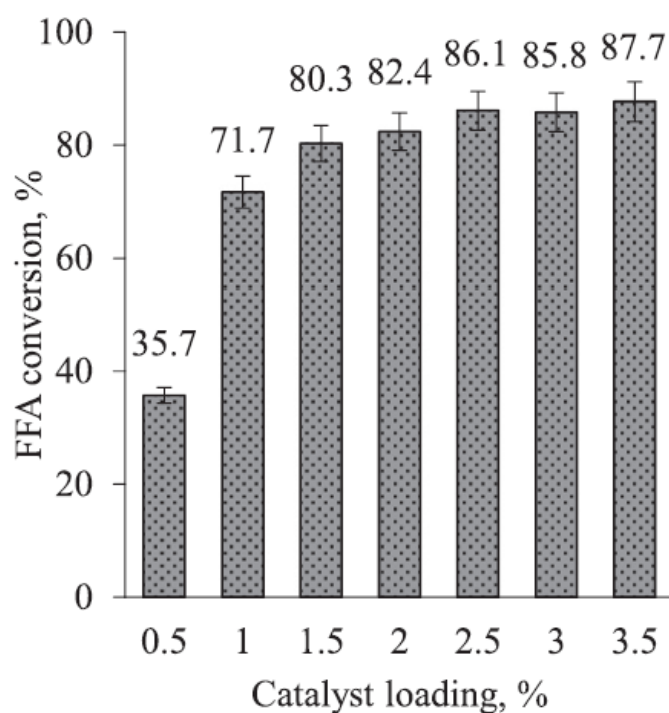
Figure 2.7: Effect of Catalyst Loading on PFAD Conversion (Lokman, et al., 2015)

In summary, all the parameters discussed above have apparent effects on the yield of biodiesel. A compilation of reaction conditions used by various sources is shown in Table 2.2. With the OVAT approach, the highest point of biodiesel yield of each independent parameters are obtainable. However, Brown, Tauler and Walczak (2009) mentioned that OVAT failed to consider the interaction between these parameters, which could affect the reaction in any possible ways. Furthermore, high number of repetitions were required in order to achieve the optimum point.

Table 2.2: Compilation of Various Reaction Conditions Used for Esterification of PFAD

| Feedstock | Catalyst Used | Range of Reaction Conditions | | | | References |
		Temperature (°C)	Time (min)	Methanol-to-oil Ratio	Catalyst Loading (wt%)	
Palm Fatty Acid Distillate (PFAD)	Solid oxide acid (ZrFeTiO, ZrFeO, FeTiO)	110 – 200	60 – 420	2:1 to 6:1	1 – 6	Olutoye, et al. (2014)
	Chromium-tungsten (CrW$_2$O$_2$, CrWO$_2$)	110 – 170	60 – 360	1:1 to 6:1	1 – 6	Wan, Lim and Hameed (2015)
	Sulphonated coconut shell biochar	40 – 60	240	6:1 to 12:1	1 – 7	Hidayat, et al. (2015)
	Sulphonated-glucose derived solid acid	65 – 90	60 – 360	1:1 to 18:1	0.5 – 3.5	Lokman, et al. (2015)

Table 2.2 (Continued)

Feedstock	Catalyst Used	Range of Reaction Conditions				References
		Temperature (°C)	Time (min)	Methanol-to-oil Ratio	Catalyst Loading (wt%)	
Palm Fatty Acid Distillate (PFAD)	Sucrose-derived solid acid	50 – 90	30 – 180	2.5:1 to 20:1	0.5 – 6	Theam, et al. (2015)
	Aliminum alginate solid acid	50 – 90	60 – 300	5:1 to 25:1	1 – 20	Cheryl-Low, Theam and Lee (2015)
	Sulphonated palm seed cake	55 – 75	60 – 360	3:1 to 13:1	0.5 – 3.5	Akinfalabi, et al. (2017)
	Sugar catalyst supported by honeycomb monolith	80	60 – 480	1:1 to 25:1	1.25 – 5	Hosseini, Janaun and Choong (2015)
	Sulphonated $ZnAl_2O_4$	80 – 200	15 – 150	3:1 to 18:1	0.5 – 3	Soltani, et al. (2016)

2.3   Carbon-based Catalyst for Biodiesel Production

It was established previously that the usage of catalyst is necessary as a result of problems faced in esterification reaction to produce biodiesel. There are developed catalysts today that are currently being used commercially. Several examples are potassium hydroxide, sulphuric acid, tungsten oxides, sulphonated zirconia, and Nafion resins (Talha and Sulaiman, 2016).

However, Narasimharao, Lee and Wilson (2007) stated that homogeneous catalyst such as sodium hydroxide and sulphuric acid were hard to be separated from the processed mixture. Issues with corrosion from sulphuric acid, and soap formation due to the use of sodium hydroxide were discussed. Thus, it can be concluded that homogeneous catalyst are not really beneficial in commercial processes as it will only increase the overall operating and maintenance cost. Moreover, catalysts that contain transition metals like tungsten oxide and sulphonated zirconia are normally expensive (Ranu, et al., 2015).

Hence, carbon-based catalyst were developed to replace the commercial catalysts as it is cheaper, easily available in huge amount, and more importantly it is chemically inert (Konwar, et al., 2015). Nonetheless, the carbon source is not functional until it undergoes carbon activation and sulphonation of the activated carbon.

2.3.1   Carbon Activation

Carbons can be activated via two methods, physical activation and chemical activation. Dizbay-Onat, Vaidya and Lungu (2017) explained that in physical activation, high carbon content material was first placed in an inert environment by limiting the concentration of oxygen in the environment. This was achieved by purging nitrogen or other inert gases. Then, to enlarge the pores, the environment was purged with carbon dioxide or steam with the temperature set between 800 °C and 1000 °C. Konwar, Boro and Deka (2013) stated that water and non-carbon substances were removed entirely from the subject during this process, leaving only porous carbon after the thermal process.

In chemical activation, activating agents such as phosphoric acid, and sodium hydroxide are normally used before the subject is carbonised (Dizbay-Onat, Vaidya and Lungu, 2017). The authors also claimed that chemical activation is more advantageous than physical activation as it is able to retain higher amount of carbon.

Besides, it consumes lesser energy as compared to physical activation. There are various methods to activate carbons by chemical activation. To increase the contact area between the subject and the activating agent, different mixing methods as shown in Table 2.3 were tested by Bagheri and Abedi (2009). It was concluded that impregnation method is the most suitable method. This is because as compared to the other methods a better distribution of activating agents were found in the carbonaceous subject, which ultimately produces porous subject with higher surface area.

Table 2.3: Chemical Activation of Carbonaceous Subject (Bagheri and Abedi, 2009)

Method	Procedure
Mixing-filtration method	The grinded subject is mixed with activating agent for an hour before it is filtered, dried and activated.
Solid-solid mixing	Dried subject and activating agent are mixed and activated directly.
Impregnation method	Dried subject is soaked in saturated activating agent and dried overnight.

2.3.2 Sulphonation of Activated Carbon

The next step to produce carbon-based catalyst is to functionalise the activated carbon through sulphonation. By undergoing this step, sulphonate groups are attached on the prepared activated carbon. An illustration of sulphonation process is shown in Figure 2.8.
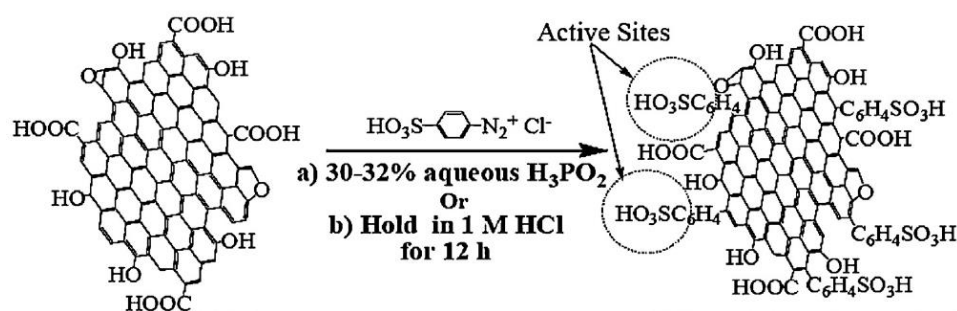
Figure 2.8: Sulfonation of activated carbon (Konwar, et al., 2013)

Malins, et al. (2015) stated that there were two ways to functionalise the activated carbons. The first method is direct sulphonation. In this method, sulphonation is simply done by mixing sulphuric acid with the activated subject at a certain temperature. The product is then filtered, washed and dried in vacuum overnight (Konwar, et al. 2015).

The second method stated by Malins, et al. (2015) was sulphonation by arylation of 4-benzenediazoniumsulphonate (4-BDS). This method is slightly more complicated as it involves more steps than the previous method. For the sulphonation process to be complete, sulphonated aryl groups from 4-BDS will need to be attached covalently to the activated subject. This can be achieved by mixing the activated carbons, 4-BDS and reducing agent, typically, hypophosphorous acid together.

Despite that both methods are feasible, however, it was claimed by Konwar, et al. (2013) that sulphonation by 4-BDS method was more efficient than direct sulphonation due to the following reasons.

(i)   Higher degree of sulphonation.

(ii)   Preservation of the structure and morphology of the carbonaceous subject as a result of the use of benign conditions.

(iii)   Enhanced resusability of the catalyst produced.

(iv)   Better capability to sulphonate more complex and rigid carbon structures.

This was further supported by a research from Konwar, et al. (2015). In the research, activated *M. ferrea L.* seed, denoted with 'MAC' was subjected to the two sulphonation methods mentioned, which are denoted as 'MACS' and 'MACH$_2$SO$_4$'. For clarification purposes, 'MACS' and 'MACH$_2$SO$_4$' represent sulphonation by 4-BDS, and sulphuric acid respectively. The result obtained is shown in Table 2.4. It is observed that, the –SO$_3$H density and total acid density of MACS was the highest among the rest. This shows that more acids were attached successfully by sulphonation of 4-BDS than direct sulphonation.

Table 2.4: Comparison of the Properties of Catalyst (Konwar, et al., 2015)

Catalyst	Specific Surface Area (m^2/g)	Pore Volume (cm^3/g)	$-SO_3H$ Density (mmol/g)	Total Acid Density $(mmolH^+/g)$
MAC	786	0.63	–	1.91
MACS	468	0.39	0.75	3.01
$MACH_2SO_4$	690	0.61	0.30	2.01

2.4 Optimisation of Biodiesel Production

It is mentioned before that although OVAT approach is a useful technique to determine the significance of a factor. Unless the factor is a prominent one, which greatly outweighs the minor factors, it is rare that a parameter is only affected by a single factor. In fact, the consideration of a factor one at a time will only negatively affect the reliability of the overall results obtained.

2.4.1 Response Surface Methodology (RSM)

The main goal of optimisation is to get the highest possible results according to the factors considered. Employment of RSM is required not only to achieve the goal, but also to identify and analyse the interaction and effects between the factors. It also provides opportunities to further improve the research as well. One of the most renowned method is Response Surface Methodology (RSM).

There are different design strategies available to fit the model of different experiments. Alvarez (2000) explained that another reason for considering the choice of these strategies was because different strategies apply different points in the experiment to determine the optimum result of the experiment. Several examples are Central Composite Design (CCD), and Box-Behnken Design (BB). Normally, BB is used in experiments involving only three factors (Stat-Ease, 2017). However, it is possible for CCD to consider more than three factors. Therefore, the choice of strategy depends on the nature of the experiment.

RSM applies mathematical and statistical techniques to analyse problems that consist multiple independent variables with the objective to optimise the responses (Bradley, 2007). This method is widely used today due to its accuracy and efficiency in predicting the result based on the data inputted. Nonetheless, Cassettari, et al. (2013)

stated that RSM still face problems with consistency, whereby, the actual values were not accurately the same as the predicted values.

2.4.2 Optimisation of Biodiesel Production

The individual effect of temperature, reaction time, methanol-to-oil ratio, and catalyst loading on the biodiesel yield as well as the optimal point of each factor were already discussed Section 2.2. However, a lower biodiesel yield may be possible if the optimal point of each individual factor is adapted as the interaction between these factors are not considered. A summary of research done on the optimisation of esterification reaction is tabulated in Table 2.5.

For instance, methanol has a boiling point of 64.7 °C at 1 atm. With the usage of higher temperature, methanol will start to evaporate, which affects the methanol-to-oil ratio and it will eventually affect the yield. Longer reaction time allows the reaction to exceed the equilibrium. This creates an opportunity for backward reaction to occur, which will reduce the final yield. Hence, to determine the actual optimal point for the reaction, consideration of the interaction between factors are required.

In a research by Ajala, et al. (2016), an increase in temperature improved the biodiesel yield as a result of increase in activity and collision at a molecular level. However, similar issue occurred when the temperature was increased beyond the boiling point of methanol. The reduction in methanol because of evaporation will contribute to the declination of biodiesel yield as backward reaction occurs more easily. A clearer picture is shown in Figure 2.9, where ESB and SBD stand for esterified shear butter and shear biodiesel respectively.
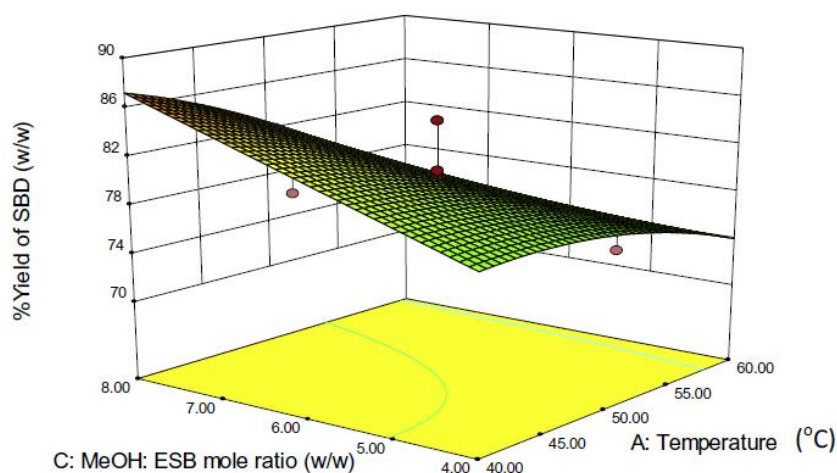
Figure 2.9: Effect of Temperature and Methanol-to-esterified Shear Butter on Biodiesel Yield (Ajala, et al., 2016)

As shown in Figure 2.10, it was observed by Mohamad, et al. (2016) that longer reaction time was not beneficial in any way. This is due to the fact that longer reaction time allows backward reaction to occur despite that it occurs slowly (Ezekannagha, Ude and Onukwuli, 2017). Furthermore, due to the presence of three phase systems between oil, methanol and catalyst, the reaction rate will take place comparably slower. A further increase of catalyst loading will only negatively affect the reaction rate and biodiesel yield. Thus, a sufficient amount of catalyst loading will be enough to reduce the time required to reach the highest possible yield.
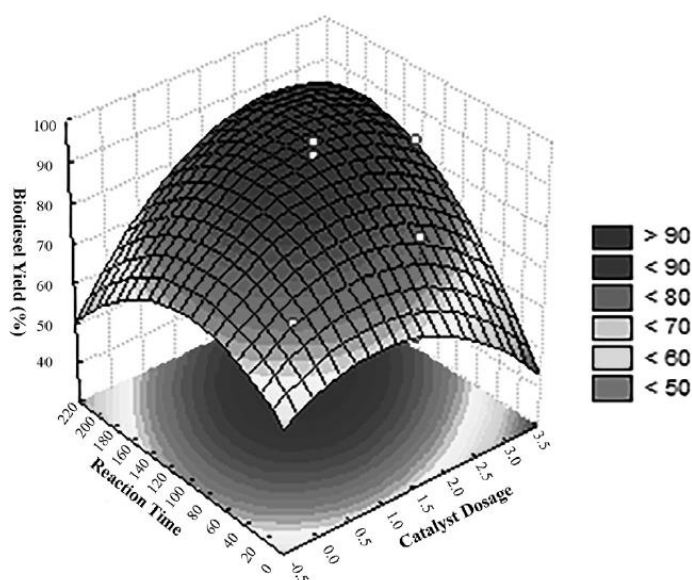
Figure 2.10: Effect of Reaction Time and Catalyst Dosage on Biodiesel Yield (Mohamad, et al., 2016)

Table 2.5: Biodiesel and Conversion after Reaction Optimisation

Feedstock	Conditions	Range of Conditions	Optimised Conditions	Conversion / Yield	References
Cotton Seed Oil	**Temperature (°C)**	20 – 60	55		
	Time (min)	25 – 65	60	Predicted Yield:	Onukwuli, et al.
	Methanol-to-Oil	3:1 to 7:1	6:1	95.57 %	(2016)
	Catalyst Loading (wt %)	0.2 – 1.0	0.6	Actual Yield: 96.00 %	
Lard Oil	**Temperature (°C)**	50 – 70	65		
	Time (min)	20 – 100	40	Predicted Yield:	Ezekannagha, Ude and
	Methanol-to-Oil	3:1 to 15:1	6:1	96.20 %	Onukwuli (2017)
	Catalyst Loading (wt %)	0.5 – 1.5	1.25	Actual Yield: 96.00 %	
Palm Fatty Acid Distillate	**Temperature (°C)**	150	150	Predicted Conversion:	
	Time (min)	130.2 – 469.8	187.2	94.39 %	Mohamad, et al.
	Methanol-to-Oil	1.17:1 to 6.83:1	5.85:1	Actual Conversion:	(2016)
	Catalyst Loading (wt %)	1.59 – 4.41	2.97	93.3 %	

Table 2.5 (Continued)

Feedstock	Conditions	Range of Conditions	Optimised Conditions	Conversion / Yield	References
Palm Fatty Acid Distillate	**Temperature (°C)**	70	70	Predicted Conversion: 95 % Actual Conversion: 92 %	Cheryl-Low, Theam and Lee (2015)
	Time (min)	90 – 240	230		
	Methanol-to-Oil	1:1 to 12:1	20:1		
	Catalyst Loading (wt %)	5.0 – 20.0	10.0		
	Temperature (°C)	70	70	Predicted Conversion: 91.40 % Actual Conversion: 93.70 % Actual Yield: 83.3 %	Theam, et al. (2015)
	Time (min)	90 – 150	142		
	Methanol-to-Oil	5:1 to 10:1	9.6:1		
	Catalyst Loading (wt %)	2.0 – 5.0	5.0		
	Temperature (°C)	65	65	Predicted Conversion: 98.8 % Actual Conversion: 94.5 % Actual Yield: 92.4 %	Lokman, Rashid and Taufiq-Yap (2015)
	Time (min)	60 – 180	134		
	Methanol-to-Oil	5:1 to 15:1	12.2:1		
	Catalyst Loading (wt %)	1.0 – 3.0	2.9		

CHAPTER 3

METHODOLOGY AND WORK PLAN

3.1 Overall View on Procedure

The overall flow of the research is summarised in Figure 3.1 for a better illustration and understanding.
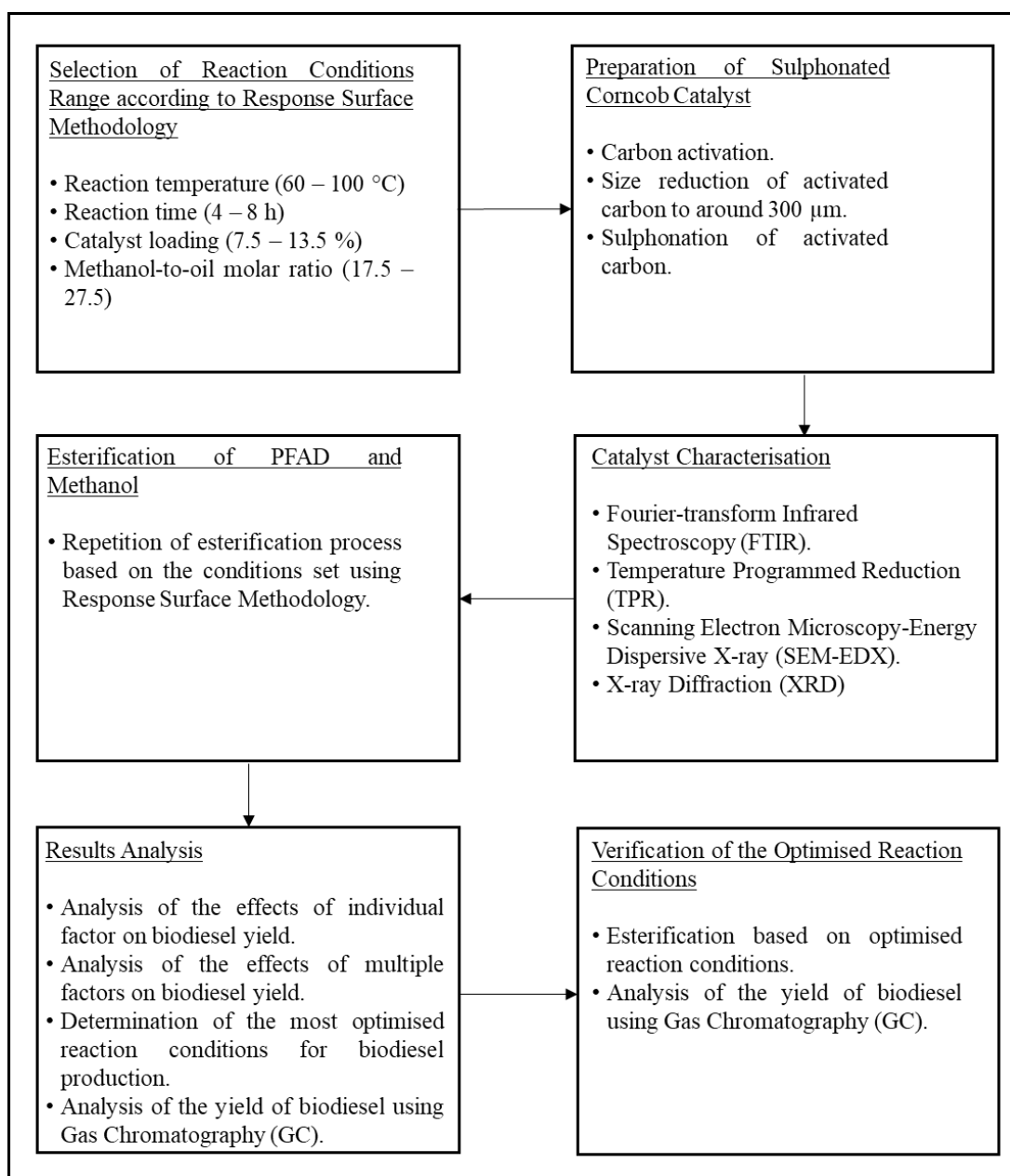
Figure 3.1: Flowchart of the Overall Procedure

3.2   Apparatus and Materials

In order to synthesise the catalysts for the purpose of esterification process, various apparatus, laboratory equipment, and materials required, which are displayed in Table 3.1, 3.2 and 3.3 respectively.

Table 3.1: List of Apparatus Used

Apparatus	Brand (Model)	Purpose
Furnace	Carbolite (RHF 15/8)	To activate powdered carbon.
Oven	Memmert	To dry materials.
Blender	Berjaya (BJY-CB2LN)	To grind corncob into very fine pieces.
Mortar and Pestle	N/A	To reduce the size of corncob into smaller pieces.
Sieve	Prada Test Sieves (850 µm, 300 µm)	To obtain corncob powders within the desired size range.
Ice Water Bath	N/A	To maintain the temperature during synthesis of 4-BDS.
Heating Mantle	MTops (MS-DMS633)	To heat up the mixture to the desired temperature.
Reflux Condenser	Favorit	To reflux evaporated methanol back for esterification process.

Table 3.2: List of Analytical Equipment Used

Equipment	Brand (Model)	Function
Energy Dispersive X-ray (EDX)	Hitachi (S-3400N)	To perform qualitative and quantitative test on the elements identified.
Fourier Transform-infrared Spectroscopy (FTIR)	Nicolet (IS10)	To determine the functional groups and structure of the catalyst.
Gas Chromatography (GC)	Perkin Elmer (Claurus 500)	To determine the biodiesel yield.
Scanning Electron Microscopy (SEM)	Hitachi (S-3400N)	To observe the morphology difference of the catalyst before and after sulphonation process.
Temperature Programme Desorption, Reduction and Oxidation (TPDRO)	Thermo Scientific (TPDRO1100)	To determine the reducibility of the catalyst.
X-ray Diffractometer (XRD)	Shidmazu (XRD-6000)	To determine the crystallinity of carbon-based catalyst produced.

Table 3.3: List of Materials Involved

Materials	Brand (Purity)	Purpose	Amount
Corncob	Sungai Long Night Market	Raw material to be used as carbon-based catalyst.	200 g
Phosphoric Acid	Merck (85 %)	Act as chemical activating and reducing agent.	1.42 L
Sulphanilic acid	Merck (99 %)	Reactant to produce 4-BDS.	450 g
Hydrochloric Acid	Merck (37 %)	Reactant to produce 4-BDS and used to determine the acid density of the catalyst produced.	0.35 L
Sodium Nitrite	ACROS Organic (98.5 %)	Reactant to produce 4-BDS.	90 g
Deionised Water	UTAR	To clean solid products.	3 L
Ethanol	Synerlab (96 %)	Involved in reduction of sulphonated catalyst.	1 L
Sodium Hydroxide	Merck (99 %)	To determine the acid density of the catalyst produced.	0.12 L

Table 3.3 (Continued)

Materials	Brand (Purity)	Purpose	Amount
Phenolphthalein	R&M Chemicals (99.9 %)	To determine the change of pH during back-titration.	0.05 L
Palm Fatty Acid Distillate	Palm Oil Mill Malaysia	Reactant involved in esterification process.	400 g
Methanol	Merck (99.9 %)	Reactant involved in esterification process.	1.5 L
Hexane	Merck (96 %)	Organic solvent used for gas chromatography	0.3 L
Methyl Heptadecanoate	Sigma Aldrich (99 %)	Internal standard to determine biodiesel yield	0.015 L

3.3   Procedures

3.3.1   Selection of Reaction Conditions

To optimise the biodiesel yield, the software Design-Expert® coupled with RSM was used to identify the reaction conditions for each run of the experiment. The upper and lower limits as shown in Table 3.4 were determined based on literature review.

In this research, CCD was applied to determine the optimum conditions for esterification reaction. There are centre points and star points, or also known as axial points, whereby these points allow the estimation of curvature of the response surface. The centre points and star points are denoted as 0 and $\pm \alpha$ respectively in Table 3.4. Besides, the behaviour of the yield from esterification process based on the four factors, which are reaction temperature, time, catalyst loading and methanol-to-PFAD molar ratio are explained with equation 3.1.

$$Y = \beta_0 + \beta_1 X_1 + \beta_2 X_2 + \beta_3 X_3 + \beta_{12} X_1 X_2 + \beta_{13} X_1 X_3 + \beta_{23} X_2 X_3 \quad (3.1)$$
$$+ \beta_{11} X_1^2 + \beta_{22} X_2^2 + \beta_{33} X_3^2$$

where,

Y = Yield of biodiesel

β_i = Interception and interaction coefficients

X_i = Independent variables

Table 3.4: Range of Reaction Conditions

Conditions	Units	$-\alpha$	-1	0	$+1$	$+\alpha$
Temperature	°C	60	70	80	90	100
Time	h	4	5	6	7	8
Catalyst Loading	wt %	7.5	9	10.5	12	13.5
Methanol-to-PFAD Molar Ratio	mol MeOH / mol PFAD	17.5	20	22.5	25	27.5

The experiment matrix obtained from Design-Expert® software is as shown in Table 3.5.

Table 3.5: Experimental Matrix of Esterification Reaction

Temperature (°C)	Time (h)	Catalyst Loading (wt %)	Methanol-to-PFAD Molar Ratio
80	8	10.5	22.5: 1
90	7	9.0	20.0 : 1
90	7	12.0	25.0 : 1
70	7	9.0	25.0 : 1
90	7	9.0	25.0 : 1
90	7	12.0	20.0 : 1
70	7	12.0	20.0 : 1
70	7	12.0	25.0 : 1
70	7	9.0	20.0 : 1
80	6	7.5	22.5 : 1
80	6	10.5	22.5 : 1
80	6	10.5	17.5 : 1
80	6	13.5	22.5 : 1
80	6	10.5	22.5 : 1
60	6	10.5	22.5 : 1
80	6	10.5	22.5 : 1
100	6	10.5	22.5 : 1
80	6	10.5	22.5 : 1
80	6	10.5	27.5 : 1
80	6	10.5	22.5 : 1
80	6	10.5	22.5 : 1
70	5	9.0	20.0 : 1
70	5	9.0	25.0 : 1
90	5	9.0	25.0 : 1
70	5	12.0	25.0 : 1
70	5	12.0	20.0 : 1
90	5	12.0	25.0 : 1
90	5	9.0	20.0 : 1
90	5	12.0	20.0 : 1
80	4	10.5	22.5 : 1

3.3.2   Preparation of Activated Carbon

100 g of fresh corncobs were cleaned and dried in an oven at 60 °C overnight. The dried corncobs were grinded into finer powders. The powders were ensured to be at least smaller than 850 µm using a sieve before they were impregnated in 700 g of 30 % v/v phosphoric acid for 24 hours. The impregnated products were repetitively washed with distilled water. Then, it was dried in the oven at 60 °C overnight. The chemically activated carbons were powdered calcined at 900 °C for two hours in a furnace with the heating rate of 5 °C/min. The activated carbons were once again powdered using pestle and mortar and sieved until all the carbons were smaller than 300 µm. An illustration of the steps mentioned above are shown in Figure 3.2.
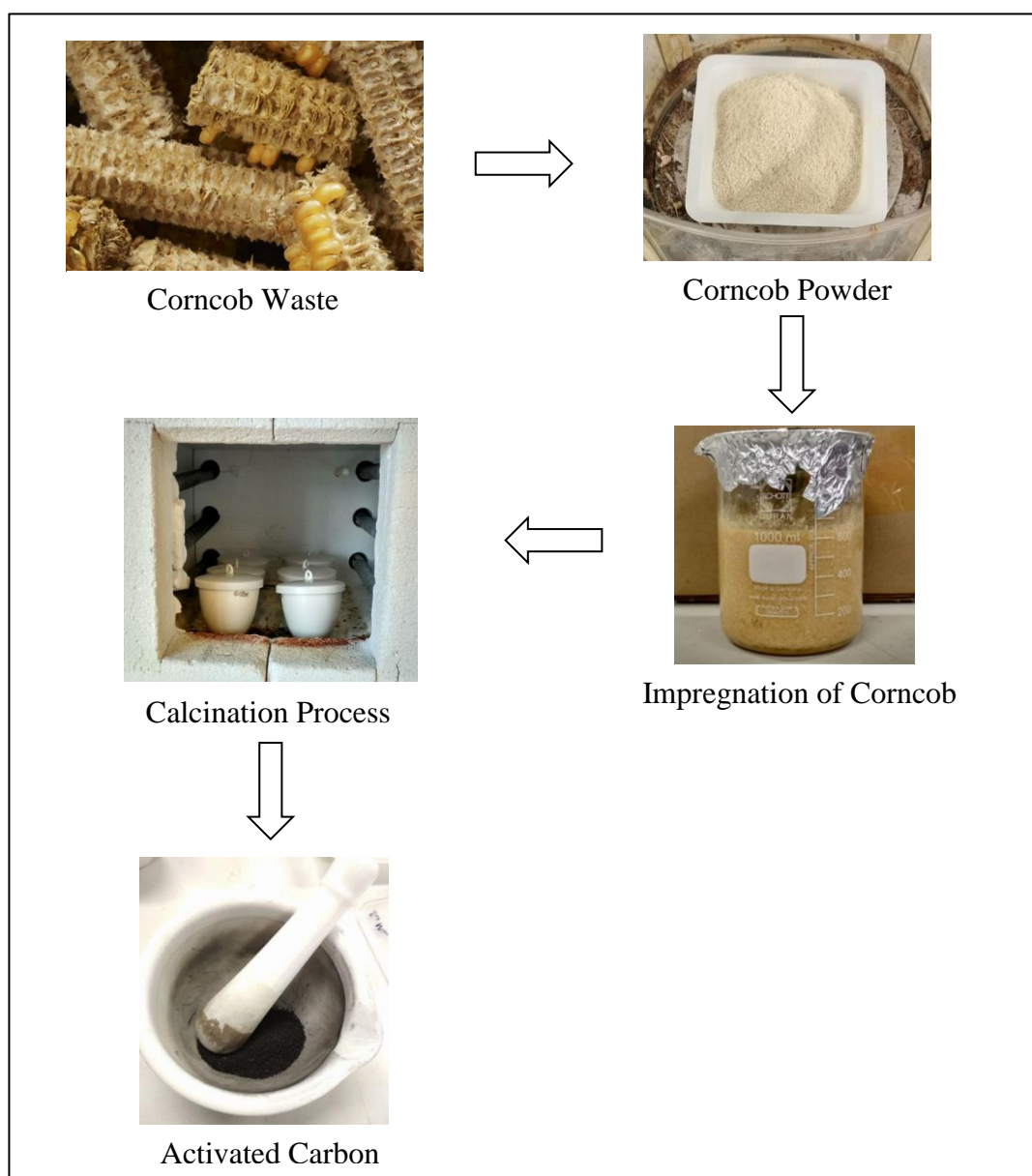
Figure 3.2: Preparation of Activated Carbon

3.3.3   Synthesis of 4-benzenediazoniumsulphonate (4-BDS)

The procedures of producing acidic carbon catalyst was adopted from a research by Konwar, et al. (2015). 33 g of sulphanilic acid was dissolved in 300 mL of 1 M hydrochloric acid in a round bottom flask. The flask containing the mixture was immersed in ice water bath. It was noted that the temperature should be maintained below 5 °C. The mixture in the flask was stirred continuously. Then, 90 mL of 1 M sodium nitrite solution was added into the mixture slowly. The mixture was stirred for an hour within the same range of temperature. Schematic diagram of this synthesis of 4-BDS is shown in Figure 3.3.
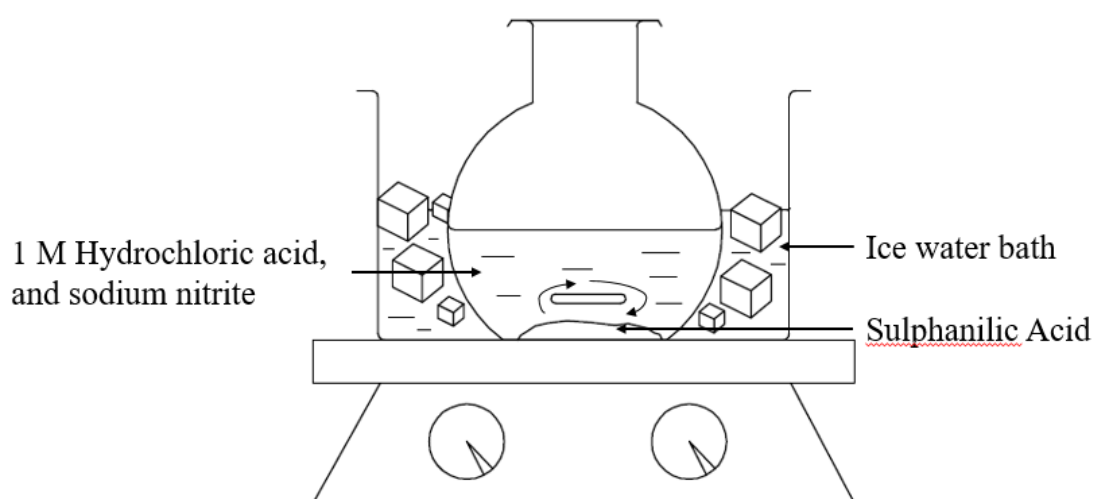
Figure 3.3: Illustration of Synthesis of 4-BDS

3.3.4   Reduction of Sulphonated Carbon-based Catalyst

The white precipitate of 4-BDS produced was filtered to remove the filtrate and washed with deionised water. The precipitate was added into a beaker consists of 200 mL of deionised water and 60 mL of ethanol. After that, 3.0 g of activated carbon was added into the mixture. The temperature of the mixture was decreased and maintained below 5 °C using ice water bath again. 100 mL of 30 % (v/v) phosphoric acid was added into the beaker and the mixture was stirred for 30 min. Then, another 50 mL of 30 % (v/v) phosphoric acid was added into the beaker and stirred for another 1.5 hours. The sulphonated carbon catalysts recovered were washed with distilled water repetitively and dried in the oven at 60 °C overnight. An illustration of this step is shown in Figure 3.4.
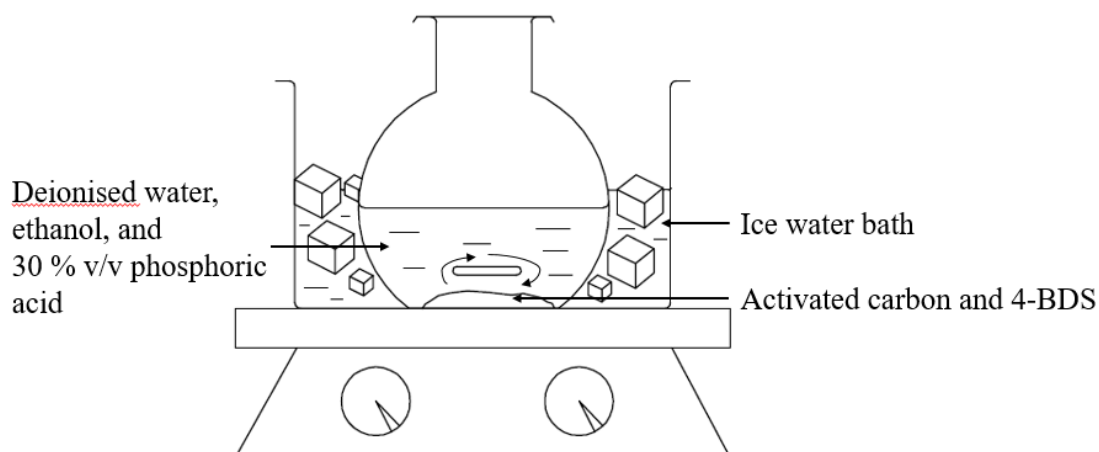
Figure 3.4: Illustration of Reduction of Sulphonated Carbon-based Catalyst

3.3.5 Biodiesel Production

Biodiesel is produced through esterification process of PFAD and methanol (Hosseini, Janaun and Choong, 2015). For instance, the amount of methanol and PFAD added were based on the molar ratio set, which is 25:1. Next, 12 wt % of catalyst was added into the mixture. By fixing the stirring rate at 500 rpm, temperature at 80 °C, the esterification process was allowed to run for an hour. After the process, the catalyst was filtered from the product. The biodiesel yield was analysed by using gas chromatography. Similar steps are repeated according to the conditions set for each run. An illustration is shown in Figure 3.5.
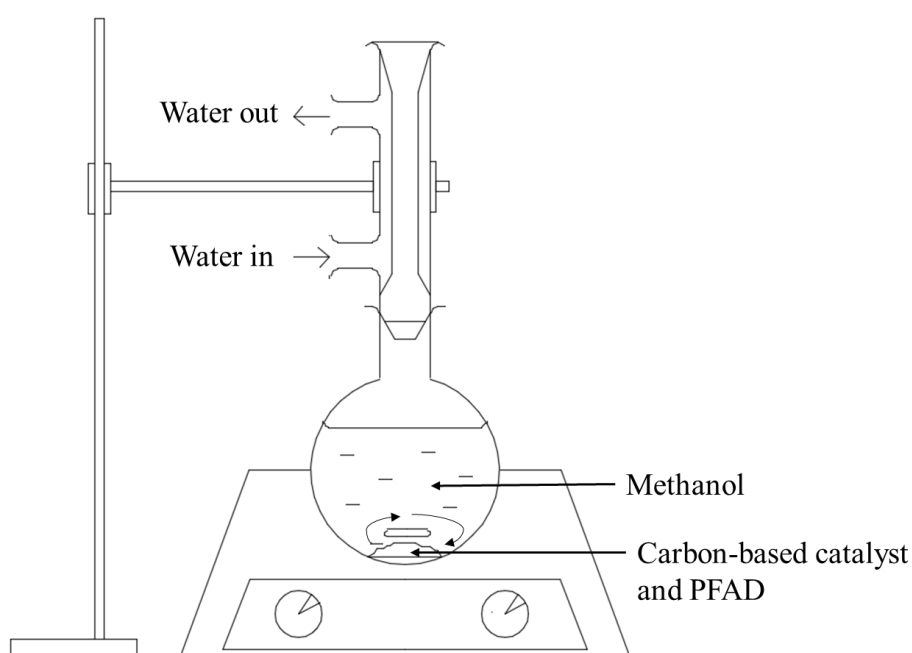
Figure 3.5: Illustration of Esterification Process

3.4 Catalyst Characterisation

In order to ensure the catalyst produced is functional with the desired properties, a few analytical tests were conducted before the catalyst is used for esterification process.

3.4.1 Fourier Transform-infrared Spectroscopy (FTIR)

FTIR is mainly used to identify the functional groups exist in chemical structure of the catalyst produced. The infrared energy emitted by the equipment will be absorbed by the catalyst particles. As every functional group only absorbs a specific amount of energy, the remaining energy transmitted from the catalyst will be recorded. As a result, the amount of energy absorbed or transmitted tells the identity of the catalyst by identifying the functional group found in the catalyst.

3.4.2 Temperature Programmed Reduction (TPR)

TPR is usually conducted to determine the ideal reduction conditions for solid catalysts. The oxidised solid catalysts were subjected to mixture of hydrogen and inert gases such as, nitrogen as the analysis proceeded. The reduction rate on the catalysts was determined based on the amount of hydrogen gas consumed throughout the analysis. Before running TPR analysis, the solid catalysts were pre-treated to remove any impurities attached on it. The conditions for pre-treatment as well as the reduction process are shown in Table 3.6.

Table 3.6: Conditions for Pre-treatment and TPR Analysis

	Type of Gas	Flow rate (cm^3/min)	Temperature (°C)	Ramp rate (°C/min)
Pre-treatment	Nitrogen	20	200	10
TPR	5.47 % Hydrogen and 94.53 % Nitrogen	25	1000	5

3.4.3 Scanning Electron Microscopy-Energy Dispersive X-ray (SEM-EDX)

The purpose of SEM coupled with EDX is to obtain a clear image as well as qualitative and quantitative test of the catalyst sample, especially before and after of the sulphonation process. This was done by emitting a focused electron beam on the catalyst surface. As the electron beam was emitted, lower energy electrons will be excited, causing it to leave the atom. The excited electrons that left the atom were

collected to produce the images observed from SEM. The vacancies left by the excited electrons allowed other high energy electrons to fill in the vacant spots and produce auger electrons and X-ray in the process. The auger electrons produced will be detected by EDX. Since, auger electrons consist of characteristic energy, it allows the identification of the elements present in the sample.

3.4.4   X-ray Diffraction (XRD)

XRD is utilised to determine the crystallinity of the samples. It is also commonly used to identify unknown compounds as each compound has its characteristics diffraction pattern according to its crystal structure. This analysis is carried out by emitting X-rays on the sample. The X-rays diffracted constructively from the sample were detected by the detector. The conditions used by Malins, et al. (2015) for XRD analysis, which are 2θ range of 5° to 60° with the scanning rate of 2°/min were taken as reference for sample analysis in this research.

3.5   Determination of Acid Density of Catalyst Synthesised

Back titration method was used to determine the acid density of the sulphonated carbon-based catalyst synthesised. 0.1 g of catalyst was first mixed with 60 mL of 0.01 M sodium hydroxide solution for half an hour and filtered to remove any solids. Then, the leftover filtrate was used to titrate with 0.02 M of hydrochloric acid. This is to identify the amount of hydrochloric acid required to neutralise the leftover sodium hydroxide solution. The amount used for titration also reflected the acid density of the catalyst, which can be explained using equation 3.3 and 3.4. To identify if the solution is neutralised by hydrochloric acid, phenolphthalein was used as an indicator.

In simple terms, the amount of acid of the catalyst is the difference between the number of moles of sodium hydroxide before and after adding the catalyst into the solution.

$$HCl + NaOH \rightarrow NaCl + H_2O \qquad (3.2)$$
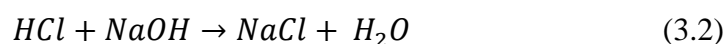
From equation 3.2, a mole of hydrochloric acid, HCl and sodium hydroxide, NaOH are required to produce a mole of sodium chloride salt, NaCl and water, H_2O. Therefore, to determine the number of moles of the final amount of sodium hydroxide, equation 3.3 was used.

$$Final\ mole\ of\ NaOH \qquad\qquad (3.3)$$
$$= Molarity\ of\ HCl\ \times Volume\ of\ HCl\ used$$

$$Acid\ Density \qquad\qquad (3.4)$$
$$= \frac{Initial\ mole\ of\ NaOH - Final\ mole\ of\ NaOH}{0.1\ g}$$

3.6   Determination of Biodiesel Yield

The biodiesel yield was obtained using gas chromatography. In order to use this technique, a mobile phase and stationary phase is needed. The reason for the need of two different phases is to aid the separation of the chemical substances for qualitative and quantitative analysis. In this case, helium gas acts as the mobile phase in Nukol capillary column to determine the yield of biodiesel. Other specifications applied are as shown in Table 3.7.

Table 3.7: Settings used in Gas Chromatography Analysis

Settings	Specifications
Flow rate of Carrier Gas	3 mL/min
Injector Temperature	250 °C
Flame Ionisation Detector Temperature	220 °C

Skoog, et al. (2004) highlighted that the internal standard in gas chromatography is able to compensate the uncertainties occurred in situations such as during injection of the biodiesel sample and any changes in column environment. Therefore, a more accurate result is possible with the introduction of internal standard in gas chromatography analysis. The authors also mentioned that the internal standard needs to fulfil the following criteria before it is selected.

(i)   The peak of internal standard should be separated from the peaks of biodiesel, fatty acid methyl ester (FAME).

(ii)   The internal standard selected should not be originally present in the biodiesel sample.

With that, methyl heptadecanoate was selected as the internal standard to determine the biodiesel yield. To determine the total biodiesel yield, external calibration curves, which are shown in Figure 3.6, 3.7, 3.8, and 3.9 were needed to identify the concentration of respective FAME. By summing the concentration of each FAME, the actual weight of biodiesel and total biodiesel yield were calculated using equation 3.5 and 3.6.

$$Actual\ FAME\ Weight \qquad\qquad\qquad (3.5)$$
$$= \frac{Total\ Concentration\ of\ Biodiesel}{Dilution\ Factor}$$
$$\times Weight\ of\ Product$$

$$Biodiesel\ Yield\ (\%) = \frac{Actual\ FAME\ Weight}{10\ g\ of\ PFAD} \times 100\% \qquad (3.6)$$
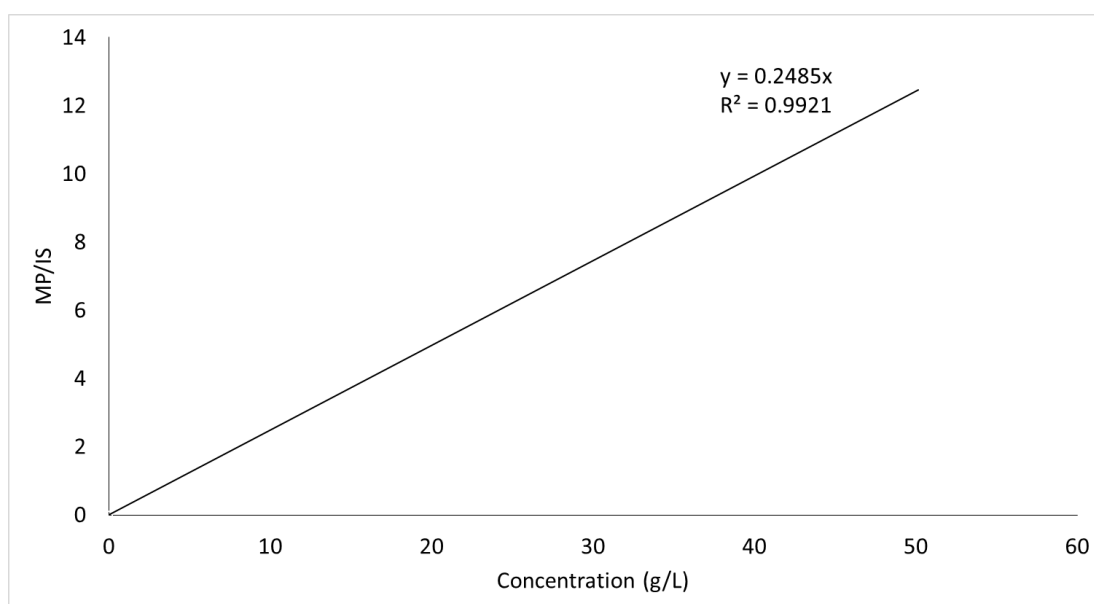
Figure 3.6: Calibration Curve of Methyl Palmitate
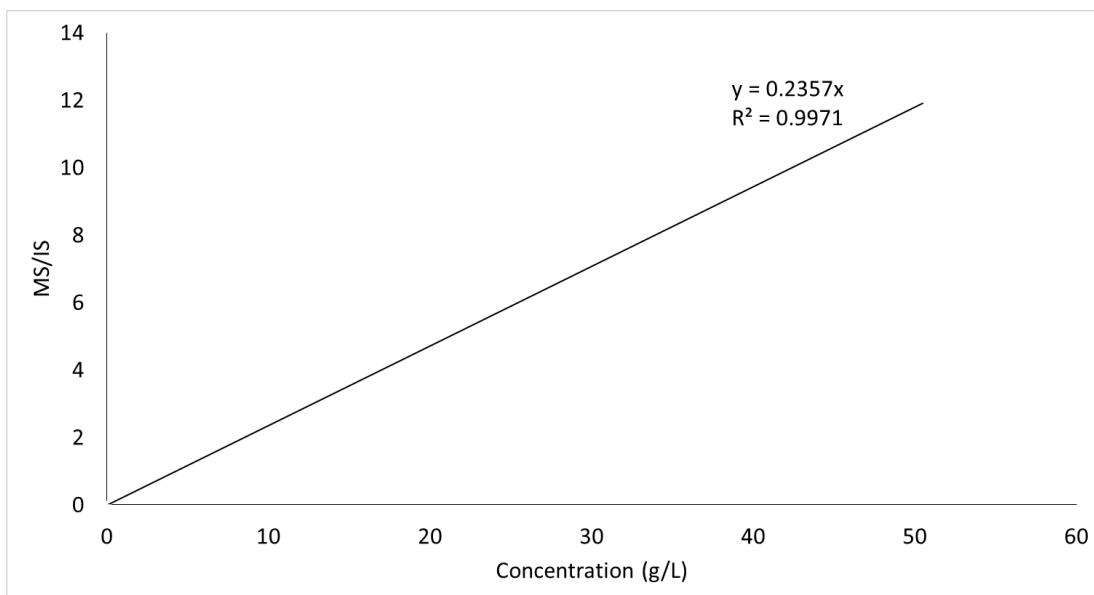
Figure 3.7: Calibration Curve of Methyl Stearate
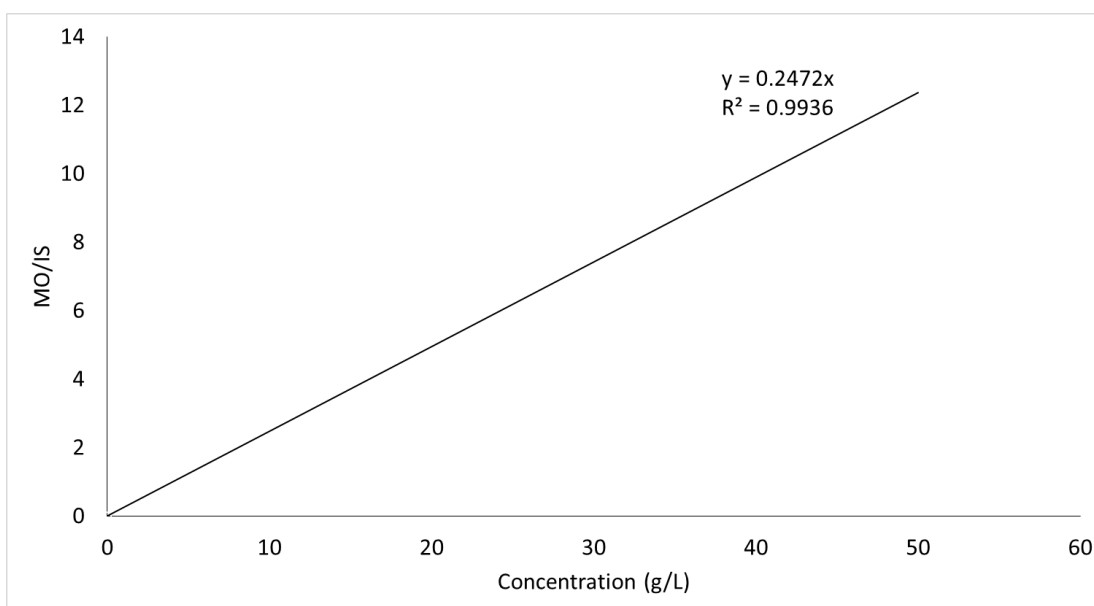
Figure 3.8: Calibration Curve of Methyl Oleate
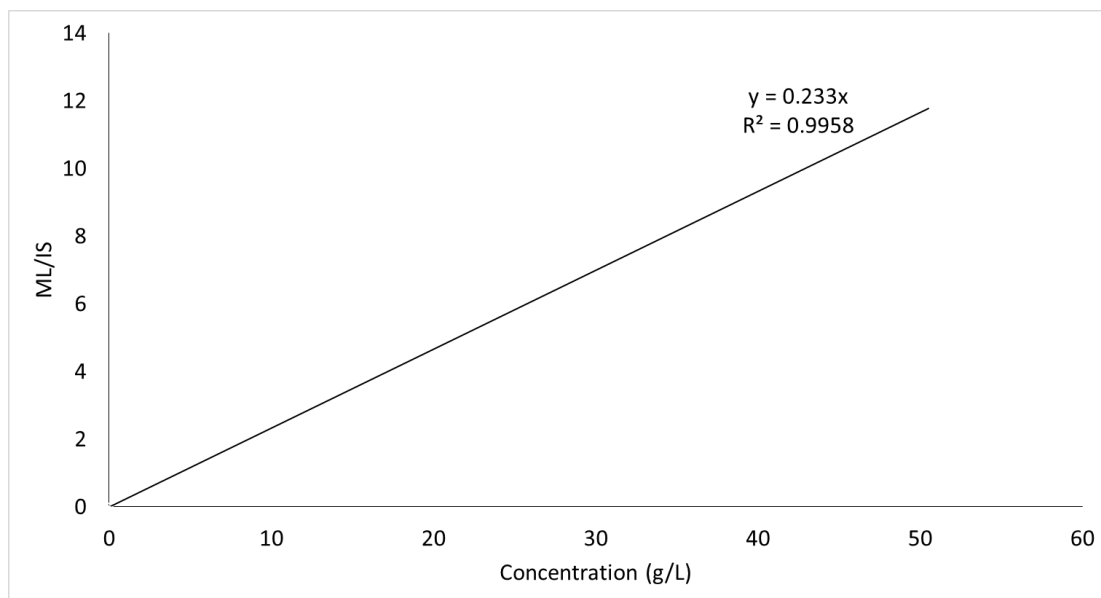
Figure 3.9: Calibration Curve of Methyl Linoleate

Besides, as shown in equation 3.7, the ester content in the biodiesel was calculated using the EN-14103 method. Gasparini, et al. (2011), stated that the purpose of this method is to determine the quality of biodiesel by quantifying the actual biodiesel content.

$$Ester\ Content\ (\%) \tag{3.7}$$
$$= \left(\frac{Total\ FAME\ Peak\ Area}{Peak\ Area\ of\ Methyl\ Heptadecanoate} - 1\right)$$
$$\times \left(\frac{Mass\ of\ Methyl\ Heptadecanoate}{Total\ Mass\ of\ FAME}\right)$$

CHAPTER 4

RESULTS AND DISCUSSION

4.1 Catalyst Characterisation

The purpose of conducting catalyst characterisation is to have a better understanding on the carbon catalyst generated as well as to ensure that the catalyst produced is desirable in terms of its properties and performance. In this research, analytical equipment including FTIR, SEM-EDX, TPR, and XRD were used to aid in the characterisation of the carbon catalyst. The acid density test was also performed to determine acid density of the carbon catalyst produced.

4.1.1 Fourier Transform-infrared Spectroscopy (FTIR)

It was mentioned previously in Section 3.4.1 that different functional groups absorb or transmit a specific amount of infrared energy, and thus, exhibit peaks or stretching that are specific to its characteristics. This helps in the identification of the acidic carbon catalyst. The required information to identify the acidic carbon catalyst is shown in Table 4.1.

Table 4.1: Infrared Characteristics of Important Functional Groups (Konwar, et al., 2015)

Functional Groups	Wavenumber (cm^{-1})
$C = C$	1580
$S = O$	1003 to 1018 and 1110 to 1118
$-SO_3H$	1171 to 1175 and 1267 to 1270

According to Konwar, et al. (2015), the peak formed ($C = C$) at 1580 cm^{-1} was due to incomplete carbonisation of the corncob waste. The presence of this peak could indicate if the material was carbonised and it could also be used to differentiate the peaks of raw corncob waste from activated carbon and carbon catalyst in Figure 4.1. As seen in Figure 4.1, this peak was observed clearly for activated carbon and faintly for the carbon catalyst. The absence of this peak for corncob waste indicated that it was not previously carbonised.

On the other hand, it is possible to tell if the carbon had been successfully sulphonated based on the characteristic peaks formed (S = O) from 1003 to 1018 cm^{-1} and 1110 to 1118 cm^{-1} as well as (–SO_3H) from 1171 to 1175 cm^{-1} and 1267 to 1270 cm^{-1}. However, from Figure 4.1, these peaks are not visible. This is mainly due to the fact that the black carbon material is able to greatly absorb and scatter the infrared radiation, which ultimately affects the infrared spectrum of activated carbon and the carbon catalyst to a great extent (Bradley, 2005).
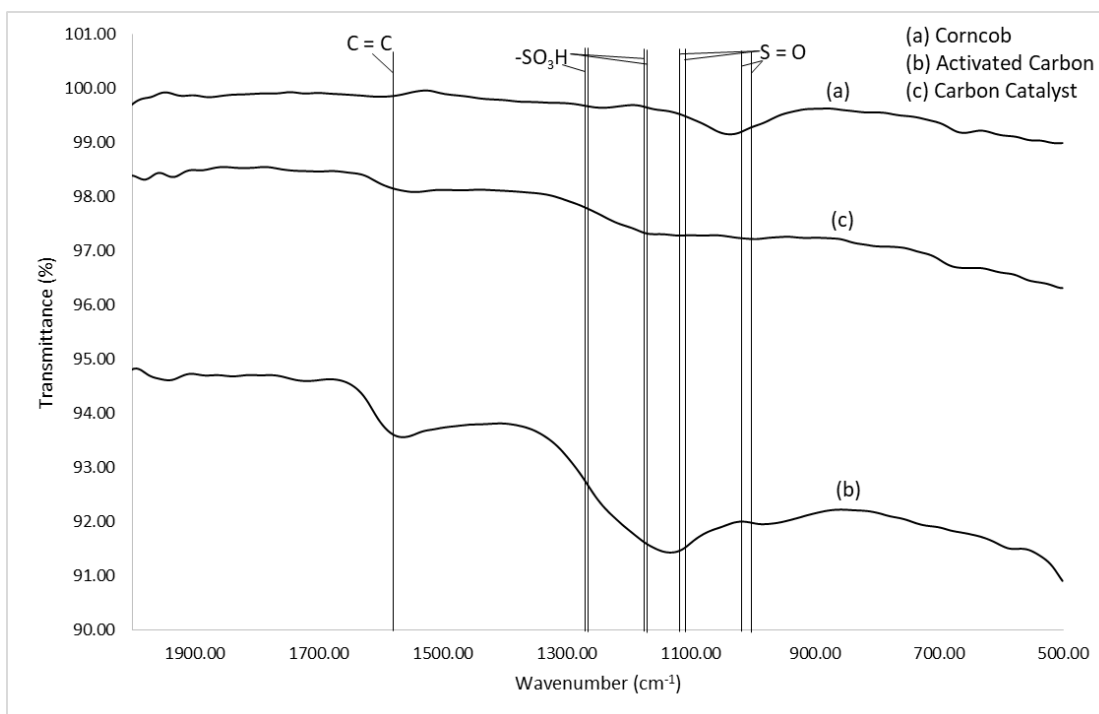
Figure 4.1: Infrared Spectrum from 500 cm^{-1} to 1900 cm^{-1}

4.1.2   Scanning Electron Microscopy-Energy Dispersive X-ray (SEM-EDX)

From Figure 4.2, it can be observed that the microstructure of raw corncob waste is well organised with the surface structures aligned in a well-mannered with the absence of pores.

(a)   (b)
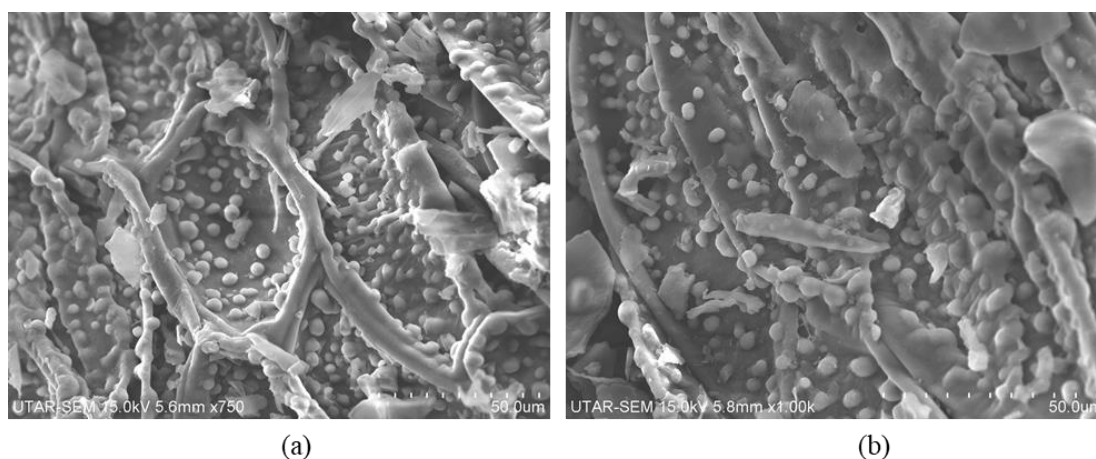
Figure 4.2: SEM Images of Raw Corncob at (a) ×750 and (b) ×1000

In Figure 4.3, it was observed that after chemical activation by 30 % (v/v) phosphoric acid and calcination at 900 °C, large pores and interstices were formed unevenly on the activated carbon. It could also be seen that smaller pores were also formed on the walls of the large pores. These pores and interstices increased the total surface area, which allowed more attachments of sulphonic groups ($-SO_3H$) after the sulphonation process as compared to non-porous structures. Also, it provided protection to the active phase from any possible damage. Besides, as compared to the microstructure of raw corncob wastes in Figure 4.2, the well-organised surface structure was badly distorted with the development of cracks on the surface of the activated carbon as a result of chemical damage as well as high temperature treatment.

After sulphonation process, it can be seen from Figure 4.4 that more cracks were formed on the surface of the catalyst. This could be due to the contribution of 30 % (v/v) phosphoric acid, which was also used in sulphonation process. However, the morphology of the catalyst did not differ greatly from activated carbon. This further proven what was claimed by Konwar, et al. (2013) that the preservation of the structure was possible through sulphonation by 4-BDS.
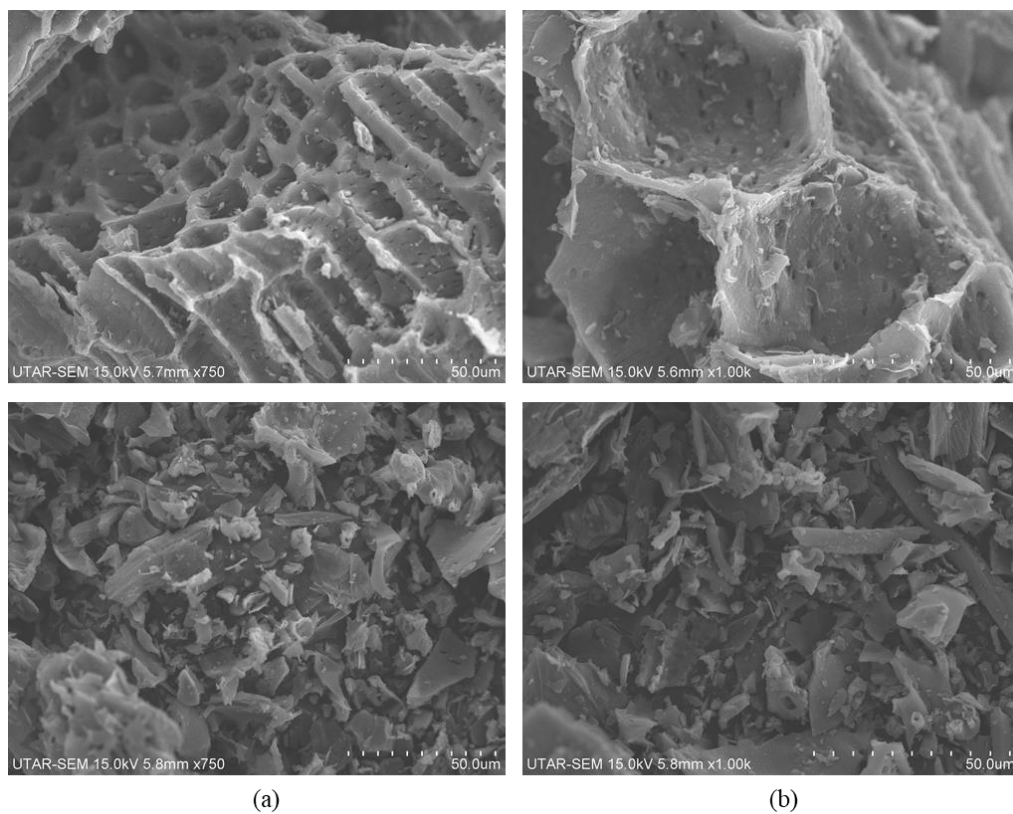
Figure 4.3: SEM Images of Activated Carbon at (a) ×750 and (b) ×1000
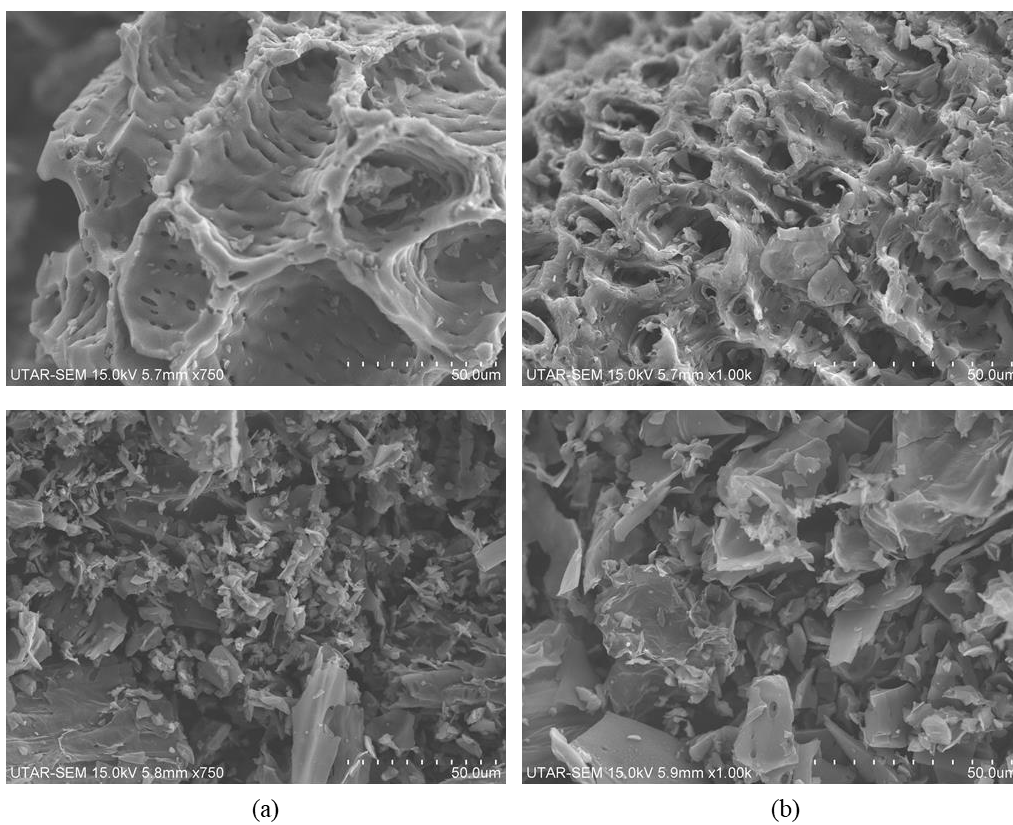
Figure 4.4: SEM Images of Acidic Carbon Catalyst at (a) ×750 and (b) ×1000

On the other hand, Energy Dispersive X-ray (EDX) analysis was also done to determine the elemental composition of the raw corncob waste, activated carbon and acidic carbon catalyst. A summary of the composition of the analysis is shown in Table 4.2.

Table 4.2: Elemental Composition from EDX Analysis

	Wt %				At %			
	CK	OK	SiK	SK	CK	OK	SiK	SK
Corncob	48.26	50.76	0.71	0.27	55.62	43.92	0.35	0.12
Activated Carbon	60.86	36.94	2.01	0.19	67.99	30.98	0.96	0.08
Carbon Catalyst	73.68	18.85	0.96	6.51	81.25	15.61	0.45	2.69

From Table 4.2, it was seen that the composition of SiK increased during the process to produce activated carbon from corncob waste and reduced after sulphonation process. It was inferred that the increment of silicon content occurred during the calcination process, whereby small amount of silicon based substance from the crucible may react with the surrounding oxygen and produce silica dioxide as it was subjected to high heat at 900 °C for 2 hours. Fortunately, the silicon content reduces during the sulphonation process. The reduction of silicon content may be due to the repetitive washing of catalyst after sulphonation process. The composition of sulphur, SK, and carbon, CK were also observed to increase after sulphonation process. This shows that the active phase of 4-BDS were successfully attached onto the active sites of the activated carbon to form acidic catalyst.

4.1.3   Temperature Programmed Reduction (TPR)

In addition to the active phase of the carbon catalyst ($-SO_3H$), other acidic functional groups such as carboxylic acid ($-COOH$) and hydroxyl group ($-OH$) were mainly found in carbon catalysts produced. The presence of oxygen-bearing groups suggested that it was possible for the catalyst to be reduced. With that, TPR was conducted to determine the most suitable temperature for reduction process.

As seen in Figure 4.5, the reading of signal initially increased at a decreasing rate until around 460 °C, where reading of signal started to increase rapidly to form a peak at 661 °C before it decreased as the temperature continued to increase. Therefore, from the plot, it was known that the reduction process was most effective at 661 °C with the hydrogen consumption of 1300 µmol H_2/g.

According to the thermogravimetric analysis (TGA) of acidic carbon catalyst by Liu, et al. (2010), the weight of catalyst was observed to continue to decrease from 95 wt% at 150 °C to 86 wt% at 800 °C as a result of thermal decomposition of sulphonic group. Thus, it was expected that most of the sulphonic group was decomposed as the temperature continued to increase from 661 °C. This explains the reason for the decrement of reduction signal after 661 °C.

Since, 661 °C was the most effective temperature to reduce the carbon catalyst, it could be implied that the carbon catalyst was not easy to be reduced at lower temperature. Hence, this catalyst may be used in other applications that undergo reduction process at lower temperature, such as, hydrogenation processes. In addition, due to the fact that the carbon catalyst was not easily reduced, it was possible for the catalyst to be reused after the suggested process.
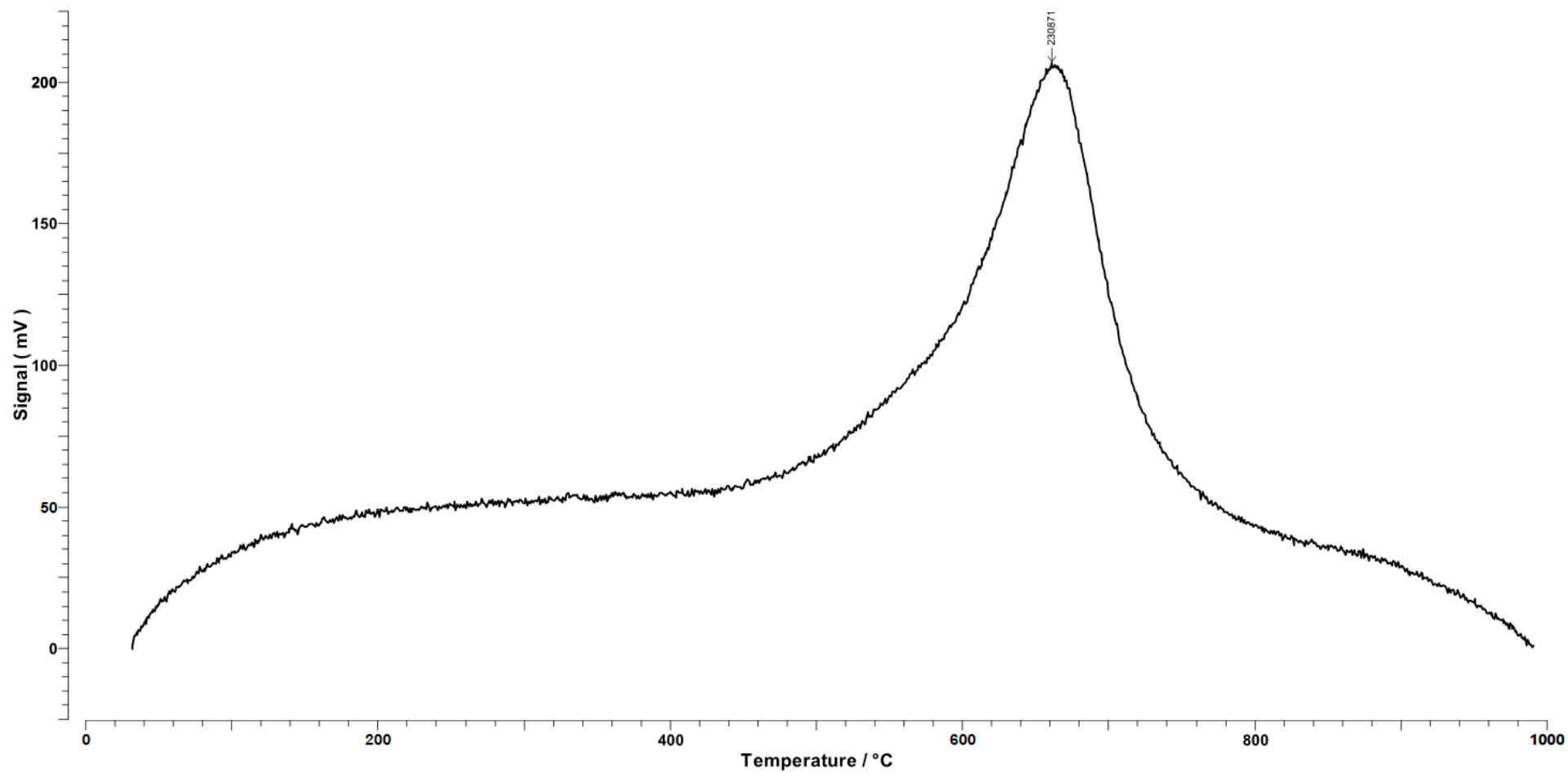
Figure 4.5: TPR Spectra of Acidic Carbon Catalyst

4.1.4   X-ray Diffraction (XRD)

XRD was also conducted for corncob wastes, activated carbon and acidic carbon catalyst to study the microstructure and to determine the crystallinity of these samples. From Figure 4.6, two broad peaks and two sharp peaks were formed. A summary of the peaks for the three samples were shown in Table 4.3.

Table 4.3: Peak Locations of Different Type of Samples

Type of Sample	2θ (°)			
	Broad Peak 1	Broad Peak 2	Sharp Peak 1	Sharp Peak 2
Corncob Waste	22	35	38	44
Activated Carbon	21	43	38	44
Carbon Catalyst	24	43	38	44

It was explained by Malins, et al. (2015) that the presence of the broad (002) and (101) peaks within the range of $15° < 2\theta < 35°$ and $40° < 2\theta < 50°$ respectively indicated that the samples were composed of amorphous carbon structures with a low level of crystalline graphite. Similar XRD patterns between activated carbon and carbon catalyst indicated that there were no microstructural changes before and after sulphonation, which further strengthen what was claimed in Section 4.1.2.

González-García (2018) mentioned that the degree of graphitisation of the samples could be determined by simply comparing the diffractogram of the samples and graphite. As compared to the diffractogram of graphite by Johra, Lee and Jung (2014), it was proven that the low level of graphitisation was observed. In addition, the broader peaks of all three sample as compared to the peaks of graphite also proven that the samples are less crystalline.

On the other hand, sharp peaks were found at 2θ of 38° and 44° for all three samples. It was suggested that the peaks were contributed by the flat aluminium sample holder for XRD analysis. This was further proven based on the diffractogram by Hu, et al. (2018) and Xiao, et al. (2018), whereby the sharp aluminium peaks were found at 2θ of 38° and 44°. It was speculated that the presence of these peaks may be due to the samples were not filled and packed appropriately, which produce gaps between sample powders that allowed X-ray to penetrate into the aluminium sample holder.
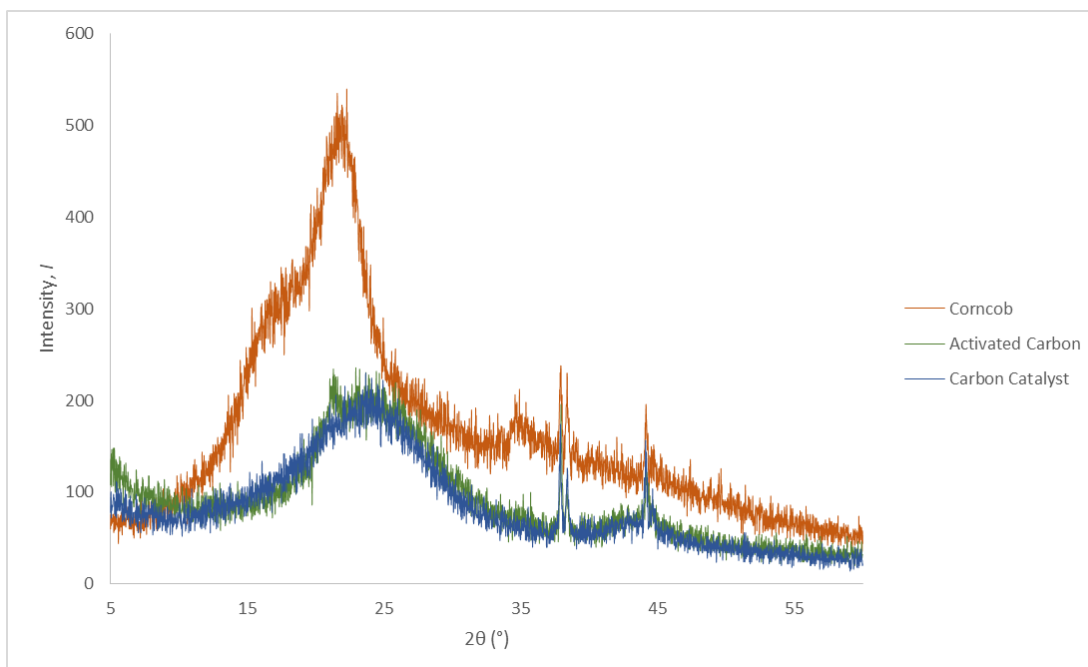
Figure 4.6: XRD Patterns of Corncob Waste, Activated Carbon and Acidic Carbon Catalyst

4.1.5 Acid Density Test

The next method to determine if the acidic active phase, $-SO_3H$ had attached to the catalyst is through acid density test. By conducting back-titration as well as applying equation 3.3 and 3.4, the acid density of the catalyst was determined. To ensure that the catalyst was successfully produced, acid density was first conducted before it was used for esterification process. A complete list of acid density test performed was tabulated in Table 4.4.

Table 4.4: Acid Density of Every Sulphonation Process Conducted

Volume of HCl consumed (mL)	Acid Density (mmol/g)
13.34	3.3320
15.70	2.8600
15.50	2.9000
16.00	2.8000
19.10	2.1800
12.40	3.5200
13.30	3.3400
16.80	2.6400

Table 4.4 (Continued)

Volume of HCl consumed (mL)	Acid Density (mmol/g)
17.40	2.5200
15.10	2.9800
15.30	2.9400
16.35	2.7300
13.60	3.2800

It can be seen from Table 4.4 that the acid density obtained for each sulphonation attempt was within the range of 2.000 to 4.000 mmol/g, yet the values obtained were inconsistent. The reason for the fluctuating values may be mainly due to the inconsistency during the final washing step. Throughout the research, the carbon catalysts were washed and filtered until the filtrate turns from dirty green to colourless. However, no other additional steps were made to act as an indicator to stop the washing process, which led to the inconsistency of acid density of the carbon catalysts. The inconsistency of acid density may possibly affect the esterification reaction as well.

4.2   Response Surface Methodology

The first step of determination of the optimised conditions to obtain the highest biodiesel yield from esterification reaction is by completing the 30 esterification runs generated by the algorithm of Design-Expert® software. The biodiesel yield for each run was calculated using equation 3.5 and 3.6. The calculated value is shown in Table 4.5.

Table 4.5: Experimental Matrix and the Corresponding Biodiesel Yield

Temperature (°C)	Time (h)	Catalyst Loading (wt %)	Methanol-to-PFAD Molar Ratio	Biodiesel Yield (%)
80	8	10.5	22.5: 1	66.82
90	7	9.0	20.0 : 1	60.77
90	7	12.0	25.0 : 1	54.25
70	7	9.0	25.0 : 1	64.45
90	7	9.0	25.0 : 1	69.85

Table 4.5 (Continued)

Temperature (°C)	Time (h)	Catalyst Loading (wt %)	Methanol-to-PFAD Molar Ratio	Biodiesel Yield (%)
90	7	12.0	20.0 : 1	44.71
70	7	12.0	20.0 : 1	51.70
70	7	12.0	25.0 : 1	46.32
70	7	9.0	20.0 : 1	45.55
80	6	7.5	22.5 : 1	53.55
80	6	10.5	22.5 : 1	52.06
80	6	10.5	17.5 : 1	27.99
80	6	13.5	22.5 : 1	30.82
80	6	10.5	22.5 : 1	48.46
60	6	10.5	22.5 : 1	44.09
80	6	10.5	22.5 : 1	24.37
100	6	10.5	22.5 : 1	29.31
80	6	10.5	22.5 : 1	69.66
80	6	10.5	27.5 : 1	31.98
80	6	10.5	22.5 : 1	53.43
80	6	10.5	22.5 : 1	46.24
70	5	9.0	20.0 : 1	59.96
70	5	9.0	25.0 : 1	40.80
90	5	9.0	25.0 : 1	43.20
70	5	12.0	25.0 : 1	57.51
70	5	12.0	20.0 : 1	58.97
90	5	12.0	25.0 : 1	44.01
90	5	9.0	20.0 : 1	47.29
90	5	12.0	20.0 : 1	49.10
80	4	10.5	22.5 : 1	42.55

The quality of biodiesel produced based on the total ester content was also calculated using the EN-14103 method, which was shown in equation 3.7. As seen in Table 4.6, most of the ester content are above 50 %, while a small portion of the results have lower ester content. This was mainly due to the lower biodiesel yield produced.

Table 4.6: Experimental Matrix and the Corresponding Ester Content

Temperature (°C)	Time (h)	Catalyst Loading (wt %)	Methanol-to-PFAD Molar Ratio	Ester Content (%)
80	8	10.5	22.5: 1	77.84
90	7	9.0	20.0 : 1	77.84
90	7	12.0	25.0 : 1	67.17
70	7	9.0	25.0 : 1	65.41
90	7	9.0	25.0 : 1	72.52
90	7	12.0	20.0 : 1	56.43
70	7	12.0	20.0 : 1	68.82
70	7	12.0	25.0 : 1	55.57
70	7	9.0	20.0 : 1	78.00
80	6	7.5	22.5 : 1	62.25
80	6	10.5	22.5 : 1	69.09
80	6	10.5	17.5 : 1	73.85
80	6	13.5	22.5 : 1	72.96
80	6	10.5	22.5 : 1	59.68
60	6	10.5	22.5 : 1	49.46
80	6	10.5	22.5 : 1	46.37
100	6	10.5	22.5 : 1	31.27
80	6	10.5	22.5 : 1	96.77
80	6	10.5	27.5 : 1	44.92
80	6	10.5	22.5 : 1	75.78
80	6	10.5	22.5 : 1	60.34
70	5	9.0	20.0 : 1	76.56
70	5	9.0	25.0 : 1	42.21
90	5	9.0	25.0 : 1	54.97
70	5	12.0	25.0 : 1	63.96
70	5	12.0	20.0 : 1	70.11
90	5	12.0	25.0 : 1	53.59
90	5	9.0	20.0 : 1	65.30
90	5	12.0	20.0 : 1	58.66

Table 4.6 (Continued)

Temperature (°C)	Time (h)	Catalyst Loading (wt %)	Methanol-to-PFAD Molar Ratio	Ester Content (%)
80	4	10.5	22.5 : 1	62.86

4.2.1 Statistics Analysis

To determine the validity of the data obtained from the experiment, analysis of variance (ANOVA) test was conducted. According to Ezekannagha, Ude and Onukwuli (2017), p-value measures the significance of regression coefficients of each factor. A p-value < 0.05 indicates that the particular coefficient is significant. Hence, from Table 4.7, it can be seen that the quadratic model was insignificant, which is not desired. Meanwhile, experimental variables such as B, BC, and D^2 were found to be significant. The fact that these variables are significant implied that these variables played an important role in affecting the biodiesel yield. Apart from that, by using the regression coefficients, a quadratic model as shown in equation 4.1 was generated to formulate a mathematical relationship between the experimental variables and the response, biodiesel yield.

Moreover, Embong, et al. (2015) stated that a high R-squared value and low coefficient of variance (C. V.) value were required to prove that the values obtained from the model was reliable. However, the R-squared value as shown in Table 4.7 was 0.6463, while the C. V. value was 19.66 %. This indicated that the model was unsatisfactory and the model could only explain 64.63 % of the results obtained. On the other hand, Boey, et al. (2013) explained that adequate precision was used to measure the suitability of the model to navigate the design space. A value higher than four was required in order to ensure that model was suitable for navigation to predict the biodiesel yield. From Table 4.7, the adequate precision value obtained was 5.5870. Thus, this model is still suitable to predict the biodiesel yield even though the final value obtained may not be reliable due to poor R-squared value. Repetition of experiment was not possible due to limited time available, which prevented further improvement in results.

Table 4.7: ANOVA Table for Quadratic Response Surface Model

Source	*F*-value	*p*-value
Model	1.96	0.1046
A : Temperature	0.063	0.8049
B: Time	6.09	0.0261
C: Catalyst Loading	0.77	0.3953
D: Molar Ratio	0.74	0.4026
AB	0.44	0.5170
AC	2.70	0.1210
AD	0.12	0.7309
BC	5.81	0.0292
BD	0.71	0.4139
CD	0.94	0.3469
A^2	1.89	0.1889
B^2	1.20	0.2911
C^2	0.39	0.5427
D^2	5.28	0.0363
Lack of fit	1.39	0.3762
R-squared value	0.6463	
Adequate precision	5.5870	
Coefficient of variance (%)	19.66	

Quadratic Model:

$Biodiesel\ Yield$ (%)   (4.1)

$$= -940.39042 + 6.50408\ A - 9.57000\ B$$
$$+ 67.19250\ C + 35.13783\ D + 0.15812\ AB$$
$$- 0.26117\ AC - 0.033400\ AD - 3.82833\ BC$$
$$+ 0.80100\ BD - 0.61700\ CD - 0.025050\ A^2$$
$$+ 1.99125\ B^2 - 0.50389\ C^2 - 0.66940\ D^2$$

4.3 Effect of Interaction between Factors on Biodiesel Yield

In this section, the effects of interaction between the four factors are discussed in order to establish a relationship between these factors before determining the optimum conditions to perform esterification reaction.

4.3.1 Effect of Interaction between Temperature and Time on Biodiesel Yield
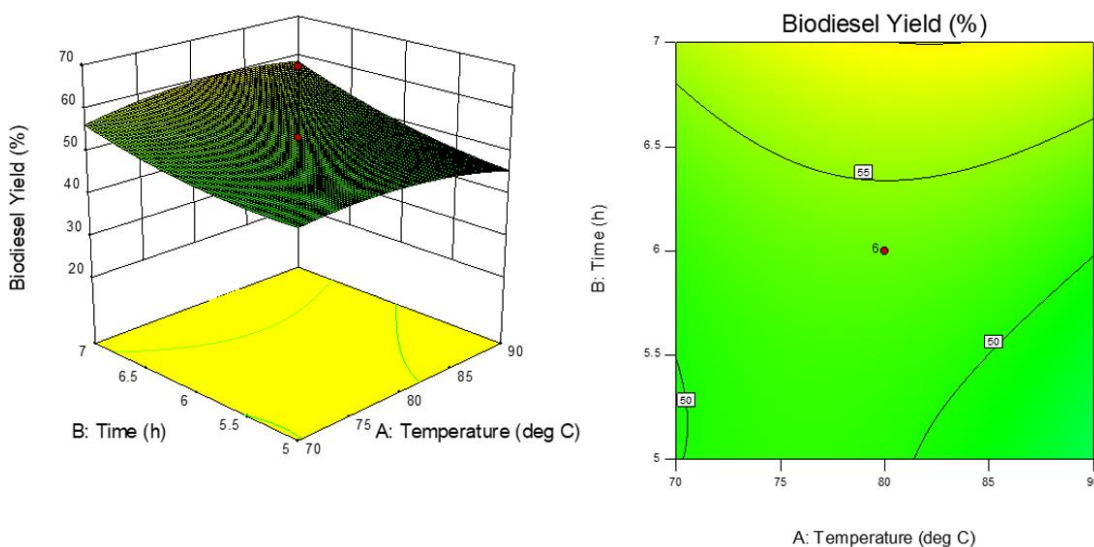
Figure 4.7: Surface Plot and Contour of Interaction between Temperature and Reaction Time at Catalyst Loading of 10.5 wt% and Methanol-to-PFAD Molar Ratio of 22.5:1

Although the interaction between temperature and time on biodiesel yield shown in Figure 4.7 may not be apparent, it can be generally agreed that a longer reaction time increased the biodiesel yield. However, a higher reaction temperature and longer reaction time did not promise the highest yield. Under reaction temperature above 64.7 °C, which was the boiling point of methanol, will cause the evaporation of methanol. This in turn reduced the amount of methanol available for esterification reaction (Latchubugata, et al., 2018). A higher reaction temperature could increase the rate of esterification reaction. However, due to the reaction is a reversible reaction, thus, the rate of backward reaction should also be expected to increase. Hence, if the reaction was carried out at the highest temperature and longest duration, more reactants might be produced as a result of backward reaction to achieve equilibrium, which lowers the biodiesel yield.

4.3.2   Effect of Interaction between Temperature and Catalyst Loading on Biodiesel Yield
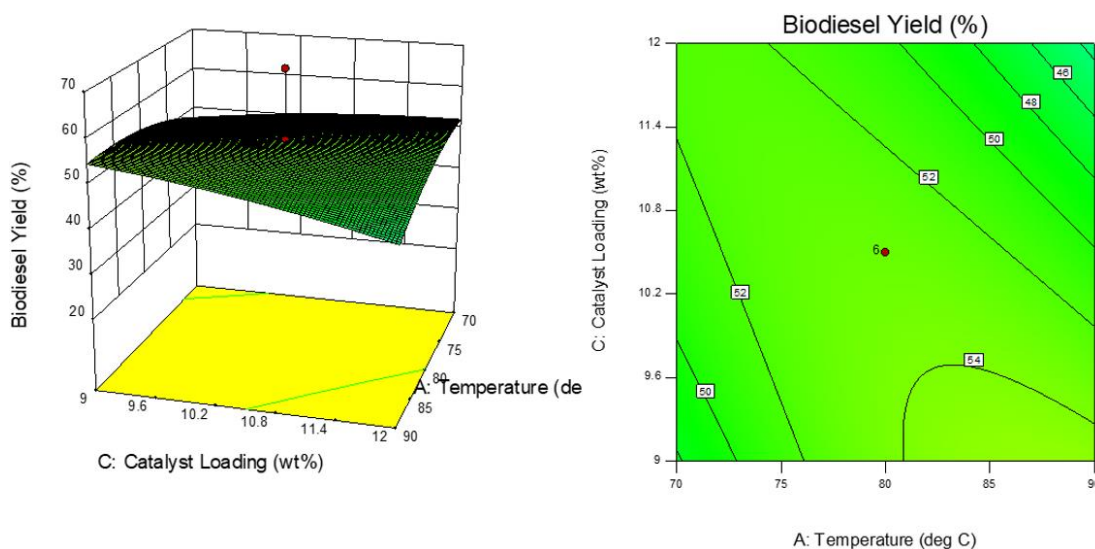
Figure 4.8: Surface Plot and Contour of Interaction between Temperature and Catalyst Loading at Methanol-to-PFAD Molar Ratio of 22.5:1 for 6 h

From Figure 4.8, a higher biodiesel yield was obtained at a higher temperature and lower catalyst loading. It was suggested that a higher reaction temperature would increase the solubility of PFAD in methanol, which promoted esterification reaction by improving effective collision between reactant particles (Ajala, et al., 2016). Although the usage of catalyst improved the reactivity of esterification reaction, according to Figure 4.8, excessive usage of catalyst affected the biodiesel yield negatively. It was inferred that a higher amount of catalyst would increase the mass transfer resistance. The mass transfer resistance might outweigh the increased movement rate of particles at higher temperature, which reduced the biodiesel yield (Muthukumaran, et al., 2017).

4.3.3 Effect of Interaction between Temperature and Methanol-to-PFAD Molar Ratio on Biodiesel Yield
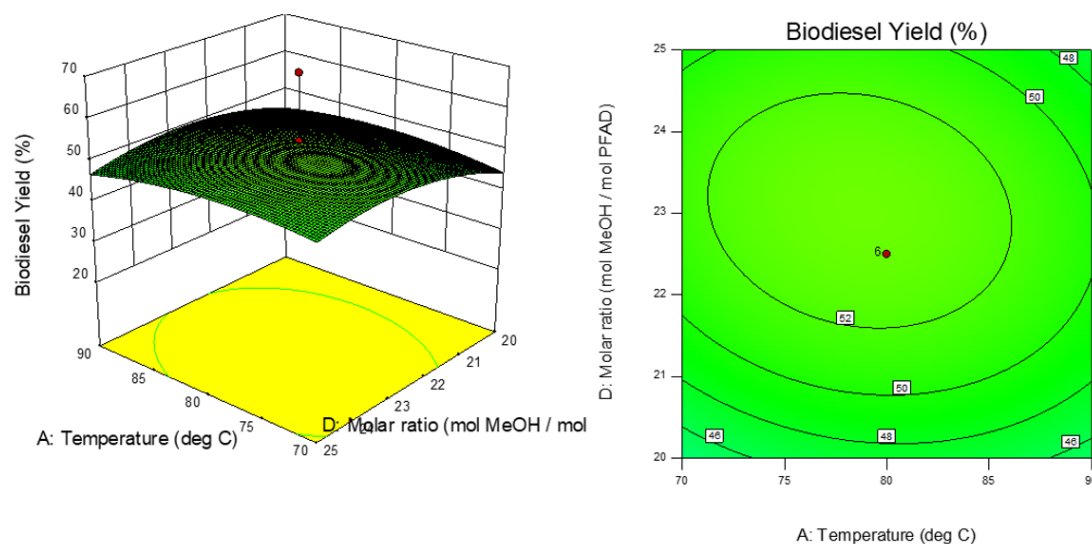
Figure 4.9: Surface Plot and Contour of Interaction between Temperature and Methanol-to-PFAD Molar Ratio at Catalyst Loading of 10.5 wt% for 6 h

The interaction between reaction temperature and methanol-to-PFAD molar ratio was depicted clearly as shown in Figure 4.9. The relationship between reaction temperature and methanol content was briefly mentioned in Section 4.3.1. Since, the reaction temperature is higher than boiling point of methanol, reflux condenser was used to trap and condense evaporated methanol. Despite that reflux condenser was used, however, the rate of evaporation at a high temperature could be greater than the condensation rate. This caused higher concentration of evaporated methanol in the apparatus set-up, and thus, reduces the methanol-to-PFAD molar ratio and the biodiesel yield. Similar surface plot pattern was also found in a research by Ezekannagha, Ude and Onukwuli (2017), where the authors used lard oil instead of PFAD to produce biodiesel.

4.3.4   Effect of Interaction between Catalyst Loading and Time on Biodiesel Yield
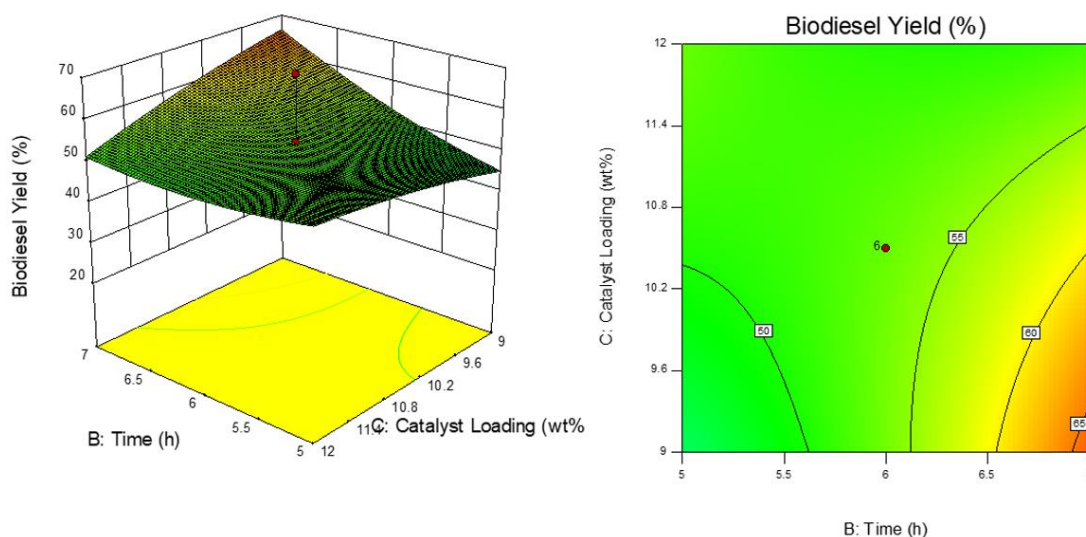
Figure 4.10: Surface Plot and Contour of Interaction between Catalyst Loading and Reaction Time at 80 °C and Methanol-to-PFAD Molar Ratio of 22.5:1

It can be observed from Figure 4.10 that the lowest catalyst loading and longest reaction time yielded the highest amount of biodiesel. It was noted by Mohamad, et al. (2016) that the presence of three phase system between PFAD, methanol and carbon catalyst reduced the reaction rate and biodiesel yield. Therefore, it was inferred that higher catalyst loading could cause greater mass transfer resistance, and thus, further contributed to the declination of biodiesel yield. It was also noticed that the biodiesel yield at reaction time of 5 h was slightly greater than reaction time of 7 h when 12 wt% of catalyst was used for esterification. This could be resulted from greater decrement of methanol content at 80 °C and the greater extent of backward reaction of biodiesel as the reaction time was increased by 2 h.

4.3.5 Effect of Interaction between Time and Methanol-to-PFAD Molar Ratio on Biodiesel Yield
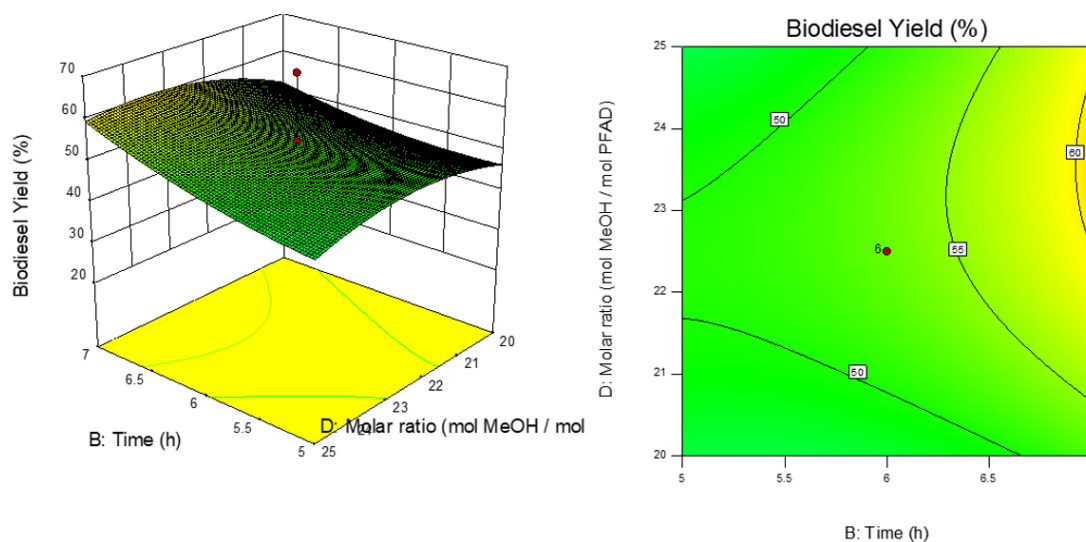
Figure 4.11: Surface Plot and Contour of Interaction between Reaction Time and Methanol-to-PFAD Molar Ratio at 80 °C and Catalyst Loading of 10.5 wt%

From the surface plot in Figure 4.11, the biodiesel yield was seen to be the highest at reaction time of 7 h and methanol-to-PFAD molar ratio of 23:1 and 24:1 and decreased slightly at molar ratio of 25:1. This indicated that the optimum point of methanol-to-PFAD molar ratio was achieved. In general, a longer reaction time and higher molar ratio will yield greater amount of biodiesel. According to Le Chatelier's principle, excess methanol is needed to push the reaction forward in order to achieve equilibrium (Boey, et al., 2013). A longer reaction time also allowed more forward reaction to be carried out, which further improves the biodiesel yield. Besides, the excess usage of methanol also ensures that there will be enough methanol for esterification reaction as methanol evaporates at temperature of 80 °C.

4.3.6   Effect of Interaction between Catalyst Loading and Methanol-to-PFAD Molar Ratio on Biodiesel Yield
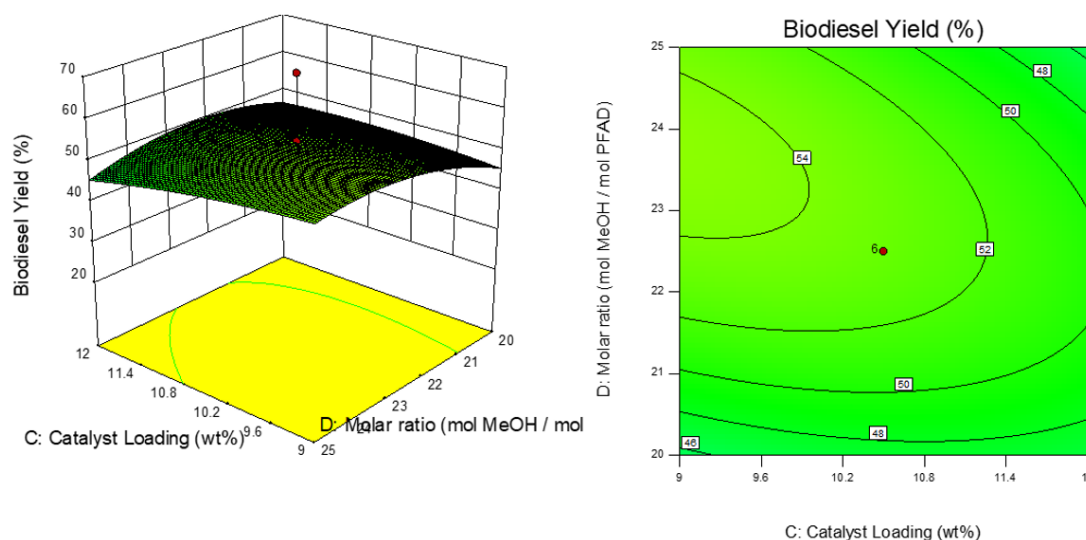
Figure 4.12: Surface Plot and Contour of Interaction between Catalyst Loading and Methanol-to-PFAD Molar Ratio at 80 °C and 6 h

It was observed in Figure 4.12 that the biodiesel yield decreased steadily as the catalyst loading increased. On the other hand, for methanol-to-PFAD molar ratio, the biodiesel yield was observed to increase until it forms a plateau from molar ratio of 23:1 to 24:1 before it started to decrease slightly. This indicated that the optimum molar ratio for the esterification reaction was achieved. Similar to the previous explanation, greater catalyst loading increases the mass transfer resistance (Mohamad, et al., 2016). This affects the diffusion of PFAD and methanol into the catalyst and therefore, reduces the biodiesel yield. Besides, lower methanol-to-PFAD molar ratio indicated that lesser methanol was used as reactant as compared to higher molar ratio. This promoted the occurrence of backward reaction to reach equilibrium due overconsumption of methanol to form biodiesel. On the other hand, too excess of methanol content might dilute the solution. This reduced the attachment of PFAD on the active sites as methanol was adsorbed on majority of the active sites, which led to the decrement of biodiesel yield.

4.4 Optimised Conditions for Esterification Reaction

The optimised conditions to yield the highest biodiesel was estimated numerically using Design-Expert® software. As discussed previously in Section 4.2.1, the model generated was suitable to predict the biodiesel yield, but the values obtained might not be reliable due to the poor R-squared value. Based on the results obtained the highest possible biodiesel yield obtained was 70.11 % at reaction temperature of 87.56 °C, time of 7 h, catalyst loading of 9.023 wt% and methanol-to-PFAD molar ratio of 24.19:1.

However, based on the surface plots in Section 4.3, it can be seen that most of the highest biodiesel yield were within the range of 50 to 60 % except for Figure 4.10, which went beyond 60 %.

It was determined by Design-Expert® software in Section 4.2.1 that the interaction between reaction time, B and catalyst loading, C, had significant effect on the biodiesel yield, hence, it was inferred that the extraordinary high biodiesel yield at reaction time of 7 h and catalyst loading of 9 wt% could be responsible in increasing the upper limit of biodiesel yield for optimisation.

To verify this theory, esterification reaction was repeated based on the optimised reaction conditions. After conducting gas chromatography analysis, the biodiesel yield was calculated to be 56.34 %, which deviated from 70.11 % by 19.64 %. This further strengthen the theory mentioned above.

Furthermore, based on the pattern of the surface plots in Section 4.3, it can be seen that no peak was formed for interaction that involved reaction time and catalyst loading. Therefore, it can be implied that optimisation of reaction time and catalyst loading were not achieved in this research. Nonetheless, it was suspected that the optimum duration and amount of catalyst required to obtain the highest biodiesel yield were 7 h and 9 wt% respectively. Further research at a wider range for reaction time and catalyst loading is required in order to determine the optimum point for the parameters.

CHAPTER 5

CONCLUSION AND RECOMMENDATIONS

5.1 Conclusion

Throughout this research, sulphonation by reductive arylation of 4-benzenediazoniumsulphonate (4-BDS) was done to functionalise activated carbon into a usable carbon catalyst for esterification. EDX analysis was conducted to further prove that the sulphonation of carbon catalyst was successful by detecting the presence of sulphur element on the catalyst.

FTIR was also conducted to identify important functional groups such as $-SO_3H$ and $S = O$, which were the active phases of the carbon catalyst. However, due to black carbon material such as, activated carbon and carbon catalyst produced, they were able to scatter infrared radiation at a great extent, the characteristic peaks of $-SO_3H$ and $S = O$ functional groups were not detected.

On the other hand, SEM was also conducted to analyse the surface properties. After undergoing chemical activation and calcination, pores and interstices were generated due to the removal of impurities from the surface of corncob wastes. Not much difference was observed on the morphology of carbon catalyst before and after the sulphonation process. This shows that the sulphonation process required only mild conditions to functionalise the activated carbon.

After conducting XRD analysis, the presence of broad peaks in diffractogram of corncob wastes, activated carbon and carbon catalyst showed that all three samples were amorphous in nature. The presence of two sharp peaks at 2θ of 38° and 44° was from the flat aluminium sample holder.

From the TPR analysis, it can be seen from the profile that the reduction of carbon catalyst was the highest at 661 °C. The low level of reduction at temperature before 661 °C implied that the catalyst might be suitable for other reductive processes.

To determine the optimum conditions to produce biodiesel, Design-Expert® software along with Response Surface Methodology (RSM) was used. Central Composite Design (CCD), which was classified under RSM was selected. 30 sets of esterification reactions with the reaction conditions set were conducted. The model with R-squared of only 0.6463 was achieved. This indicated that the model generated from this research was less reliable. Nonetheless, the model was used to determine the

optimum conditions. The optimum conditions of temperature at 87.56 °C, reaction time of 7 h, catalyst loading of 9.023 wt% and methanol-to-PFAD molar ratio of 24.19:1 were determined numerically using the software. It was estimated by the software that biodiesel yield of 70.11 % was achievable from the conditions. However, biodiesel yield of only 56.34 % was achieved, which further showed the unreliability of the response surface model.

The unreliability of the model was speculated to be from different sources. Throughout the research, high concentration of fatty acid methyl ester (FAME) such as methyl palmitate, methyl stearate, methyl linoleate and methyl oleate were expected to be produced from the esterification. However, after all 30 runs, it was found out that the concentration of methyl stearate and methyl oleate were lower than expected. Thus, it was suspected that the palm fatty acid distillate (PFAD) used may already be degraded as a result of storage for a long time, which affected the biodiesel yield.

Next, the unsteady performance of carbon catalysts could be another reason. The variation of acid densities for each batch of carbon catalysts might be due to inconsistency of washing of catalyst after sulphonation. Without any indicators to stop washing, the catalysts might be over washed which caused the catalyst to lose its acidic active phase.

All in all, the acidic carbon catalyst was successfully synthesised and characterised. The performance of the carbon catalyst was acceptable but it was believed that there were room for improvements. In addition, further research is required in order to be able to optimise the biodiesel yield.

5.2   Recommendations for Future Research

Despite that the research was conducted accordingly to as what was mentioned in literature review, unfortunately, the shortcoming of the results were inevitable. Therefore, to further improve the results and eventually optimising the biodiesel yield, certain improvements are required. Listed below are the recommendations which may be useful for future research.

(i)   Constant monitoring of temperature during the synthesis of 4-BDS and sulphonation process is required to ensure that the temperature is lower than 5 °C.

(ii)   The catalysts should be washed immediately after the sulphonation process to prevent the loss of acidic active phase.

(iii)   To ensure the catalysts produced are consistent, additional step such as pH control on filtrate should be done during the washing step to indicate if the catalysts are washed adequately.

(iv)   It is suggested to use hot oil bath for esterification instead of heating mantle. This is due to the fact that without the use of thermocouple, the temperature displayed on heating mantle may not be the actual experimental temperature. However, care must be taken if hot oil bath is used.

(v)   Any equipment used should be consistent throughout the research to minimise discrepancies.

(vi)   Analysis on catalyst and biodiesel should be done as soon as possible to prevent inaccuracy in results due to sample degradation.

(vii)   To prevent bias in the results, the 30 esterification runs should be conducted in random order.

(viii)   A wider experimental range, notably reaction duration and catalyst loading are required to obtain the absolute optimum conditions for producing biodiesel.

REFERENCES

Aalam, C. and Saravanan, C., 2015. Biodiesel production techniques: A review. *International Journal for Research in Applied Science and Engineering*, 3(6), pp.41-44.

Akinfalabi, S., Rashid, U., Yunus, R. and Taufiq-Yap, Y., 2017. Synthesis of biodiesel from palm fatty acid distillate using sulfonated palm seed cake catalyst. *Renewable Energy*, 111, pp.611-619.

Ajala, E., Aberuagba, F., Olaniyan, A., Ajala, M. and Sunmonu, M., 2016. Optimization of a two stage process for biodiesel production from shea butter using response surface methodology. *Egyptian Journal of Petroleum*, 26(4), pp.943-955.

Alsobaai, A., 2013. Thermal cracking of petroleum residue oil using three level factorial design. *Journal of King Saud University - Engineering Sciences*, 25(1), pp.21-28.

Alvarez, L., 2000. *Design optimization based on genetic programming: Approximation model building for design optimization using the response surface methodology and genetic programming*. Degree of Doctor of Philosophy. University of Bradford.

Arpornpong, N., Attaphong, C., Charoensaeng, A., Sabatini, D. and Khaodhiar, S., 2014. Ethanol-in-palm oil/diesel microemulsion-based biofuel: Phase behavior, viscosity, and droplet size. *Fuel*, 132, pp.101-106.

Ateeq, E., 2015. *Biodiesel viscosity and flash point determination*. Master. An–Najah National University.

Avhad, M. and Marchetti, J., 2015. A review on recent advancement in catalytic materials for biodiesel production. *Renewable and Sustainable Energy Reviews*, 50, pp.696-718.

Bagheri, N. and Abedi, J., 2009. Preparation of high surface area activated carbon from corn by chemical activation using potassium hydroxide. *Chemical Engineering Research and Design*, 87(8), pp.1059-1064.

Bakirtas, T. and Akpolat, A., 2018. The relationship between energy consumption, urbanization, and economic growth in new emerging-market countries. *Energy*, 147, pp.110-121.

Boey, P., Ganesan, S., Maniam, G., Khairuddean, M. and Efendi, J., 2013. A new heterogeneous acid catalyst for esterification: Optimization using response surface methodology. *Energy Conversion and Management*, 65, pp.392-396.

Bradley, M., 2005. Carbon black analysis comparison with diamond ATR and germanium crystals. Available at: http://www.acm2.com/prilojenia/Carbon%20Black%20analysis/FTIR_BlackRubber Analysis.pdf [Accessed 18 Aug. 2018].

Bradley, N., 2007. *The response surface methodology*. Master of Science. Indiana University of South Bend.

Brown, S., Tauler, R. and Walczak, B., 2009. *Comprehensive chemometrics*. 1st ed. Amsterdam, The Netherlands: Elsevier, p.551.

Bujang, A., Bern, C. and Brumm, T., 2016. Summary of energy demand and renewable energy policies in Malaysia. *Renewable and Sustainable Energy Reviews*, 53, pp.1459-1467.

Cassettari, L., Mosca, R., Revetria, R. and Rolando, F., 2013. Effectiveness and limits of response surface methodology in application to discrete and stochastic simulation of manufacturing plants. *Applied Mathematical Sciences*, 7, pp.4137-4172.

Cheryl-Low, Y., Theam, K. and Lee, H., 2015. Alginate-derived solid acid catalyst for esterification of low-cost palm fatty acid distillate. *Energy Conversion and Management*, 106, pp.932-940.

Clark, J., 2013. *Le Chatelier's Principle*. Chemguide.co.uk. Available at: https://www.chemguide.co.uk/physical/equilibria/lechatelier.html [Accessed 26 Mar. 2018].

Clark, J., 2015. *Esterification - alcohols and carboxylic acids*. Chemguide. Available at: https://www.chemguide.co.uk/organicprops/alcohols/esterification.html [Accessed 14 Mar. 2018].

Dizbay-Onat, M., Vaidya, U. and Lungu, C., 2017. Preparation of industrial sisal fiber waste derived activated carbon by chemical activation and effects of carbonization parameters on surface characteristics. *Industrial Crops and Products*, 95, pp.583-590.

Ejikeme, P., Anyaogu, I., Ejikeme, C., Nwafor, N., Egbuonu, C., Ukogu, K. and Ibemesi, J., 2010. Catalysis in Biodiesel Production by Transesterification Processes-An Insight. *E-Journal of Chemistry*, 7(4), pp.1120-1132.

Ezekannagha, C., Ude, C. and Onukwuli, O., 2017. Optimization of the methanolysis of lard oil in the production of biodiesel with response surface methodology. *Egyptian Journal of Petroleum*, 26(4), pp.1001-1011.

Farnetti, E., Monte, R. and Kašpar, J., 2009. *Inorganic and bio-inorganic chemistry: Homogeneous and heterogeneous catalysis*. 2nd ed. Oxford: Eolss Publishers, p.50.

Fong, Y., 2016. *Biodiesel production from palm fatty acid distillate (PFAD) catalyzed by acid catalysts and biodiesel purification via polymeric membranes*. Master. Universiti Tunku Abdul Rahman.

Gasparini, F., Lima, J., Ghani, Y., Hatanaka, R., Sequinel, R., Flumignan, D. and Oliveira, J., 2011. EN 14103 adjustments for biodiesel analysis from different raw materials, including animal tallow containing C17. pp.101-108. Available at: http://www.ep.liu.se/ecp/057/vol1/014/ecp57vol1_014.pdf [Accessed 18 Aug. 2018].

González-García, P., 2018. Activated carbon from lignocellulosics precursors: A review of the synthesis methods, characterization techniques and applications. *Renewable and Sustainable Energy Reviews*, 82, pp.1393-1414.

Hajjari, M., Tabatabaei, M., Aghbashlo, M. and Ghanavati, H., 2017. A review on the prospects of sustainable biodiesel production: A global scenario with an emphasis on waste-oil biodiesel utilization. *Renewable and Sustainable Energy Reviews*, 72, pp.445-464.

Hanna, R. and Zoughaib, A., 2017. Atomization of high viscosity liquids through hydraulic atomizers designed for water atomization. *Experimental Thermal and Fluid Science*, 85, pp.140-153.

Hasan, M. and Rahman, M., 2017. Performance and emission characteristics of biodiesel–diesel blend and environmental and economic impacts of biodiesel production: A review. *Renewable and Sustainable Energy Reviews*, 74, pp.938-948.

Hidayat, A., Rochmadi, Wijaya, K., Nurdiawati, A., Kurniawan, W., Hinode, H., Yoshikawa, K. and Budiman, A., 2015. Esterification of palm fatty acid distillate with high amount of free fatty acids using coconut shell char based catalyst. *Energy Procedia*, 75, pp.969-974.

Hosseini, S., Janaun, J. and Choong, T., 2015. Feasibility of honeycomb monolith supported sugar catalyst to produce biodiesel from palm fatty acid distillate (PFAD). *Process Safety and Environmental Protection*, 98, pp.285-295.

Hu, Z., Chen, F., Xu, J., Nian, Q., Lin, D., Chen, C., Zhu, X., Chen, Y. and Zhang, M., 2018. 3D printing graphene-aluminum nanocomposites. *Journal of Alloys and Compounds*, 746, pp.269-276.

Hua, Y., Oliphant, M. and Hu, E., 2016. Development of renewable energy in Australia and China: A comparison of policies and status. *Renewable Energy*, 85, pp.1044-1051.

Johra, F., Lee, J. and Jung, W., 2014. Facile and safe graphene preparation on solution based platform. *Journal of Industrial and Engineering Chemistry*, 20(5), pp.2883-2887.

Konwar, L., Boro, J. and Deka, D., 2013. Review on latest developments in biodiesel production using carbon-based catalysts. *Renewable and Sustainable Energy Reviews*, 29, pp.546-564.

Konwar, L., Das, R., Thakur, A., Salminen, E., Mäki-Arvela, P., Kumar, N., Mikkola, J. and Deka, D., 2013. Biodiesel production from acid oils using sulfonated carbon catalyst derived from oil-cake waste. *Journal of Molecular Catalysis A: Chemical*, 388-389, pp.167-176.

Konwar, L., Mäki-Arvela, P., Salminen, E., Kumar, N., Thakur, A., Mikkola, J. and Deka, D., 2015. Towards carbon efficient biorefining: Multifunctional mesoporous solid acids obtained from biodiesel production wastes for biomass conversion. *Applied Catalysis B: Environmental*, 176-177, pp.20-35.

Knothe, G. and Razon, L., 2017. Biodiesel fuels. *Progress in Energy and Combustion Science*, 58, pp.36-59.

Latchubugata, C., Kondapaneni, R., Patluri, K., Virendra, U. and Vedantam, S., 2018. Kinetics and optimization studies using Response Surface Methodology in biodiesel production using heterogeneous catalyst. *Chemical Engineering Research and Design*, 135, pp.129-139.

Lemoine, G. and Thompson, R., 2014. A preliminary study of acid catalyzed transesterification of a Jatropha-like bio-oil. *Biomass and Bioenergy*, 69, pp.169-174.

Liu, X., Huang, M., Ma, H., Zhang, Z., Gao, J., Zhu, Y., Han, X. and Guo, X., 2010. Preparation of a carbon-based solid acid catalyst by sulfonating activated carbon in a chemical reduction process. *Molecules*, 15(10), pp.7188-7196.

Lokman, I., Rashid, U. and Taufiq-Yap, Y., 2015. Production of biodiesel from palm fatty acid distillate using sulfonated-glucose solid acid catalyst: Characterization and optimization. *Chinese Journal of Chemical Engineering*, 23(11), pp.1857-1864.

Lokman, I., Rashid, U., Taufiq-Yap, Y. and Yunus, R., 2015. Methyl ester production from palm fatty acid distillate using sulfonated glucose-derived acid catalyst. *Renewable Energy*, 81, pp.347-354.

Mahmudul, H., Hagos, F., Mamat, R., Adam, A., Ishak, W. and Alenezi, R., 2017. Production, characterization and performance of biodiesel as an alternative fuel in diesel engines – A review. *Renewable and Sustainable Energy Reviews*, 72, pp.497-509.

Malins, K., Kampars, V., Brinks, J., Neibolte, I. and Murnieks, R., 2015. Synthesis of activated carbon based heterogenous acid catalyst for biodiesel preparation. *Applied Catalysis B: Environmental*, 176-177, pp.553-558.

Mohamad, M., Ngadi, N., Wong, S., Jusoh, M. and Yahya, N., 2016. Prediction of biodiesel yield during transesterification process using response surface methodology. *Fuel*, 190, pp.104-112.

Muda, N. and Tey, J., 2012. On prediction of depreciation time of fossil fuel in malaysia. *Journal of Mathematics and Statistics*, 8(1), pp.136-143.

Muthukumaran, C., Praniesh, R., Navamani, P., Swathi, R., Sharmila, G. and Manoj Kumar, N., 2017. Process optimization and kinetic modeling of biodiesel production using non-edible Madhuca indica oil. *Fuel*, 195, pp.217-225.

Narasimharao, K., Lee, A. and Wilson, K., 2007. Catalysts in production of biodiesel: A review. *Journal of Biobased Materials and Bioenergy*, 1(1), pp.1-10.

Olutoye, M., Wong, C., Chin, L. and Hameed, B., 2014. Synthesis of FAME from the methanolysis of palm fatty acid distillate using highly active solid oxide acid catalyst. *Fuel Processing Technology*, 124, pp.54-60.

Onukwuli, D., Emembolu, L., Ude, C., Aliozo, S. and Menkiti, M., 2016. Optimization of biodiesel production from refined cotton seed oil and its characterization. *Egyptian Journal of Petroleum*, 26(1), pp.103-110.

Parvizsedghy, R., Sadrameli, S. and Towfighi Darian, J., 2015. Upgraded Biofuel Diesel Production by Thermal Cracking of Castor Biodiesel. *Energy & Fuels*, 30(1), pp.326-333.

PBL Netherlands Environmental Assessment Agency, 2017. Trends in global CO2 and total greenhouse gas emissions. pp. 13-14.

Rajalingam, A., Jani, S., Kumar, A. and Khan, M., 2016. Production methods of biodiesel. *Journal of Chemical and Pharmaceutical Research*, 8(3), pp.170-173.

Ranu, B., Chatterjee, T., Mukherjee, N., Maity, P. and Majhi, B., 2015. Synthesis of bioactive five- and six-membered heterocycles catalyzed by heterogeneous supported metals. *Green Synthetic Approaches for Biologically Relevant Heterocycles*, pp.7-43.

Ritter, K., 2016. *Global carbon emissions have not risen for the first time in three years*. The Independent.

Silva, P., Silva, C., Guimarães, L. and Pliego, J., 2014. Acid-catalyzed transesterification and esterification in methanol: A theoretical cluster-continuum investigation of the mechanisms and free energy barriers. *Theoretical Chemistry Accounts*, 134(1), pp.1-13.

Skoog, D., West, D., Holler, F. and Crouch, S., 2004. *Fundamentals of analytical chemistry*. 8th ed. Belmont, Calif.: Thomson- Brooks/Cole.

Soltani, S., Rashid, U., Yunus, R. and Taufiq-Yap, Y., 2016. Biodiesel production in the presence of sulfonated mesoporous ZnAl2O4 catalyst via esterification of palm fatty acid distillate (PFAD). *Fuel*, 178, pp.253-262.

Specht, E., Redemann, T. and Lorenz, N., 2016. Simplified mathematical model for calculating global warming through anthropogenic CO2. *International Journal of Thermal Sciences*, 102, pp.1-8.

Stat-Ease, 2017. *Box-behnken design*. Design-Expert. Available at: https://www.statease.com/docs/v11/designs/box-behnken.html [Accessed 3 Apr. 2018].

Talha, N. and Sulaiman, S., 2016. Overview of catalysts in biodiesel production. *ARPN Journal of Engineering and Applied Sciences*, 11(1), pp.439-445.

Thangaraja, J., Anand, K. and Mehta, P., 2016. Biodiesel NOx penalty and control measures - a review. *Renewable and Sustainable Energy Reviews*, 61, pp.1-24.

Theam, K., Islam, A., Lee, H. and Taufiq-Yap, Y., 2015. Sucrose-derived catalytic biodiesel synthesis from low cost palm fatty acid distillate. *Process Safety and Environmental Protection*, 95, pp.126-135.

U.S. Energy Information Administration, 2017. International energy outlook executive summary. pp. 1 to 2.

Wan, Z., Lim, J. and Hameed, B., 2015. Chromium–tungsten heterogeneous catalyst for esterification of palm fatty acid distillate to fatty acid methyl ester. *Journal of the Taiwan Institute of Chemical Engineers*, 54, pp.64-70.

World Bank, 2017. *Malaysia economic monitor, December 2017*. Available at: http://www.worldbank.org/en/country/malaysia/publication/malaysia-economic-monitor-december-2017 [Accessed 23 Feb. 2018].

Xiao, F., Guo, Y., Li, J. and Yang, R., 2018. Hydrogen generation from hydrolysis of activated aluminum composites in tap water. *Energy*, 157, pp.608-614.

APPENDICES

APPENDIX A: Sample reports of Gas Chromatography (GC)

APPENDIX B: Sample reports of Energy Dispersive X-ray (EDX)

APPENDIX C: Sample reports of Temperature Programmed Reduction (TPR)

APPENDIX D: Sample reports of X-ray Diffraction (XRD)

Software Version	: 6.3.1.0504
Operator	: FES
Sample Number	:
AutoSampler	: NONE
Instrument Name	: Clarus500
Instrument Serial #	: 650N7041802
Delay Time	: 0.00 min
Sampling Rate	: 12.5000 pts/s
Sample Volume	: 1.000000 ul
Sample Amount	: 1.0000
Data Acquisition Time	: 7/6/2018 11:41:30 AM

Date	: 7/6/2018 12:08:26 PM
Sample Name	:
Study	:
Rack/Vial	: 0/0
Channel	: A
A/D mV Range	: 1000
End Time	: 19.50 min
Area Reject	: 0.000000
Dilution Factor	: 1.00
Cycle	: 1

Raw Data File : C:\Documents and Settings\FES\Desktop\Result\2018\Chon Wen-Xian\28-6-2018-T 80-t 6-load 10.5%-ratio 22.5 to 1.raw

Result File : C:\Documents and Settings\FES\Desktop\Result\2018\Chon Wen-Xian\28-6-2018-T 80-t 6-load 10.5%-ratio 22.5 to 1.rst

Inst Method : C:\GC\Method\Nukol 25327 (18092017) from C:\Documents and Settings\FES\Desktop\Result\2018\Chon Wen-Xian\28-6-2018-T 80-t 6-load 10.5%-ratio 22.5 to 1.raw

Proc Method : C:\GC\Method\Nukol 25327 (18092017) from C:\Documents and Settings\FES\Desktop\Result\2018\Chon Wen-Xian\28-6-2018-T 80-t 6-load 10.5%-ratio 22.5 to 1.rst

Calib Method : C:\GC\Method\Nukol 25327 (18092017) from C:\Documents and Settings\FES\Desktop\Result\2018\Chon Wen-Xian\28-6-2018-T 80-t 6-load 10.5%-ratio 22.5 to 1.rst

Report Format File: C:\GC\Method\Nukol 25327 (18092017).rpt

Sequence File : C:\GC\Method\28-6-2018-T 80-t 6-load 10.5%-ratio 22.5 to 1.seq

DEFAULT REPORT

Peak #	Time [min]	Area [µV·s]	Height [µV]	Area [%]	Norm. Area [%]	BL	Area/Height [s]
1	1.922	970882.81	855236.81	98.13	98.13	BE	1.1352
2	1.969	7739.60	7836.55	0.78	0.78	EB	0.9876
3	10.229	116.35	51.96	0.01	0.01	BB	2.2390
4	12.194	4925.87	1768.71	0.50	0.50	BB	2.7850
5	13.315	1335.12	390.28	0.13	0.13	BB	3.4209
6	14.675	316.16	76.98	0.03	0.03	BB	4.1072
7	15.053	3121.62	705.26	0.32	0.32	BB	4.4262
8	15.862	709.95	155.20	0.07	0.07	BB	4.5745
9	18.228	200.89	26.58	0.02	0.02	BB	7.5570
		989348.37	866248.34	100.00	100.00		

Missing Component Report

Component Expected Retention (Calibration File)

All components were found

7/6/2018 12:08:26 PM Result: C:\Documents and Settings\FES\Desktop\Result\2018\Chon Wen-Xian\28-6-2018-T 80-t 6-load 10.5%-ratio 22.5 to 1.rst

Chromatogram

Software Version : 6.3.1.0504
Sample Name :
Data Acquisition Time : 7/6/2018 11:41:30 AM

Date : 7/6/2018 12:08:26 PM
Sample Number :

Raw Data File : C:\Documents and Settings\FES\Desktop\Result\2018\Chon Wen-Xian\28-6-2018-T 80-t 6-load 10.5%-ratio 22.5 to 1.raw
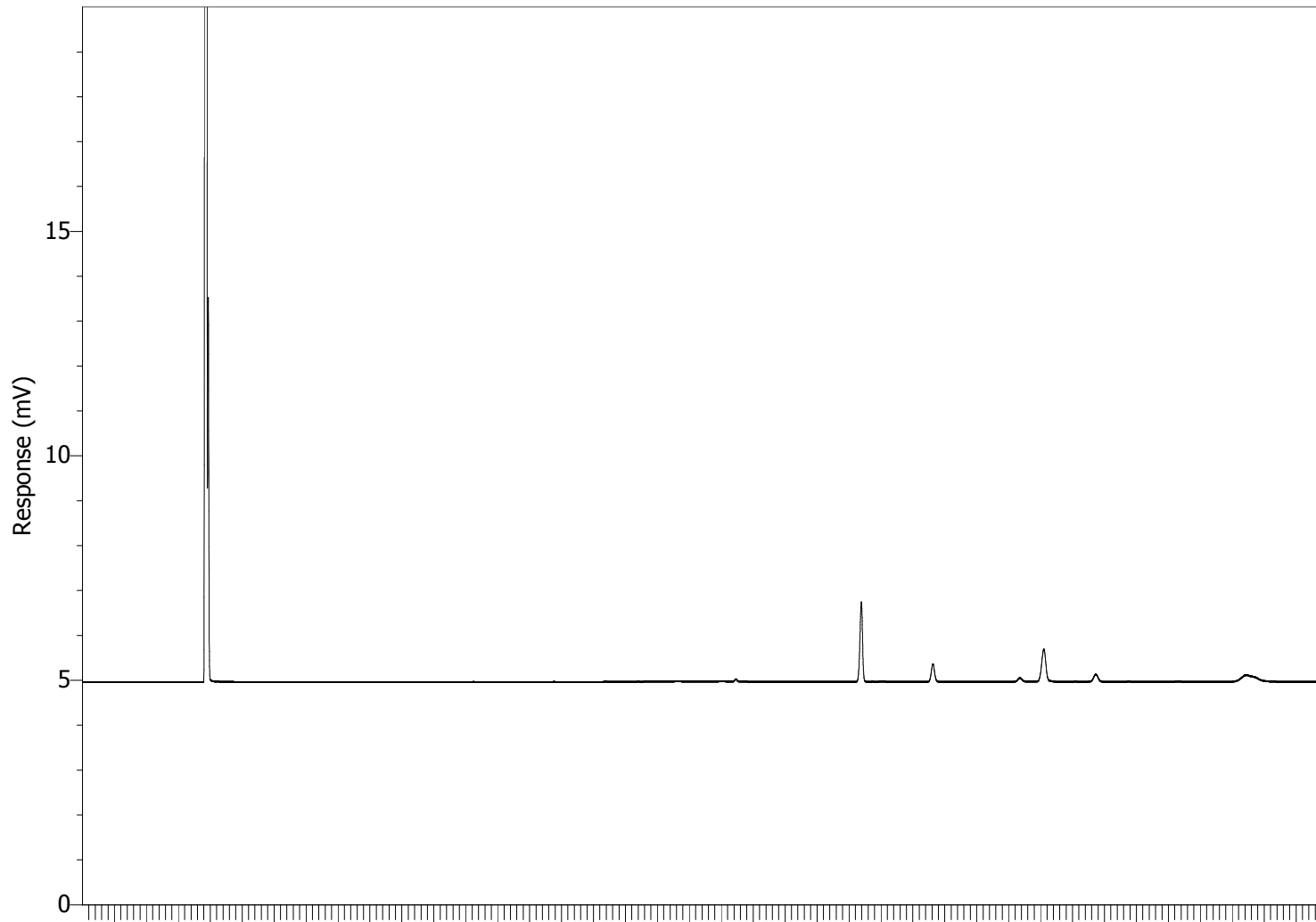
Software Version	: 6.3.1.0504	Date	: 7/27/2018 12:25:29 PM
Operator	: FES	Sample Name	:
Sample Number	:	Study	:
AutoSampler	: NONE	Rack/Vial	: 0/0
Instrument Name	: Clarus500	Channel	: A
Instrument Serial #	: 650N7041802	A/D mV Range	: 1000
Delay Time	: 0.00 min	End Time	: 19.50 min
Sampling Rate	: 12.5000 pts/s		
Sample Volume	: 1.000000 ul		
Sample Amount	: 1.0000	Area Reject	: 0.000000
Data Acquisition Time	: 7/27/2018 12:02:32 PM	Dilution Factor	: 1.00
		Cycle	: 1

Raw Data File : C:\Documents and Settings\FES\Desktop\Result\2018\Chon Wen-Xian\19-7-2018-T 70-t 7-load 9%-ratio 20 to 1.raw
Result File : C:\Documents and Settings\FES\Desktop\Result\2018\Chon Wen-Xian\19-7-2018-T 70-t 7-load 9%-ratio 20 to 1.rst
Inst Method : C:\GC\Method\Nukol 25327 (18092017) from C:\Documents and Settings\FES\Desktop\Result\2018\Chon Wen-Xian\19-7-2018-T 70-t 7-load 9%-ratio 20 to 1.raw
Proc Method : C:\GC\Method\Nukol 25327 (18092017) from C:\Documents and Settings\FES\Desktop\Result\2018\Chon Wen-Xian\19-7-2018-T 70-t 7-load 9%-ratio 20 to 1.rst
Calib Method : C:\GC\Method\Nukol 25327 (18092017) from C:\Documents and Settings\FES\Desktop\Result\2018\Chon Wen-Xian\19-7-2018-T 70-t 7-load 9%-ratio 20 to 1.rst
Report Format File: C:\GC\Method\Nukol 25327 (18092017).rpt
Sequence File : C:\GC\Method\19-7-2018-T 70-t 7-load 9%-ratio 20 to 1.seq

DEFAULT REPORT

Peak #	Time [min]	Area [µV·s]	Height [µV]	Area [%]	Norm. Area [%]	BL	Area/Height [s]
1	1.926	1061255.37	887901.55	96.18	96.18	BE	1.1952
2	1.973	8315.96	7831.74	0.75	0.75	EB	1.0618
3	10.172	264.27	117.82	0.02	0.02	BB	2.2430
4	12.144	11897.41	4109.00	1.08	1.08	BB	2.8955
5	13.234	2167.09	699.90	0.20	0.20	BB	3.0963
6	14.347	1272.45	140.92	0.12	0.12	BV	9.0295
7	14.573	8103.30	715.97	0.73	0.73	VV	11.3180
8	14.964	8312.84	1854.52	0.75	0.75	VB	4.4825
9	15.752	1813.68	409.39	0.16	0.16	BB	4.4302
		1103402.37	903780.82	100.00	100.00		

Missing Component Report
Component Expected Retention (Calibration File)

All components were found

7/27/2018 12:25:29 PM Result: C:\Documents and Settings\FES\Desktop\Result\2018\Chon
 Wen-Xian\19-7-2018-T 70-t 7-load 9%-ratio 20 to 1.rst

Chromatogram

Software Version : 6.3.1.0504   Date : 7/27/2018 12:25:30 PM
Sample Name :   Sample Number :
Data Acquisition Time : 7/27/2018 12:02:32 PM

Raw Data File : C:\Documents and Settings\FES\Desktop\Result\2018\Chon Wen-Xian\19-7-2018-T 70-t 7-load 9%-ratio
 20 to 1.raw
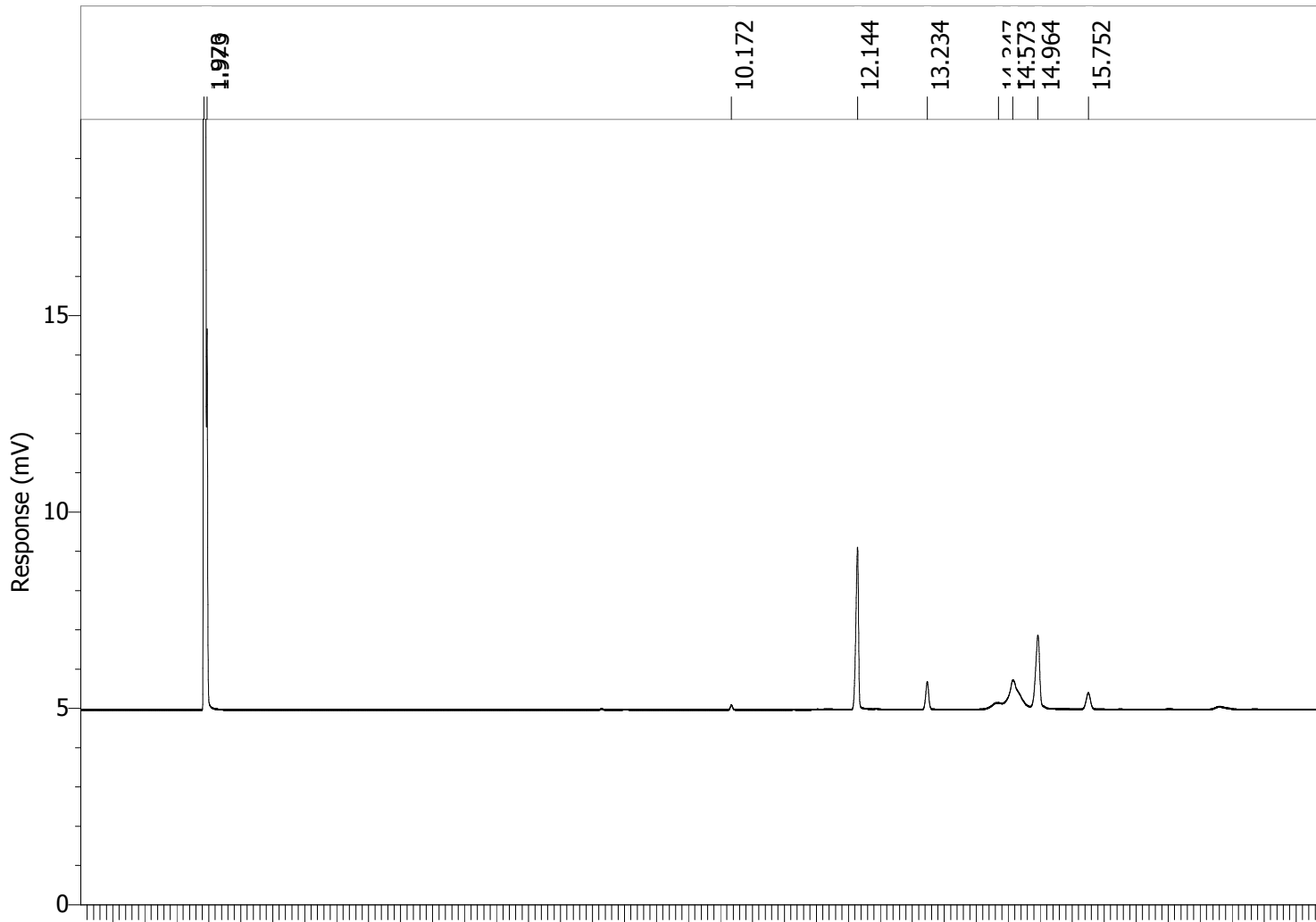
Software Version	: 6.3.1.0504	Date	: 7/11/2018 12:01:42 PM
Operator	: FES	Sample Name	:
Sample Number	:	Study	:
AutoSampler	: NONE	Rack/Vial	: 0/0
Instrument Name	: Clarus500	Channel	: A
Instrument Serial #	: 650N7041802	A/D mV Range	: 1000
Delay Time	: 0.00 min	End Time	: 19.50 min
Sampling Rate	: 12.5000 pts/s		
Sample Volume	: 1.000000 ul		
Sample Amount	: 1.0000	Area Reject	: 0.000000
Data Acquisition Time	: 7/11/2018 11:40:32 AM	Dilution Factor	: 1.00
		Cycle	: 1

Raw Data File : C:\Documents and Settings\FES\Desktop\Result\2018\Chon Wen-Xian\9-7-2018.raw
Result File : C:\Documents and Settings\FES\Desktop\Result\2018\Chon Wen-Xian\9-7-2018.rst
Inst Method : C:\GC\Method\Nukol 25327 (18092017) from C:\Documents and Settings\FES\Desktop\Result\2018\Chon Wen-Xian\9-7-2018.raw
Proc Method : C:\GC\Method\Nukol 25327 (18092017) from C:\Documents and Settings\FES\Desktop\Result\2018\Chon Wen-Xian\9-7-2018.rst
Calib Method : C:\GC\Method\Nukol 25327 (18092017) from C:\Documents and Settings\FES\Desktop\Result\2018\Chon Wen-Xian\9-7-2018.rst
Report Format File: C:\GC\Method\Nukol 25327 (18092017).rpt
Sequence File : C:\GC\Method\9-7-2018.seq

DEFAULT REPORT

Peak #	Time [min]	Area [µV·s]	Height [µV]	Area [%]	Norm. Area [%]	BL	Area/Height [s]
1	1.924	1273622.57	922518.07	98.31	98.31	BB	1.3806
2	10.238	229.99	98.31	0.02	0.02	BB	2.3393
3	12.219	10367.61	3455.63	0.80	0.80	BB	3.0002
4	13.332	2133.86	576.44	0.16	0.16	BB	3.7018
5	14.697	704.53	153.41	0.05	0.05	BB	4.5925
6	15.081	6965.98	1458.40	0.54	0.54	BB	4.7764
7	15.888	1542.36	316.73	0.12	0.12	BB	4.8696
		1295566.91	928577.00	100.00	100.00		

Missing Component Report

Component	Expected Retention (Calibration File)

All components were found

7/11/2018 12:01:42 PM Result: C:\Documents and Settings\FES\Desktop\Result\2018\Chon
 Wen-Xian\9-7-2018.rst

Chromatogram

Software Version : 6.3.1.0504   Date : 7/11/2018 12:01:42 PM
Sample Name :   Sample Number :
Data Acquisition Time : 7/11/2018 11:40:32 AM

Raw Data File : C:\Documents and Settings\FES\Desktop\Result\2018\Chon Wen-Xian\9-7-2018.raw
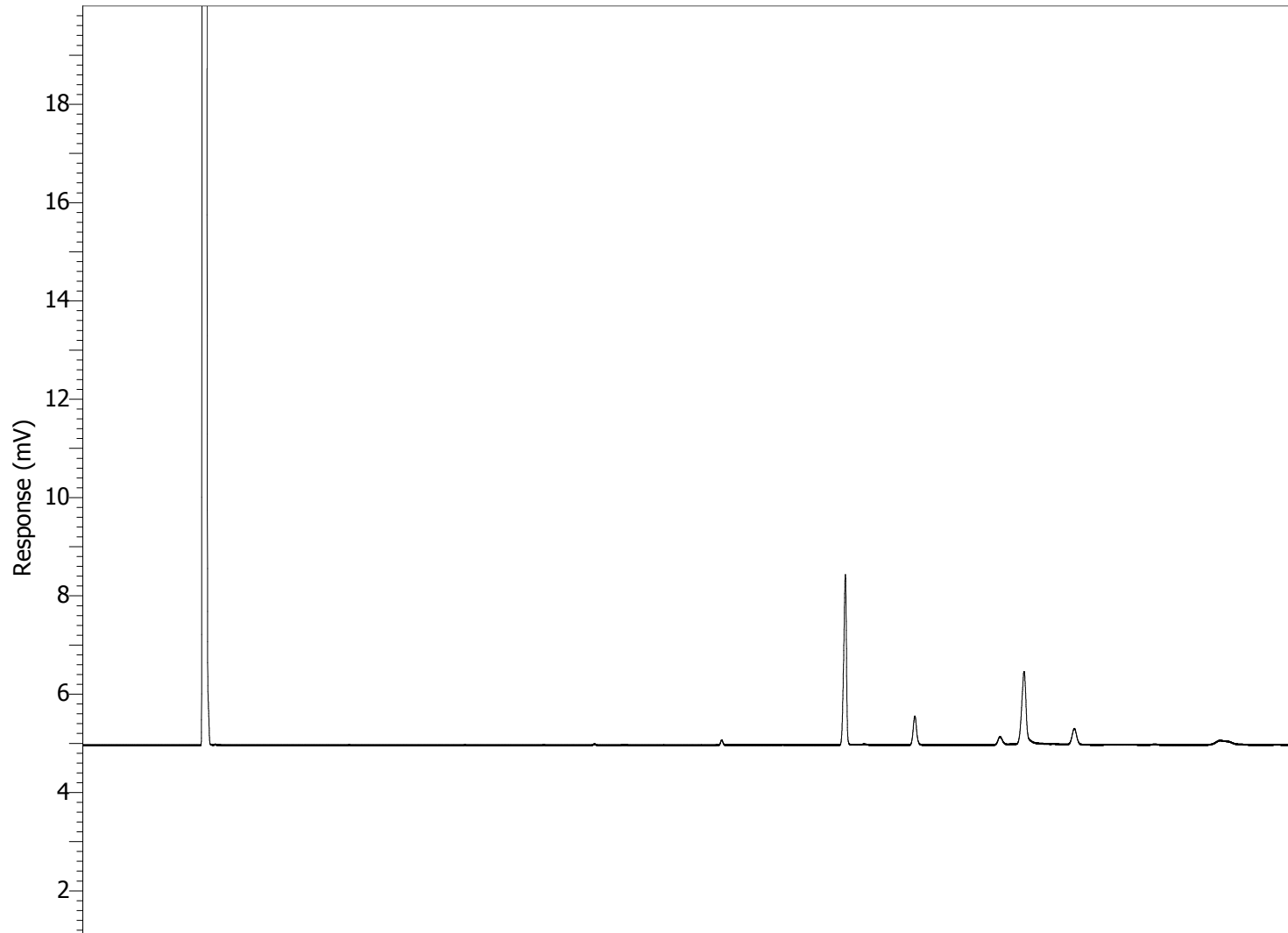
Software Version	: 6.3.1.0504		Date	: 6/12/2018 4:00:37 PM
Operator	: FES		Sample Name	:
Sample Number	:		Study	:
AutoSampler	: NONE		Rack/Vial	: 0/0
Instrument Name	: Clarus500		Channel	: A
Instrument Serial #	: 650N7041802		A/D mV Range	: 1000
Delay Time	: 0.00 min		End Time	: 19.50 min
Sampling Rate	: 12.5000 pts/s			
Sample Volume	: 1.000000 ul			
Sample Amount	: 1.0000		Area Reject	: 0.000000
Data Acquisition Time	: 6/12/2018 3:11:11 PM		Dilution Factor	: 1.00
			Cycle	: 1

Raw Data File : C:\GC\Data\Result 3.raw
Result File : C:\Documents and Settings\FES\Desktop\Result\2018\Chon Wen-Xian\Result 3.rst
Inst Method : C:\GC\Method\Nukol 25327 (18092017) from C:\GC\Data\Result 3.raw
Proc Method : C:\GC\Method\Nukol 25327 (18092017) from C:\Documents and Settings\FES\Desktop\Result\2018\Chon Wen-Xian\Result 3.rst
Calib Method : C:\GC\Method\Nukol 25327 (18092017) from C:\Documents and Settings\FES\Desktop\Result\2018\Chon Wen-Xian\Result 3.rst
Report Format File: C:\GC\Method\Nukol 25327 (18092017).rpt
Sequence File : C:\GC\Method\Result 3.seq

DEFAULT REPORT

Peak #	Time [min]	Area [µV·s]	Height [µV]	Area [%]	Norm. Area [%]	BL	Area/Height [s]
1	1.911	1172605.06	872165.83	95.97	95.97	BE	1.3445
2	1.957	19991.47	19020.09	1.64	1.64	EB	1.0511
3	2.152	77.73	54.53	0.01	0.01	BB	1.4254
4	8.096	53.70	27.15	0.00	0.00	BB	1.9776
5	10.116	274.72	120.65	0.02	0.02	BB	2.2770
6	12.074	12062.61	4172.12	0.99	0.99	BB	2.8912
7	13.155	2336.75	712.85	0.19	0.19	BB	3.2781
8	14.351	2548.00	230.51	0.21	0.21	BV	11.0539
9	14.476	1759.70	322.12	0.14	0.14	VB	5.4629
10	14.865	8255.98	1898.16	0.68	0.68	BB	4.3495
11	15.639	1828.59	404.42	0.15	0.15	BB	4.5215
		1221794.31	899128.42	100.00	100.00		

Missing Component Report
Component Expected Retention (Calibration File)

All components were found

6/12/2018 4:00:37 PM Result: C:\Documents and Settings\FES\Desktop\Result\2018\Chon Wen-Xian\Result 3.rst

---

Chromatogram

Software Version : 6.3.1.0504

Date : 6/12/2018 4:00:37 PM

Sample Name :

Sample Number :

Data Acquisition Time : 6/12/2018 3:11:11 PM

Raw Data File : C:\Documents and Settings\FES\Desktop\Result\2018\Chon Wen-Xian\Result 3.raw
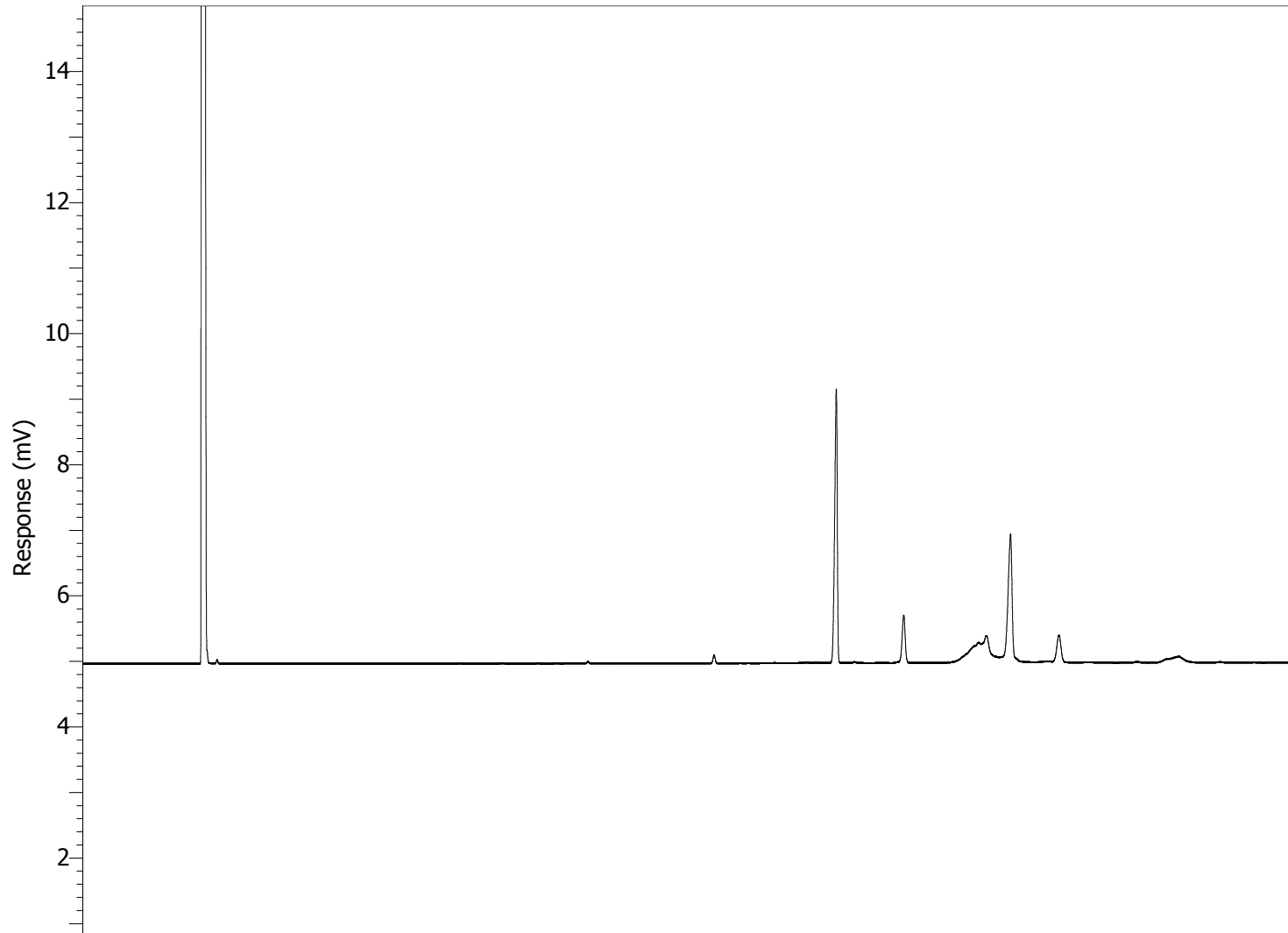
Software Version	: 6.3.1.0504		Date	: 6/29/2018 12:18:49 PM
Operator	: FES		Sample Name	:
Sample Number	:		Study	:
AutoSampler	: NONE		Rack/Vial	: 0/0
Instrument Name	: Clarus500		Channel	: A
Instrument Serial #	: 650N7041802		A/D mV Range	: 1000
Delay Time	: 0.00 min		End Time	: 19.50 min
Sampling Rate	: 12.5000 pts/s			
Sample Volume	: 1.000000 ul			
Sample Amount	: 1.0000		Area Reject	: 0.000000
Data Acquisition Time	: 6/29/2018 11:55:35 AM		Dilution Factor	: 1.00
			Cycle	: 1

Raw Data File : C:\Documents and Settings\FES\Desktop\Result\2018\Chon Wen-Xian\14-6-2018 (8.43 am)-T 70-t 5-load 9%-ratio 25 to 1.raw

Result File : C:\Documents and Settings\FES\Desktop\Result\2018\Chon Wen-Xian\14-6-2018 (8.43 am)-T 70-t 5-load 9%-ratio 25 to 1.rst

Inst Method : C:\GC\Method\Nukol 25327 (18092017) from C:\Documents and Settings\FES\Desktop\Result\2018\Chon Wen-Xian\14-6-2018 (8.43 am)-T 70-t 5-load 9%-ratio 25 to 1.raw

Proc Method : C:\GC\Method\Nukol 25327 (18092017) from C:\Documents and Settings\FES\Desktop\Result\2018\Chon Wen-Xian\14-6-2018 (8.43 am)-T 70-t 5-load 9%-ratio 25 to 1.rst

Calib Method : C:\GC\Method\Nukol 25327 (18092017) from C:\Documents and Settings\FES\Desktop\Result\2018\Chon Wen-Xian\14-6-2018 (8.43 am)-T 70-t 5-load 9%-ratio 25 to 1.rst

Report Format File: C:\GC\Method\Nukol 25327 (18092017).rpt

Sequence File : C:\GC\Method\14-6-2018 (8.43 am)-T 70-t 5-load 9%-ratio 25 to 1.seq

DEFAULT REPORT

Peak #	Time [min]	Area [µV·s]	Height [µV]	Area [%]	Norm. Area [%]	BL	Area/Height [s]
1	1.927	1149136.95	949760.60	98.08	98.08	BE	1.2099
2	1.975	8887.78	9054.62	0.76	0.76	EB	0.9816
3	2.127	173.89	122.02	0.01	0.01	BB	1.4252
4	10.235	138.70	63.40	0.01	0.01	BB	2.1876
5	12.207	6082.06	2196.21	0.52	0.52	BB	2.7694
6	13.329	1834.68	559.11	0.16	0.16	BB	3.2814
7	14.696	429.90	105.42	0.04	0.04	BB	4.0779
8	15.071	4044.16	926.77	0.35	0.35	BB	4.3637
9	15.883	959.04	206.16	0.08	0.08	BB	4.6520
		1171687.16	962994.30	100.00	100.00		

Missing Component Report

Component	Expected Retention (Calibration File)

All components were found

6/29/2018 12:18:49 PM Result: C:\Documents and Settings\FES\Desktop\Result\2018\Chon
 Wen-Xian\14-6-2018 (8.43 am)-T 70-t 5-load 9%-ratio 25 to 1.rst

Chromatogram

Software Version : 6.3.1.0504
Sample Name :
Data Acquisition Time : 6/29/2018 11:55:35 AM

Date : 6/29/2018 12:18:49 PM
Sample Number :

Raw Data File : C:\Documents and Settings\FES\Desktop\Result\2018\Chon Wen-Xian\14-6-2018 (8.43 am)-T 70-t 5-load
 9%-ratio 25 to 1.raw

Microanalysis Report
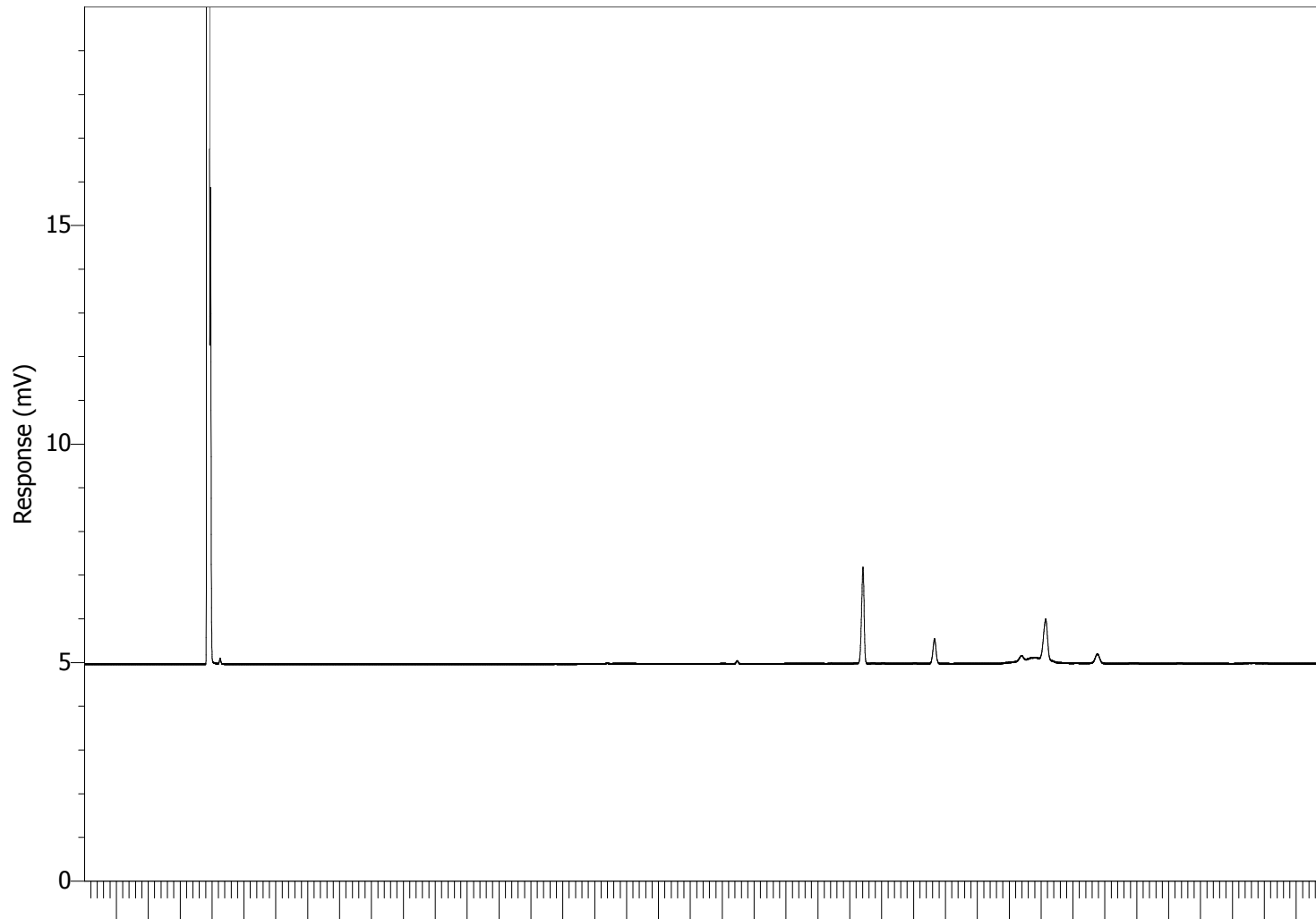
Prepared for: *Company Name Here*

Prepared by: *Your Name Here*   *7/27/2018*

c:\edax32\genesis\genmaps.spc 27-Jul-2018 09:11:20
LSecs : 8
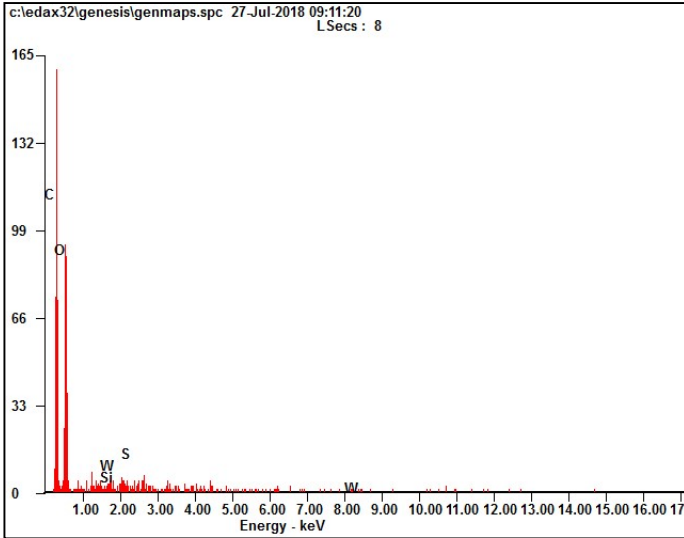
Element	Wt%	At%
CK	48.26	55.62
OK	50.76	43.92
SiK	00.71	00.35
SK	00.27	00.12
WL	00.00	00.00
Matrix	Correction	ZAF
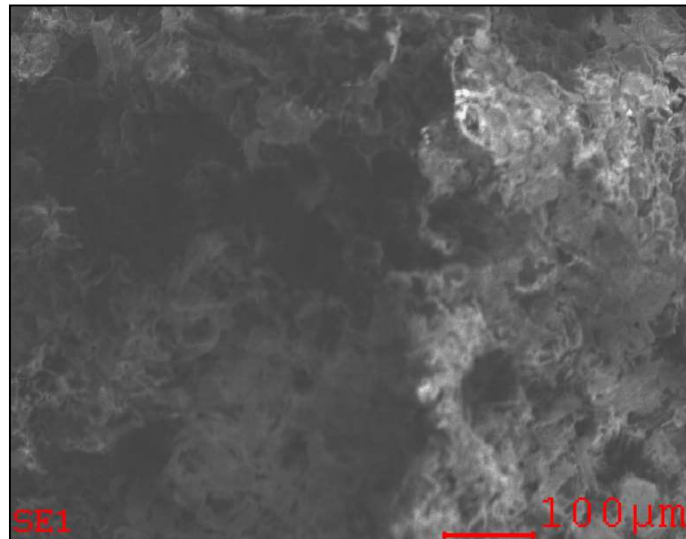
SE1   100 μm

Prepared for: *Company Name Here*

Prepared by: *Your Name Here* *7/27/2018*

EDAX' TSL
advanced microanalysis solutions
AMETEK®

c:\edax32\genesis\genmaps.spc 27-Jul-2018 09:36:01
LSecs : 8
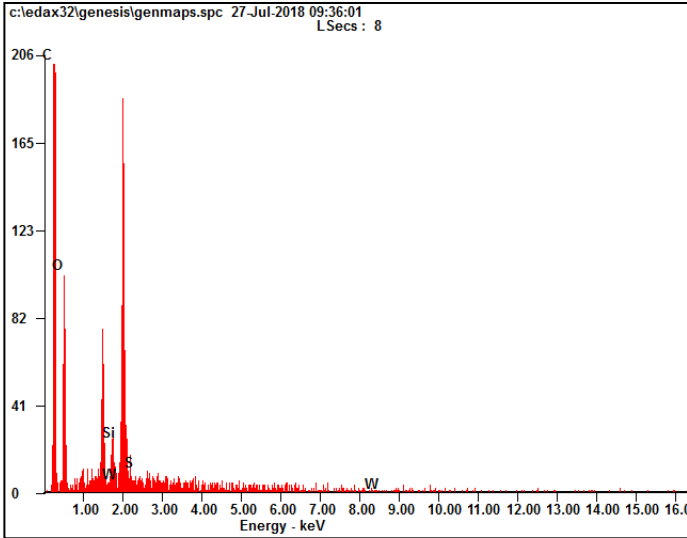
Element	Wt%	At%
CK	60.86	67.99
OK	36.94	30.98
SiK	02.01	00.96
SK	00.19	00.08
WL	00.00	00.00
Matrix	Correction	ZAF
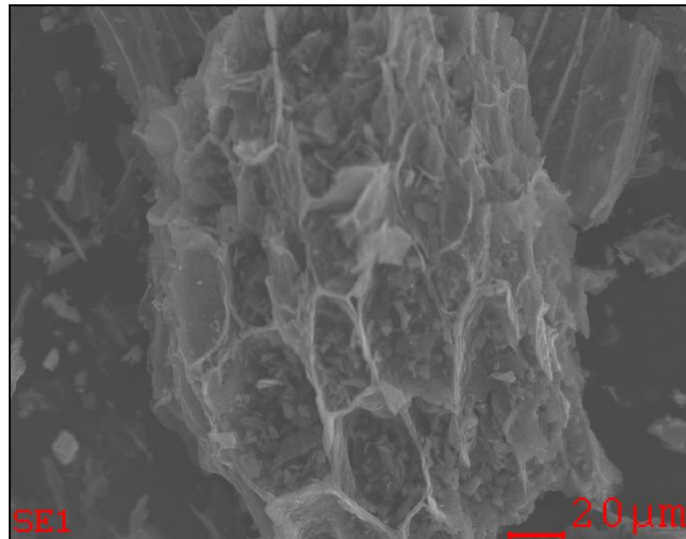
SE1 20 µm

Microanalysis Report

Prepared for: *Company Name Here*

Prepared by: *Your Name Here*   *7/27/2018*

c:\edax32\genesis\genmaps.spc   27-Jul-2018 09:43:05
LSecs : 8
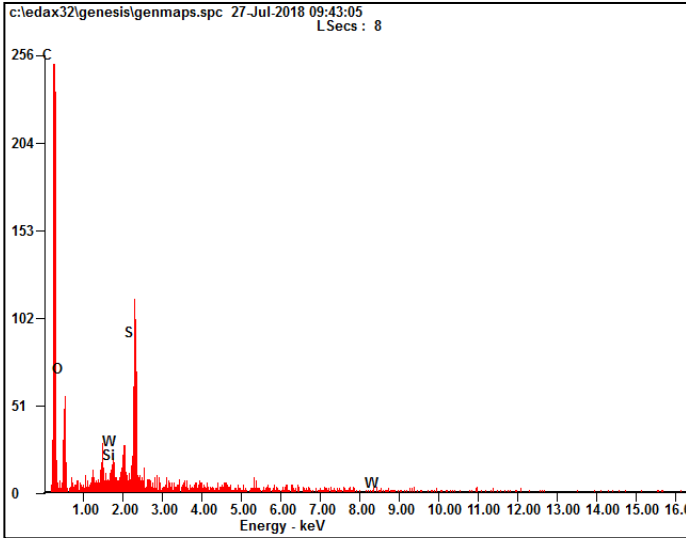
Element	Wt%	At%
CK	73.68	81.25
OK	18.85	15.61
SiK	00.96	00.45
SK	06.51	02.69
WL	00.00	00.00
Matrix	Correction	ZAF
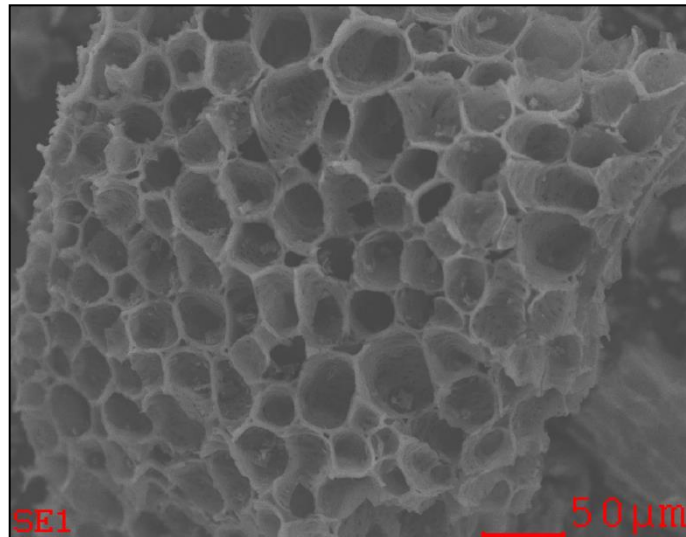
TPD/R/O 1100

Standard Data Report

Thermo Electron

Run Nr.:1564

File: C:\Thermo\data\Dr Steven\Chon Wen Xian\TPR_CATALYST1.110
Comment:
Operator: WX
Room Temperature 24°C   Atmospheric Pressure 1000hPa

Sample

Producer: Chon Wen Xian   Sample-Code: 0
Name: catalyst1   Customer-Code: 0
Mass: 0.0215 g   Support:
Info: Metals: 0
Preparation:

Pretreatment

Name: TPR Pretreatment_2018   Info:
On Instrument: Instrument 1 with Ser.Nr.20117691 on Right Oven
Started: 13/6/2018 at 10:24:15 AM finished 11:54:49 AM

Phase	With Gas	Flow [ccm/min]	Start at T [°C]	Ramp[°C/min]	Stop at T [°C]	Hold for [min]
Cleaning	Nitrogen	20	Off			5
1:	Nitrogen	20	Off	10	200	60
2:	Off					
3:	Off					
4:	Off					

End Pretreatment with Oven Off

TPD/R/O

Method Name: Ana_2018   Info:
On Instrument: Instrument 1 with Ser.Nr.20117691 on Right Oven
Started: 13/6/2018 at 12:28:47 PM finished 3:43:38 PM
Gas Port when Ready: (a) Nitrogen
Gas Port when End: (a) Nitrogen
Sample rate: 1 s
Gain: 10
Polarity: Positive

With Gas	Flow [ccm/min]	Start at T [°C]	Ramp°C/min	Stop at T [°C]	Hold for [min]
Hydrogen 5.47% in Nitrogen 0		25	30	5	1000

Results

Amount gas adsorbed: 1300.29808 µmol/g

Baseline

Start at 0.0167 min 1.22070 mV. Stop at 194.7000 min 47.30225 mV

Calibration

Use Calibration Factor: 1.210911 *10e-7 mmol/mVs

Peaks

#	Start [min]	Stop [min]	Maximum [min]	T [°C]	Integral [mVs]	[µmol/g]	[%]
1	115.6000	140.1833	127.7000	661	230870.82	1300.29810	100.00
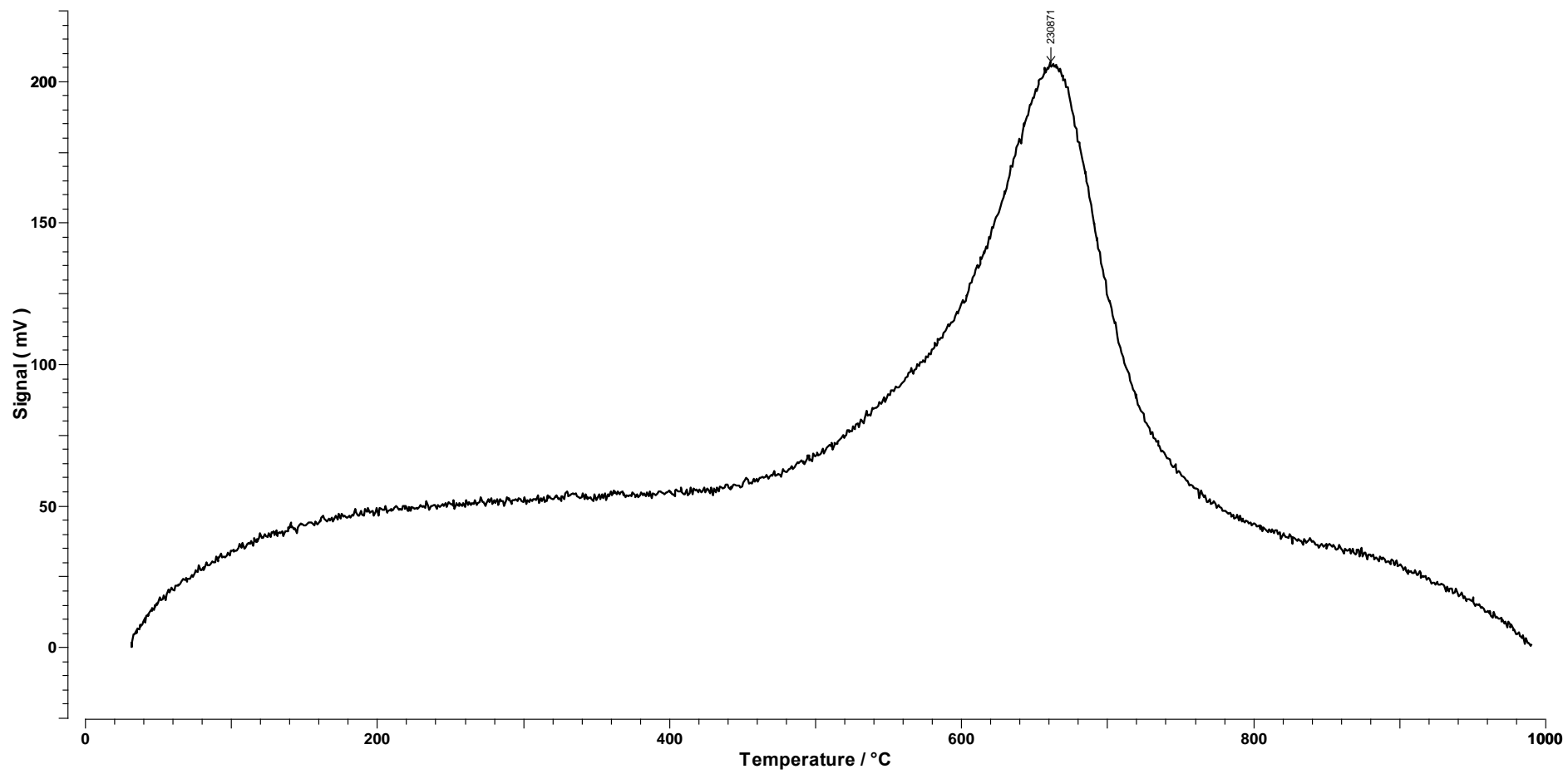
```
          ***   Basic Data Process   ***

Group      : StevenLim
Data       : corncob_2

# Strongest 3 peaks
  no. peak   2Theta        d        I/I1    FWHM      Intensity    Integrated Int
      no.    (deg)        (A)               (deg)     (Counts)     (Counts)
   1    9    21.7000    4.09215    100    3.38660       187          20016
   2    8    21.0600    4.21504     88    0.00000       164              0
   3    7    19.7800    4.48482     55    0.00000       103              0

# Peak Data List
      peak   2Theta        d        I/I1    FWHM      Intensity    Integrated Int
      no.    (deg)        (A)               (deg)     (Counts)     (Counts)
       1     13.8000    6.41186      8    0.84000        15            876
       2     16.1000    5.50068     33    2.60000        62           4229
       3     16.2600    5.44691     33    0.00000        62              0
       4     16.6800    5.31069     37    0.00000        70              0
       5     17.3800    5.09834     38    0.00000        71              0
       6     18.4200    4.81277     40    0.00000        75              0
       7     19.7800    4.48482     55    0.00000       103              0
       8     21.0600    4.21504     88    0.00000       164              0
       9     21.7000    4.09215    100    3.38660       187          20016
      10     23.7200    3.74804     38    0.00000        71              0
      11     23.9800    3.70798     31    0.00000        58              0
      12     24.6400    3.61014     19    0.76000        35           2204
      13     25.8200    3.44776      9    0.74000        16            808
      14     27.2600    3.26882      5    0.24000         9            244
      15     29.1300    3.06309      3    0.10000         6             86
      16     33.5650    2.66780      4    0.11000         7             92
      17     34.6600    2.58599     13    0.70660        24           1053
      18     35.3200    2.53916      8    0.00000        15              0
      19     35.8800    2.50080      4    0.00000         8              0
      20     36.6300    2.45130      5    0.54000        10            483
      21     37.9560    2.36866     18    0.72800        33           1386
      22     39.0366    2.30554      5    0.24670         9            135
      23     40.5100    2.22502      4    0.18000         8            218
      24     42.1700    2.14119      3    0.30000         6            175
      25     44.1650    2.04899     12    0.67000        23            714
      26     44.8200    2.02056      6    0.42000        12            360
      27     47.6400    1.90732      3    0.12000         6             83
      28     49.4600    1.84131      3    0.20000         6            138
```

```
        ***  Basic Data Process  ***


# Data Infomation
         Group              : StevenLim
         Data               : corncob_2
         Sample Nmae        : corncob_2
         Comment            :
         Date & Time        : 08-14-18 14:47:27

# Measurement Condition
   X-ray tube
         target             : Cu
         voltage            : 40.0 (kV)
         current            : 30.0 (mA)
   Slits
         Auto Slit          : not Used
         divergence slit    :   1.00000 (deg)
         scatter slit       :   1.00000 (deg)
         receiving slit     :   0.30000(mm)
   Scanning
         drive axis         : Theta-2Theta
         scan range         :    5.0000 - 60.0000 (deg)
         scan mode          : Continuous Scan
         scan speed         :    2.0000 (deg/min)
         sampling pitch     :    0.0200 (deg)
         preset time        :    0.60 (sec)

# Data Process Condition
   Smoothing               [ AUTO ]
         smoothing points   : 51
   B.G.Subtruction         [ AUTO ]
         sampling points    : 51
         repeat times       : 30
   Ka1-a2 Separate         [ MANUAL ]
         Ka1 a2 ratio       : 50 (%)
   Peak Search             [ AUTO ]
         differential points : 51
         FWHM threhold      : 0.050 (deg)
         intensity threhold : 30 (par mil)
         FWHM ratio  (n-1)/n : 2
   System error Correction  [ NO ]
   Precise peak Correction  [ NO ]
```

< Group: StevenLim   Data: corncob_2 >

```
              ***   Basic Data Process   ***

Group        : StevenLim
Data         : Activated_carbon_corn

# Strongest 3 peaks
   no. peak      2Theta         d         I/I1      FWHM      Intensity    Integrated Int
       no.       (deg)         (A)                  (deg)     (Counts)     (Counts)
    1   12       21.3800     4.15267      100      2.16000       61          5987
    2   13       22.9200     3.87702       85      0.00000       52             0
    3   14       24.2000     3.67477       82      0.00000       50             0

# Peak Data List
       peak      2Theta         d         I/I1      FWHM      Intensity    Integrated Int
       no.       (deg)         (A)                  (deg)     (Counts)     (Counts)
         1        5.3250    16.58247       11      0.31000        7           226
         2        7.6000    11.62298        3      0.04000        2            13
         3        9.0950     9.71552        7      0.25000        4            68
         4       11.6000     7.62248        3      0.08000        2            22
         5       12.5650     7.03916        5      0.05000        3            20
         6       14.0900     6.28053        3      0.10000        2            34
         7       15.0400     5.88589        3      0.04000        2             9
         8       15.8700     5.57988        8      0.10000        5            63
         9       16.8350     5.26214        5      0.03000        3             7
        10       18.9400     4.68179       16      0.84000       10           555
        11       20.1400     4.40546       49      0.68000       30           973
        12       21.3800     4.15267      100      2.16000       61          5987
        13       22.9200     3.87702       85      0.00000       52             0
        14       24.2000     3.67477       82      0.00000       50             0
        15       25.8000     3.45039       79      0.00000       48             0
        16       27.5800     3.23161       49      0.00000       30             0
        17       28.5200     3.12720       38      1.64000       23          1765
        18       29.5000     3.02551       20      0.66000       12           383
        19       30.4533     2.93293       15      0.65330        9           412
        20       32.1200     2.78445        7      0.08000        4            44
        21       34.9150     2.56768        7      0.11000        4            49
        22       37.9466     2.36922       49      0.65330       30           990
        23       40.8400     2.20780        3      0.04000        2            20
        24       41.0600     2.19648        3      0.00000        2             0
        25       41.8400     2.15732       13      0.64000        8           329
        26       42.7800     2.11206       15      0.76000        9           424
        27       44.1600     2.04921       41      0.68000       25          1065
        28       45.6000     1.98779        8      0.12000        5            66
        29       49.2100     1.85008        3      0.06000        2            12
        30       52.9600     1.72757        3      0.08000        2            21
        31       53.6900     1.70579        3      0.14000        2            24
        32       56.0200     1.64024        5      0.08000        3            27
```

```
          ***  Basic Data Process  ***

# Data Infomation
          Group              : StevenLim
          Data               : Activated_carbon_corn
          Sample Nmae        : Activated_carbon_corn
          Comment            :
          Date & Time        : 08-14-18 13:35:50

# Measurement Condition
     X-ray tube
          target             : Cu
          voltage            : 40.0 (kV)
          current            : 30.0 (mA)
     Slits
          Auto Slit          : not Used
          divergence slit    :   1.00000 (deg)
          scatter slit       :   1.00000 (deg)
          receiving slit     :   0.30000 (mm)
     Scanning
          drive axis         : Theta-2Theta
          scan range         :    5.0000 - 60.0000 (deg)
          scan mode          : Continuous Scan
          scan speed         :    2.0000 (deg/min)
          sampling pitch     :    0.0200 (deg)
          preset time        :    0.60 (sec)

# Data Process Condition
     Smoothing               [ AUTO ]
          smoothing points   : 51
     B.G.Subtruction         [ AUTO ]
          sampling points    : 51
          repeat times       : 30
     Ka1-a2 Separate         [ MANUAL ]
          Ka1 a2 ratio       : 50 (%)
     Peak Search             [ AUTO ]
          differential points : 51
          FWHM threhold       : 0.050 (deg)
          intensity threhold  : 30 (par mil)
          FWHM ratio  (n-1)/n : 2
     System error Correction [ NO ]
     Precise peak Correction [ NO ]
```

< Group: StevenLim   Data: Activated_carbon_corn >

```
            ***   Basic Data Process   ***

Group       : StevenLim
Data        : corncob_catalyst2

# Strongest 3 peaks
   no. peak    2Theta       d        I/I1     FWHM      Intensity    Integrated Int
       no.     (deg)       (A)                (deg)     (Counts)     (Counts)
    1   16    23.6600     3.75740    100    0.00000        49            0
    2   17    24.9000     3.57303     92    0.00000        45            0
    3   15    22.7200     3.91069     88    0.00000        43            0

# Peak Data List
       peak    2Theta       d        I/I1     FWHM      Intensity    Integrated Int
       no.     (deg)       (A)                (deg)     (Counts)     (Counts)
        1      5.4300    16.26205     16    0.38000         8           272
        2      8.1050    10.89988      8    0.21000         4            90
        3     10.0200     8.82061      2    0.00000         1             0
        4     12.9500     6.83074      6    0.06000         3            18
        5     13.6050     6.50331      6    0.05000         3            17
        6     15.2500     5.80531      4    0.06000         2            18
        7     16.0000     5.53483      4    0.08000         2            20
        8     17.2600     5.13352     12    0.16000         6           125
        9     18.1400     4.88642     18    0.32000         9           430
       10     18.8800     4.69653     20    0.00000        10             0
       11     19.0400     4.65742     20    0.00000        10             0
       12     19.8800     4.46249     45    1.16000        22          1721
       13     20.8000     4.26714     65    0.00000        32             0
       14     21.4000     4.14883     69    0.00000        34             0
       15     22.7200     3.91069     88    0.00000        43             0
       16     23.6600     3.75740    100    0.00000        49             0
       17     24.9000     3.57303     92    0.00000        45             0
       18     25.8000     3.45039     84    0.00000        41             0
       19     26.7400     3.33119     69    0.00000        34             0
       20     27.4000     3.25243     49    0.00000        24             0
       21     27.6800     3.22016     45    0.00000        22             0
       22     28.2200     3.15976     37    1.44000        18           924
       23     29.1600     3.06001     22    0.96000        11           505
       24     31.0950     2.87386      4    0.05000         2             9
       25     32.4000     2.76102      2    0.00000         1             0
       26     33.9600     2.63767      4    0.04000         2             8
       27     34.5000     2.59761      2    0.00000         1             0
       28     37.9283     2.37033     55    0.72330        27          1142
       29     39.6800     2.26963      2    0.00000         1             0
       30     42.0200     2.14849     12    0.84000         6           207
       31     42.2400     2.13781     12    0.00000         6             0
       32     42.8600     2.10831     18    0.64000         9           384
       33     44.1450     2.04987     61    0.71000        30          1237
       34     45.8550     1.97733      6    0.13000         3            30
       35     46.7000     1.94350      2    0.00000         1             0
       36     59.5800     1.55045      4    0.20000         2            24
```

```
         ***  Basic Data Process  ***

# Data Infomation
          Group              : StevenLim
          Data               : corncob_catalyst2
          Sample Nmae        : corncob_catalyst2
          Comment            :
          Date & Time        : 06-20-18 12:48:30

# Measurement Condition
    X-ray tube
          target             : Cu
          voltage            : 40.0 (kV)
          current            : 30.0 (mA)
    Slits
          Auto Slit          : not Used
          divergence slit    :   1.00000 (deg)
          scatter slit       :   1.00000 (deg)
          receiving slit     :   0.30000(mm)
    Scanning
          drive axis         : Theta-2Theta
          scan range         :    5.0000 - 60.0000 (deg)
          scan mode          : Continuous Scan
          scan speed         :    2.0000 (deg/min)
          sampling pitch     :    0.0200 (deg)
          preset time        :    0.60 (sec)

# Data Process Condition
    Smoothing               [ AUTO ]
          smoothing points   : 51
    B.G.Subtruction         [ AUTO ]
          sampling points    : 51
          repeat times       : 30
    Ka1-a2 Separate         [ MANUAL ]
          Ka1 a2 ratio       : 50 (%)
    Peak Search             [ AUTO ]
          differential points : 51
          FWHM threhold      : 0.050 (deg)
          intensity threhold : 30 (par mil)
          FWHM ratio  (n-1)/n : 2
    System error Correction  [ NO ]
    Precise peak Correction  [ NO ]
```

< Group: StevenLim   Data: corncob_catalyst2 >